Copernicus assisted environmental monitoring across the Black Sea Basin – PONTOS

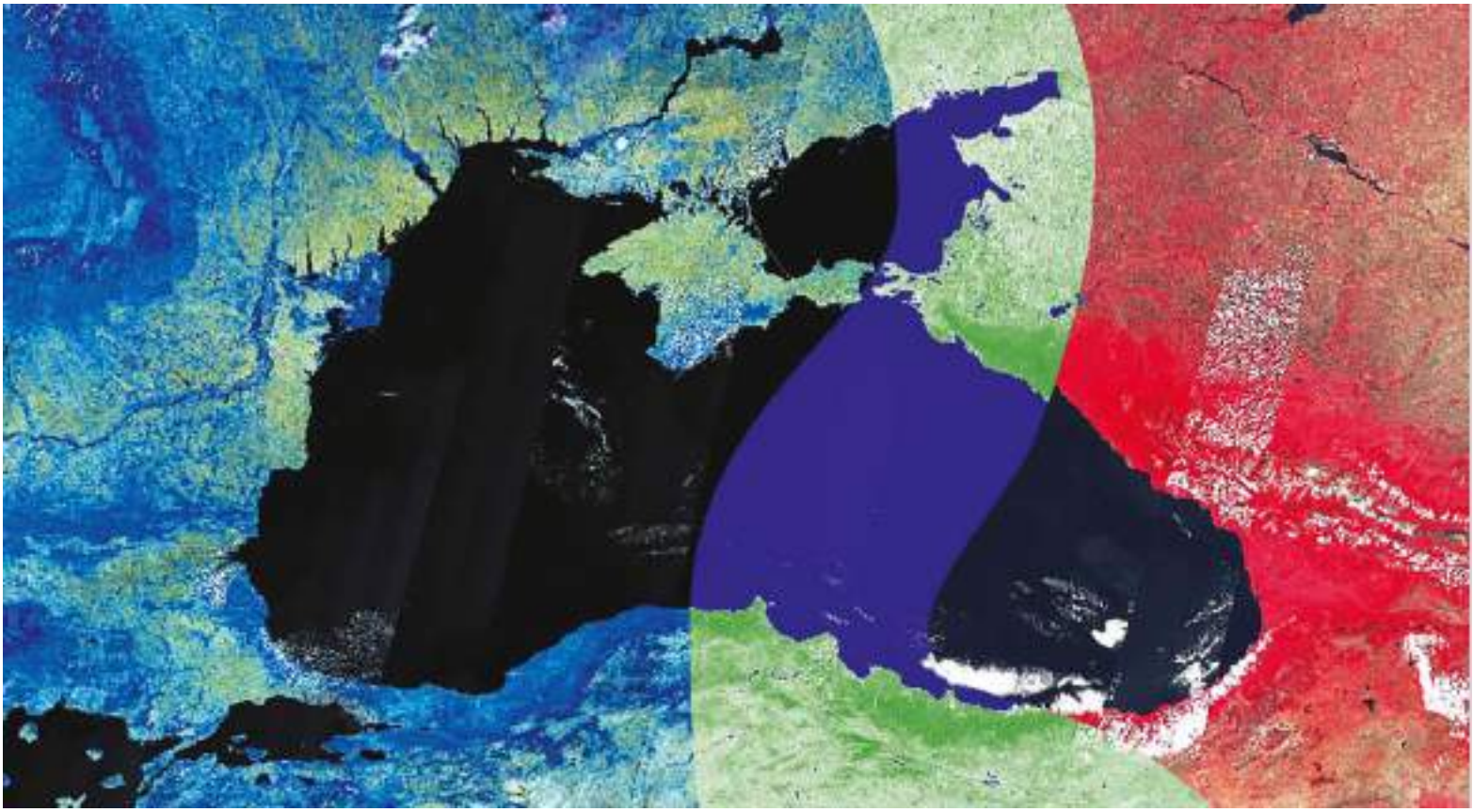

Integrated assessment on chlorophyll concentration and eutrophication dynamics

Deliverable D.T1.2.5

PONTOS-UA (Ukraine)

Authors: Medinets V.I., Gazyetov Ye.I., Kovalova N.V., Kristich V.F., Konareva O.P, Soltys I.E., Snihirov S.M., Medinets S.V.

Table of Contents

1. Introduction

As is known [EEA, 2019, Borum, J. 1996], eutrophication is a long-term and cyclic in time process of aquatic ecosystem quality degradation as the result of enrichment with nutrients – first of all nitrogen and phosphorus compounds, which breaks the usual biogeochemical cycles of a water ecosystem functioning and causes changes in a water body's production processes, in the first instance as the temperature goes up in summer. Eutrophication can result from the water body's natural aging or anthropogenic pollution (with wastewater, fertilizers etc.)

There are two types of eutrophication.

1. Natural eutrophication is a normal process of nutrients entering water bodies from their catchment causing changes in those water bodies, ageing above all others, particularly in lakes and other water bodies with slow velocity of water flows and therefore when the loaded nutrients accumulated in borders of concrete water ecosystem. This leads to decrease in depth, appearing of aquatic vegetation and disappearing of the water body in a hundred or thousand years' time.

2. Anthropogenic (Cultural) eutrophication is the process that speeds up natural eutrophication because of additional inflow of nutrients due to human activities. Due to some of the reasons like urbanization, land runoff is accelerated and more nutrients are supplied to lakes and rivers, and then to coastal estuaries and bays. Extra nutrients are also supplied by treatment plants, fertilizers, farms, as well as untreated sewage in many cities.

The main difference between natural and anthropogenic eutrophication is that the natural process is very slow, occurring on geological time scales (hundreds and thousands of years). The anthropogenic eutrophication has more intensive processes that speeds up natural eutrophication because of human activities etc. in the time scale of dozens of years.

Eutrophication process is developing in 5 stages as follows:

1. Excessive content of nutrients at higher temperature causes rapid development of algae and microalgae (first of all phytoplankton). At that increase in number of zooplankton feeding on phytoplankton is observed.

2. The algae and bacteria reproducing in the water body as the result have much bigger total body surface and biomass than a usual plant complex would have. At that, no photosynthesis takes place in those plants at night, while they continue to breath and this requires oxygen.

3. Consequently, especially in warm days, oxygen concentration in water goes down reaching the critical values (less than 30-40 % of saturation level) and the organisms begin to die of oxygen depletion – hypoxia (the so-called 'summer mortality'). Such mortalities are periodically observed in summer practically in all the estuaries, lakes and reservoirs in Odesa Region.

4. As a result, water transparency decreases sharply, the depth of sunrays penetration decreases that entails death of bottom plants due to the lack of light. After the bottom plants death other organisms, whose live cycle was connected with the plants, also die away.

5. Large quantities of phytoplankton, plants and other organisms that died away are settling down from the water layers to the bottom where bacterial destruction of dead organic

matter happens with significant oxygen consumption. This entails the decrease of oxygen content down to practically zero level, due to which the process of bottom hypoxia starts, causing death of all the benthic organisms and fish. The similar phenomenon is observed most often in autumn and at the beginning of winter period in shallow water bodies and marine coastal waters. At that, anaerobic decomposition of dead organisms starts in the oxygen free bottom soils, producing such compounds and phenols and hydrogen sulphide, which cause even bigger mortality of water organisms and duration of hypoxia phenomena is extending!!!

Thus, the main consequences of eutrophication process, using which we can assess the possible risks, are as follows:

1. Sharp increase in primary production of aquatic ecosystem (blooms of microalgae) and change in the primary producers' biodiversity.

2. Development of aquatic vegetation and algae decreases penetration of light into the water column (transparency).

3. Hypoxia and mortality events caused by decrease in dissolved oxygen concentration leading to death of plants, fish, benthos and changes in the aquatic ecosystems' biodiversity and trophic chains, namely to decrease in specific weight of the highly organised forms of life (benthos, fish) …

4. Organic and inorganic compounds of nitrogen and phosphorus accumulation in the ecosystems entails transformation of an aerobic environment into anaerobic accompanied with the changes causing drop in aquatic environment quality down to a critical level, toxins, decrease in water bodies recreation value and attractiveness, as well as increase of greenhouse gases emissions.

Other effects of Eutrophication.

- Primary productivity increases and diversity of primary producers varies.

- Growth of aquatic plants and algae reduces the light penetration and also increases the turbidity . Death of resident organisms takes place.

- DO level decreases and sedimentation rate increases.

- Species diversity is altered, in turn overall aquatic ecosystem is effected.

- Accumulation of organic and inorganic nutrients.

- Conversion of aerobic environment to anaerobic in turn altering the appearance, odour of the water body.

- Anaerobes produce toxins and usage of this water causes health and recreation problems.

- Aquatic ecosystem is depleted.

The main indicators of eutrophication (characterising concrete stages) used by researchers and managers to identify eutrophication:

- Concentration of nutrients – nitrogen and phosphorus compounds (stage 1)
- Concentrations and levels of saturation with oxygen in the surface and bottom water layers (stages 2 and 3)

- Phytoplankton biomass (stage 2)
- Chlorophyll *a* concentration (stage 2)
- Water transparency (stages 2 and 3)
- Visual characteristics (dead organisms)- (stage 4)
- Aquatic vegetation (stage 2)
- Hydrogen sulphide availability in bottom soils (stages 4 and 5)
- Bacterioplankton number (availability of allochthonous organics)

Additional criteria and indices used to assess a trophic index of the aquatic environment:

- TRIX trophic index (trophic state of an ecosystem in general)
- TSI trophic index (trophic state of an ecosystem in general)

The assessment of eutrophic conditions is a formal requirement of several European Directives [Greenwood et al, 2019]. Typically, these eutrophication assessments use a set of primary indicators which include dissolved inorganic nutrients, chlorophyll, dissolved oxygen and secondary information such as phytoplankton community data.

The methodology of the PONTOS Project is based on the use of the most accessible eutrophication state indicator - chlorophyll concentration, which can be obtained from the space images Landsat 8 (9 spectral channels) and Sentinel 2 (13 spectral channels), as well as Sentinel 3 (21 spectral channels).

The following is required in order to fulfil this task:

1. To master the existing standard methods of images processing using the SNAP (SeNtinel's Application Platform) developed for marine areas and using all the above mentioned satellites.

2. To plan and perform special field (in situ) studies to receive real experimental data with in-fact measured chlorophyll concentrations required to assess reliability of the SNAP data obtained and recalibration of the SNAP results.

3. In case the results of standard SNAP calculation do not satisfy the customer, the possibility to receive primary results as to spectral characteristics of water surface is used, taking into account atmospheric correction or w/o atmospheric correction. This enables a user to determine independently the algorithm of chlorophyll *a* calculation.

4. Identification of real dependence of chlorophyll *a* concentration on the intensity of concrete spectral parts of a space image for more reliable chlorophyll concentration determination.

5. Based on the experimental dependencies, the recalculations of the chlorophyll fields will have to be made, which could be used for the real analysis of eutrophication processes in the pilot area.

The aims of our studies within the PONTOS project for the Ukrainian pilot area (the Dniester Delta) were as follows:

- To quantitatively assess the long-term changes in the main eutrophication indicators in the Dniester Delta based on historical data.
- To develop a methodology for using the Landsat and Sentinel satellite images to monitor chlorophyll concentration and assess the state of eutrophication.
- To formulate recommendations as to implementation of the satellite observations methodology to assess eutrophication in the Dniester Delta water bodies and other water objects
- To provide a wide range of users with objective information on the real dynamics of eutrophication phenomena and chlorophyll concentration in the Dniester Delta water bodies.

2. Background

One of the manifestations of negative consequences of anthropogenic impact on the lake, river and estuarine ecosystems in the Black Sea area is their progressive eutrophication (Materials, 2012). Eutrophication is a serious cause of aquatic ecosystems degradation, in particular the Dniester Estuary ecosystem (*Kovalova et al, 2012, 2018, 2021*). Its shallowness (average depth is ca. 2 m), the inflow of large amounts of nutrients with industrial effluents, run-off from the fields and secondary pollution from bottom sediments during floods, water releases from reservoirs and wind impact contribute to the Dniester Estuary's eutrophication. One of the water bodies' eutrophication level indicators is the chlorophyll *a* concentration calculated from the Earth Observation Space images processing and its concentration is widely and effectively used to assess the state of the aquatic environment eutrophication level (*Ogashawara et al., 2017*) for marine and freshwater bodies (rivers, lakes and estuaries) (*O'Reilly J. E. et al. 1998; O'Reilly & Werdell, 2019, Watanabe F. et al., 2018; Ogashawara et al., 2017, (Voronova, 2020)*.

The intensity of eutrophication processes' in water bodies is assessed using both separate simple indicators (chlorophyll *a*, bacterioplankton, nitrogen and phosphorus concentration) *OECD, 1982, (V.D. Romanenko, V.M. Zhukinskyi, O.P. Oksiyuk et.al., 1998)* and the complex trophic indices. The TRIX index (*Vollenweider R.A., 1998)*, which uses four parameters (chlorophyll *a* concentration, relative oxygen content (% of saturation), concentration of total nitrogen and total phosphorus) enables us to compare the level of eutrophication in fresh, sea and estuarine waters. The complex trophic index application is the most feasible under the condition of sea and fresh water mixing, which is typical of the water area studied. As is known (*L.A. Sirenko, N.Yu. Evtushenko, F. Komsrovskiy et.al., 1992)*, water exchange between the Dniester Estuary and the sea is one of the most significant factors influencing the environmental state of the estuary and the adjacent coastal area of the Black Sea.

The overview used and analysed the historical materials from the surveys performed by the staff of the Regional Centre for Integrated Environmental Monitoring (Odesa National I.I. Mechnikov University) in 2006-2020 in accordance with the EU Water Framework Directive methodology (*Kovalova N.V., Medinets V.I., Konareva O.P., Snigirov S.M., Medinets S.V., Soltys I.E., 2010, Kovalova N.V., Medinets V.I., 2012, Kovalova N.V., Medinets V.I., Medinets S.V., 2018, 2019)*. The programme of observations in the Dniester Estuary and the Black Sea coastal area comprised a network of stations given in the papers (*Kovalova N.V., Medinets V.I., Medinets S.V., 2020, 2021)* and included physicochemical, hydrobiological and microbiological studies of the aquatic environment. Altogether, 647 water samples from the estuary and 30 samples from the Black Sea deltaic area were analysed in 2006-2020 for chlorophyll *a* concentration, total nitrogen, total phosphorus, bacterioplankton number and other parameters. The methodologies described earlier in the papers (*Kovalova N.V., Medinets V.I., Konareva O.P., Snigirov S.M., Medinets S.V., Soltys I.E., 2010, Kovalova N.V., Medinets V.I., 2012, Kovalova N.V., Medinets V.I., Medinets S.V., 2018, 2019*, *Kovalova N.V., Medinets V.I., Medinets S.V., 2020, 2021*) were used for sampling and analysing of physicochemical characteristics. TRIX index [*Vollenweider R.A., 1998*] was used to assess water trophic status, the range of values from 1 to 10 included the trophic range from oligotrophic to hypertrophic waters. Besides, we used the (OECD, 1982) and JRC EC scales (Cardozo et al, 2001) for lakes and estuaries trophic status

assessment using chlorophyll *a*, as well as the national classification of inland waters quality where bacterioplankton number indicator is used (*V.D. Romanenko, V.M. Zhukinskyi, O.P. Oksiyuk et.al., 1998)*.

3. Materials and Methods

3.1. Methodological Framework Description

The objective of this study is to map and assess Chl-a concentration in the UA2 pilot areas water bodies such as Dniester Estuary and Bile lake in Odessa Region of Ukraine.

Chl-a values were initially assessed using the well-known C2RCC algorithm. As the interference of (a) the shallow sea bottom reflection, (b) the sun glint and (c) the presence of non-algal particles on the optical signal (spectral reflectances) measured by satellites has not been adequately evaluated then we should attempt to recalibrate the C2RCC processor using in-situ Chl-a concentration data or find the empirical algorithms without C2RCC processor using respective spectral radiance or reflectance values for calculation Chl-a concentration values.

During the initial stage of the task **we used** the PONTOS methodological framework for eutrophication assessment scheme presented in Figure 3.2, preliminary agreed between the PONTOS partners and described in detailed in [DUTH, 22] as the basic scheme.

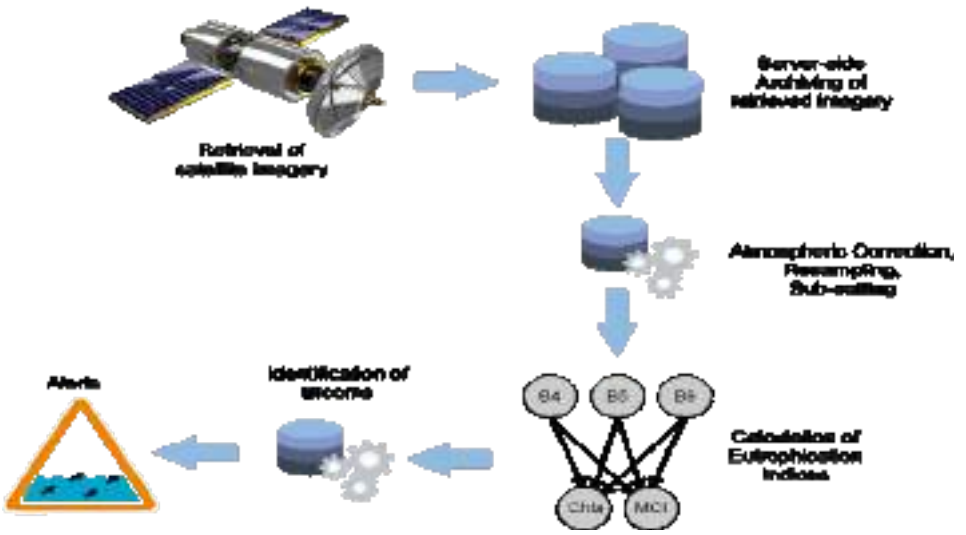

Figure 3.1. The PONTOS methodological framework for eutrophication assessment [DUTH, 22].

At that, in their report [DUTH, 22] the Greek partners described the main steps (Fig. 3.2) of the Methodological framework [DUTH, 22] use.

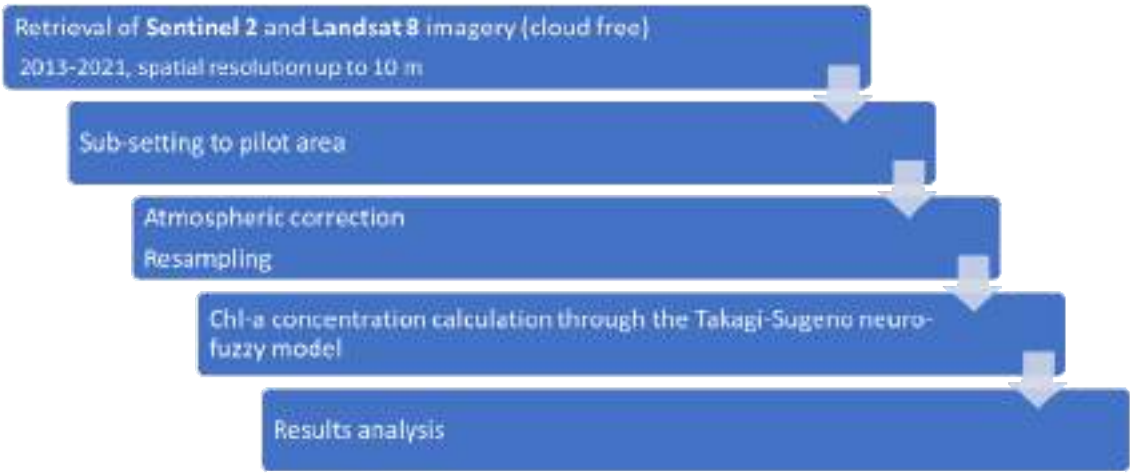

Figure 3.2. Methodological steps used and described by the Greek partners [DUTH, 2022].

In the course of work, we had to partially expand and change the list of steps of the methodological framework of PONTOS eutrophication assessment and monitoring for the Ukrainian pilot area UA2. Sentinel-2, Landsat 8 and Sentinel-3 satellite images were collected for the study area and period. We proposed and used the following steps of the methodological framework of PONTOS eutrophication assessment and monitoring:

Step 1. Retrieval and downloading of space images (cloude free) for: LandSat 8 (2016-2021), spatial resolution (SR) to 30 m, (https://earthexplorer.usgs.gov); Sentinel-2 (2016-2021) SP 10-60 m, (https://scihub.copernicus.eu); Sentinel-3 (2017-2021). SP to 300 m, (https://coda.eumetsat.inthttps://scihub.copernicus.eu, https://scihub.copernicus.eu).

Step 2. Subsetting to UA2 pilot area and resampling of space images for the best cells resolution (for Sentinel-2 only).

Step 3. Calculation of Chlorophyll concentration using SNAP-C2RCC algorithm and checking the level representativeness of results of calculation using comparison with experimental data from historical experimental data.

Step 4. Planning and realisation of pilot field trip programme in 2021

Step 5. Extraction Top-of-Atmosphere (TOA) spectral radiance for LandSat 8 and Sentinel-3 and Bottom-Of-Atmosphere (BOA) reflectances for Sentinel-2 in the SNAP environment by Export Mask Pixels instrument.

Step 6. Retrieval of types of empirical algorithms with maximal rate of determination and correlation between experimental chlorophyll *a* concentrations and arguments which used radiance / reflectance values of some remote sensing bands only.

Step 7. Decision about further algorithms using for each satellite images and procedures of further processing of space image

Step 8. Final processing and calculations of chlorophyll *a* concentrations for pilot water bodies areas using empirical algorithms for each satellites space image of LandSat 8, Sentinel-2, Sentinel-3.

Step 9. Definition and Exclusion from Consideration of clouds and water vegetation areas and finalise the raster images for analysis

Step 10. Results Analysis and above all of the final maps of chlorophyll concentrations.

At that, the following additions and assumptions should be pointed out.

The main criterion of the satellite images selection was full coverage of the studied water body or a part of the water body on condition of parallel in-situ studies, as well as absence of clouds or haze. SNAP, ArcGIS, QGIS, Excel and GIMPsoftware was used to process the LandSat 8, Sentinel-2 and Sentinel-3 images.

All images were stored on the local ONU working station purchased under the PONTOS project for that purpose. Satellite images were imposed on resampling, subsetting, atmospheric correction (only for S2 and L8). Chl-a field data were derived from historical and carried out during PONTOS project 2021 field trips.

Furthermore, field and satellite data of Chl-a concentration were examined to assess the reliability of the calculations from the satellite images and after the additional calibrations used to build maps of chlorophyll *a* distribution in water. Using those maps we further assessed location and acreage of the areas with exceeded concentrations, which characterise the beginning of eutrophication.

The parts of the water bodies that were overgrown with aquatic vegetation or covered with clouds were excluded from the final results analysed in this overview.

Working on this chapter, the ONU group considered and applied two methodological approaches to the calculation of chlorophyll *a* concentration in the surface waters of the pilot water bodies using the data from space images.

The first of them is to use the C2RCC processor (Case 2 Regional CoastColour) of the SNAP platform, where chlorophyll *a* concentration is calculated directly from the space images based on the neural (neural network?) algorithms that take into account the bio-optical components of light absorption by particles in aquatic environment (Brockmann et al., 2016). These algorithms were developed based on the Inherent Optical Properties (IOP) of different waters derived from NOMAD data set (NOMAD, 2008) on big quantity marine date. Lack of such data of observation for the areas of the freshwater lakes, rivers and estuaries in the standard NOMAD database brings down significantly the quality of chlorophyll concentration calculation in the SNAP platform. For shallow lakes and estuarine waters one should use his own data measured in the study areas.

The second approach is based of empirical algorithms using experimental data on the chlorophyll content in the surface water of the studied water bodies and the respective values of the TOA radiance / BOA reflectance values of the selected spectral channels of space images as those values are fixing representatively different levels of radiation absorption by chlorophyll in different optical and infrared spectra (O'Reilly J. E. et al. 1998; Dall'Olmo, G., & Gitelson A., 2005; Gitelson A. et al., 2007; Gitelson A. et al. 2011; Kopelevich O.V. et al., 2015; Tikhomirov O.A. et al. 2016; Watanabe F. et al. 2018).

3.2. In-situ field data collection

In the course of the study, the historical (2016-2020) and the measured during the PONTOS project field surveys (2021) data on the Dniester Estuary and the Bile Lake were collected for the period 2016-2021. Water samples of the surface water were collected and Chl-a concentration and other hydrological, hydrochemical and hydrobiological characteristics determined. A database of 179 Chl-a values and the related data for 2021 was created. Those in-situ Chl-a concentration values were used to evaluate and calibrate the remote sensing data (space) images from Sentinel -2, Landsat -8 and Sentinel – 3.

Location of the stations for which the historical information was collected for 2016-2020 is presented on Fig. 3.3 and the scheme of the stations selected for the pilot studies within the framework of the PONTOS project in 2021 – on Fig. 3.4.

The information on the number of analysed samples from the UA2 pilot area and those selected for the further calibration of the space images is presented in Table 3.1.

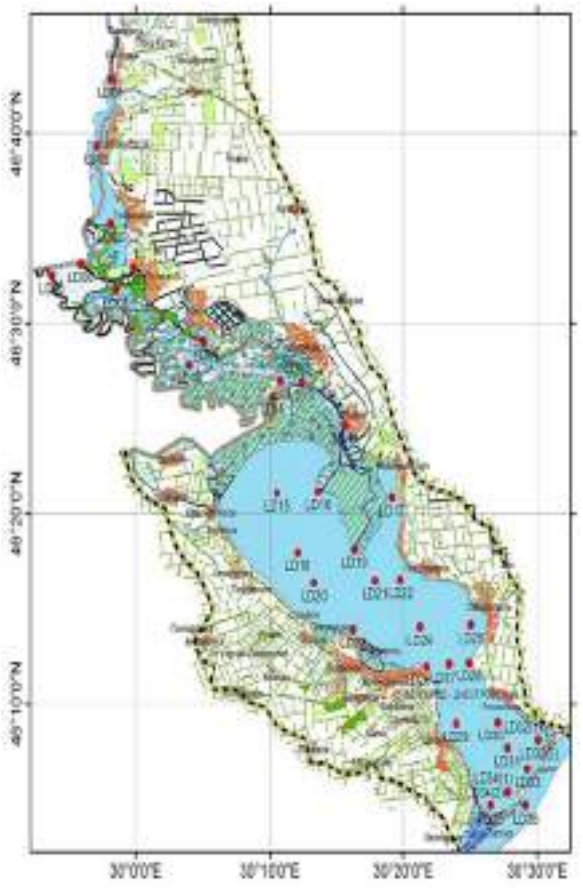

Figure 3.3. Scheme of water sampling stations for chlorophyll analysis in the water bodies of the Dniester River deltaic part in 2003-2020

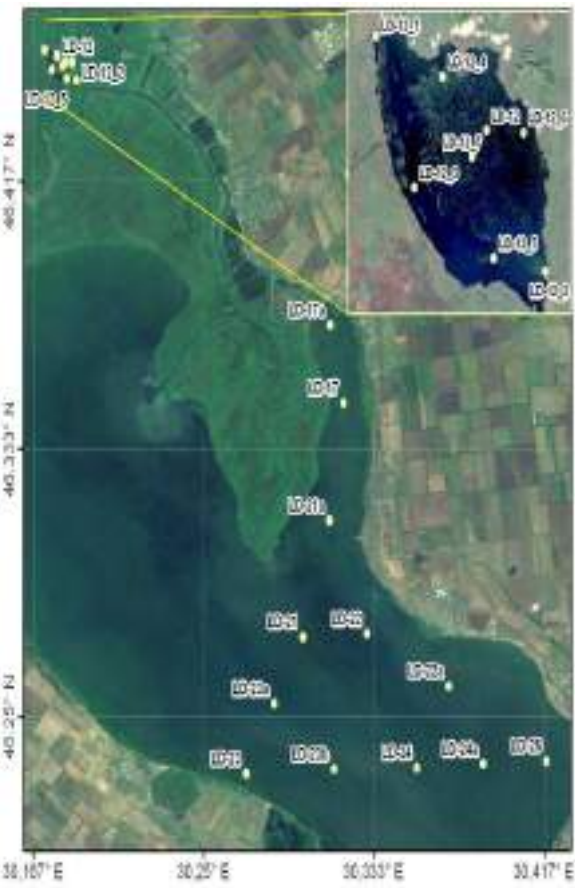

Figure 3.4. Scheme of pilot water sampling stations for chlorophyll analysis in the Bile Lake and the Dniester Estuary within the

Table 3.1. The number of samples analysed for Chl-a concentration and related parameters, as well as the number of samples used to find the empirical algorithms for the space images from Sentinel 2, Sentinel 3 and Landsat 8

Year	Number of samples analysed for Chl-a concentration and related parameters	Of these, used to calibrate the space images		
		S2	S3	L8
2016	56	0	0	5
2017	76	6	6	3
2018	78	6	9	4
2019	87	2	7	0
2020	85	6	14	8
2021	161	57	84	22
Total	543	78	120	42

Note. The parameters related to the Chl-a concentration determination in samples were as follows.

- Hydrology: depth, water transparency, temperature and conductivity;

- Hydrochemistry: - pH, dissolved oxygen, ammonium nitrogen, nitrit nitrogen, nitrate nitrogen, total nitrogen, phosphate, total phosphorus;

- Hydrobiology – number and biomass of bacterioplankton and phytoplankton.

Analysis of the information presented in the table has shown that most of the experimental (*in-situ*) determinations of chlorophyll - 78 and 120 were accordingly used for calibration of space images of Sentinel 2, 3 and Landsat 8 .

3.3 Satellite images retrieved for the Ukrainian UA2 pilot site

Space images LandSat 8, Sentinel-2 and Sentinel-3 retreived from the sites https://scihub.copernicus.eu/, https://glovis.usgs.gov/, https://earthexplorer.usgs.gov [Lansat 8, Sentinel-2, Sentinel-3] were used to build the maps of Chl *a* concentration in the surface waters of the Dniester Estuary and the Bile Lake.

Landsat 8 images have 15-meter panchromatic and 30-meter multi-spectral spatial resolutions along a 185 km orbital swath width. Landsat 8 carries two sensors: Operational Land Imager sensor (OLI) and Thermal Infrared Sensor (TIRS). The OLI measures in 9 spectral bands: visible, near infrared, and shortwave infrared portions (VNIR, NIR, and SWIR) of the spectrum. The TIRS measures land surface temperature in two thermal bands. Landsat 8 satellite orbit is a sun-synchronous, near-polar (98.2 degrees inclination); an altitude of 705 km; completes one Earth orbit every 99 minutes; has a 16-day repeat cycle.

Sentinel-2 was launched in 2015 and carried out an optical instrument - Multispectral Imager's (MSI) with 13 spectral bands: four bands at 10 m, six bands at 20 m and three bands at 60 m spatial resolution. This instrument is possible to use for the monitoring of small waterbodies with algorithms based on neural networks, like the Case-2 Regional Coast Colour (C2RCC) developed by ESA CoastColour project [Doerffer & Brockmann, 2014; CoastColour project]. The orbital swath width of Sentinel-2 is 290 km. The time coverage of Sentinel-2A and Sentinel-2B satellites is 10-15 days.

Sentinel-3 with satellite sensor OLCI (Ocean and Land Colour Instrument) was launched in February 2016 by the European Space Agency (ESA). The OLCI have 21 spectral bands at 300 m spatial resolution and based on the opto-mechanical and imaging design of Envisat's the Medium Resolution Imaging Spectrometer (MERIS) instrument. The OLCI is an excellent tool for marine environmental monitoring especially for estimating of Chl *a* concentration in turbid coastal waters by C2RCC processor. The orbital swath width of the OLCI is 1270 km. The time coverage of Sentinel-3 satellites of the same areas is 1-2 days.

3.3.1. Landsat 8

We used the LandSat 8 images with the following orbital characteristics: WRS Path=181 & WRS Row=028 and WRS Path=180 & WRS Row=028. Location of coverage of the images with these orbital characteristics is presented on Fig. 3.1-3.2.

Figure 3.1. Coverage of LandSat 8 images with orbital characteristics: WRS Path=180 & WRS Row=028 (full coverage of the PONTOS UA2 pilot area)

Figure 3.2. Coverage of LandSat 8 images with orbital characteristics: WRS Path=181 & WRS Row=028 (coverage of the northern part of the Dniester Delta including the northern and central parts of the Dniester Estuary)

Operational Land Imager (OLI) spectral bands, including a panchromatic band, comprises the following set (Table 3.1).

Table 3.1. Spectral characteristics of OLI and TIRS sensors of LandSat 8

Spatial Resolution (m)	Band Number	Band Name	Lower Wavelength (nm)	Higher Wavelength (nm)
30	1	Coastal Aerosol	433	453
30	2	Blue	450	515
30	3	Green	525	600
30	4	Red	630	680
30	5	Near-Infrared	845	885
30	6	SWIR 1	1560	1660
30	7	SWIR 2	2100	2300
30	8	Panchromatic	500	680
15	9	Cirrus	1360	1390
100	10	TIRS 1	10300	11300
100	11	TIRS 2	11500	12500

Altogether 8 LandSat 8 images were used for Chl a concentration mapping in the Dniester Estuary surface water within the framework of the PONTOS project (Table 3.2).

Table 3.2. List of the LandSat 8 for 2016-2021 used for the PONTOS UA2 pilot area

Nos.	Codes of LandSat 8 images	Sensing date	Sensing time
1	LC08_L1TP_180028_20160722_20200906_02_T1	22.07.16	11:44
2	LC08_L1TP_180028_20170725_20200903_02_T1	25.07.17	11:44
3	LC08_L1TP_181028_20180719_20200831_02_T1	19.07.18	11:49

Nos.	Codes of LandSat 8 images	Sensing date	Sensing time
4	LC08_L1TP_180028_20200717_20200911_02_T1	17.07.20	11:44
5	LC08_L1TP_181028_20210422_20210422_01_RT	22.04.21	11:50
6	LC08_L1TP_180028_20210720_20210729_02_T1	20.07.21	11:44
7	LC08_L1TP_181028_20210727_20210804_02_T1	26.07.21	11:50
8	LC08_L1TP_181028_20210929_20211012_02_T1	29.09.21	11:50

3.3.2. Sentinel-2

Sentinel-2 images with the following orbital characteristics were used: OrbitRelative=7 & Tile Number=T35TQM and OrbitRelative=107 & Tile Number=T35TQM. Coverage by the imagery with such orbital characteristics is presented on Fig. 3.3-3.4 where the PONTOS UA2 pilot area is shown.

Figure 3.3. Coverage by Sentinel-2 images with orbital characteristics: OrbitRelative=7 & Tile Number=T35TQM (full coverage of the PONTOS UA2 pilot area)

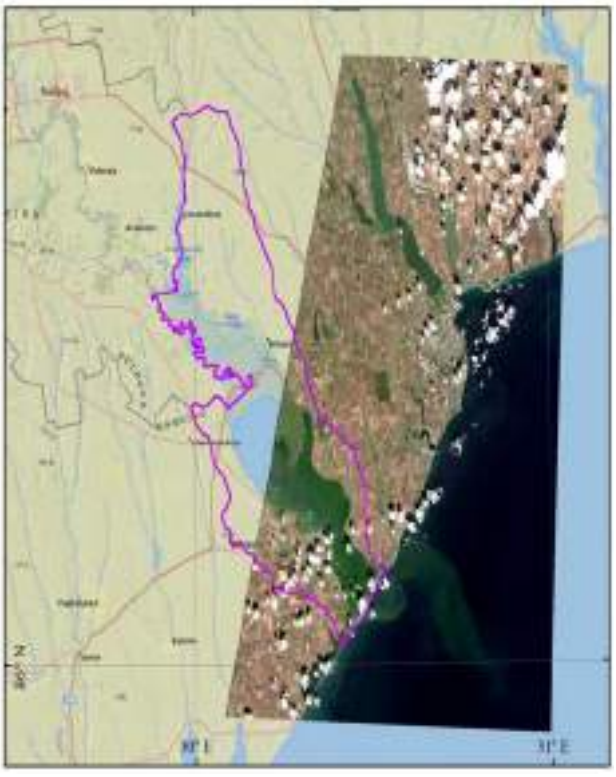

Figure 3.4. Coverage by Sentinel-2 images with orbital characteristics: OrbitRelative=107 & Tile Number=T35TQM (coverage of the Karagolska Bay, central and southern parts of the Dniester Estuary)

Sentinel-2 MultiSpectral Instrument includes 13 spectral bands: 10 m, 20 m and 60 m spatial resolution (Table 3.3).

Table 3.3. Spectral characteristics of Sentinel-2 MSI Bands

Spatial Resolution (m)	Band Number	S2A		S2B	
		Central Wavelength (nm)	Bandwidth (nm)	Central Wavelength (nm)	Bandwidth (nm)
10	2	492.4	66	492.1	66
	3	559.8	36	559.0	36
	4	664.6	31	664.9	31
	8	832.8	106	832.9	106
20	5	704.1	15	703.8	16
	6	740.5	15	739.1	15
	7	782.8	20	779.7	20
	8a	864.7	21	864.0	22
	11	1613.7	91	1610.4	94
	12	2202.4	175	2185.7	185
60	1	442.7	21	442.2	21
	9	945.1	20	943.2	21
	10	1373.5	31	1376.9	30

The Sentinel-2 was developed by an industrial consortium led by Astrium GmbH (Germany). Astrium SAS (France) is responsible for the [Sentinel-2]. The MSI works passively, by collecting sunlight reflected from the Earth. The incoming light beam is split at a filter and focused onto two separate focal plane assemblies within the instrument; one for Visible and Near-Infra-Red (VNIR) bands and one for Short Wave Infra-Red (SWIR) bands. Altogether 17 Sentinel-2 images were used within the framework of the PONTOS project to analyse Chl concentration in the Dniester Estuary water (Table 3.4).

Table 3.4. List of Sentinel-2 images for 2016-2021used for the PONTOS UA2 pilot area

Nos.	Codes of Sentinel-2 images	Sensing date	Sensing time
1	S2B_MSIL1C_20170717T090019_N0205_R007_T35TQM	17.07.17	12:00
2	S2A_MSIL1C_20180714T084601_N0206_R107_T35TQM	14.07.18	11:46
3	S2A_MSIL1C_20180717T085601_N0206_R007_T35TQM	17.07.18	11:56
4	S2A_MSIL1C_20190712T085601_N0208_R007_T35TQM	12.07.19	11:56
5	S2B_MSIL1C_20190717T085609_N0208_R007_T35TQM	17.07.19	11:56
6	S2A_MSIL1C_20200716T085601_N0209_R007_T35TQM	16.07.20	11:56
7	S2B_MSIL1C_20200718T084559_N0209_R107_T35TQM	18.07.20	11:45
8	S2A_MSIL1C_20210422T085551_N0300_R007_T35TQM	22.04.21	11:55
9	S2B_MSIL1C_20210424T084559_N0300_R107_T35TQM	24.04.21	11:45
10	S2A_MSIL1C_20210611T085601_N0300_R007_T35TQM	11.06.21	11:56
11	S2B_MSIL1C_20210716T085559_N0301_R007_T35TQM	16.07.21	11:56
12	S2A_MSIL1C_20210718T084601_N0301_R107_T35TQM	18.07.21	11:46
13	S2B_MSIL1C_20210726T085559_N0301_R007_T35TQM	20.07.21	11:56
14	S2A_MSIL1C_20210820T085601_N0301_R007_T35TQM	20.08.21	11:56
15	S2A_MSIL1C_20210909T085601_N0301_R007_T35TQM	09.09.21	11:56
16	S2A_MSIL1C_20210929T085751_N0301_R007_T35TQM	29.09.21	11:56
17	S2B_MSIL1C_20211004T085729_N0301_R007_T35TQM	04.10.21	11:56

3.3.3. Sentinel-3

Sentinel-3 images with a set of different orbital characteristics were used: Duration, Cycle number and Relative orbit number (see Table 3.5). Their coverage is presented on Fig. 3.5 where PONTOS UA2 pilot area is marked.

Figure 3.5. Coverage of 19 Sentinel-3 images with localisation of the PONTOS UA2 pilot area

The OLCI instrument was developed to provide continuity with measurements made by MERIS instrument. OLCI is a visible imaging push-broom radiometer with more spectral bands, improved signal-to-noise ratio, among other improvements, compared to MERIS. The OLCI has 21 spectral bands from 400 to 1200 nm (Table 3.5).

Table 3.5. Spectral characteristics of Sentinel-3 Ocean and Land Colour Instrument (OLCI)

Spatial Resolution (m)	Band Number	Band Name	Band centre λ (nm)	Band Width (nm)
300	1	Oa1	400.00	15
300	2	Oa2	412.50	10
300	3	Oa3	442.50	10
300	4	Oa4	442.00	10
300	5	Oa5	510.00	10
300	6	Oa6	560.00	10
300	7	Oa7	620.00	10
300	8	Oa8	665.00	10
300	9	Oa9	673.75	7,5
300	10	Oa10	681.25	7,5
300	11	Oa11	708.75	10
300	12	Oa12	753.75	7,5
300	13	Oa13	761.25	2,5
300	14	Oa14	764.38	3,75
300	15	Oa15	767.50	2,5
300	16	Oa16	778.75	15
300	17	Oa17	865.00	20
300	18	Oa18	885.00	10
300	19	Oa19	900.00	10
300	20	Oa20	940.00	20
300	21	Oa21	1020.00	40

The OLCI swath is not centered at nadir which minimizes the occurrence of sun glint. Altogether 19 Sentinel-3 images were used within the framework of the PONTOS project to analyse Chl concentration in the Dniester Estuary water (Table 3.6).

Table 3.6. List of Sentinel-3 images for 2017-2021 used for the PONTOS UA2 pilot area

Nos.	Codes of Sentinel-3 images (the last three numbers: Duration, Cycle number and Relative orbit number)	Sensing date	Sensing time
1	S3A_OL_1_EFR_20170717T080927_0179_020_078	17.07.2017	11:09
2	S3B_OL_1_EFR_20180714T082403_0179_010_235	14.07.2018	11:24
3	S3B_OL_1_EFR_20180717T084630_0179_010_278	17.07.2018	11:46
4	S3A_OL_1_EFR_20190712T081324_0179_047_021	12.07.2019	11:13
5	S3B_OL_1_EFR_20190717T084453_0180_027_335	17.07.2019	11:44
6	S3A_OL_1_EFR_20200716T082056_0179_060_292	16.07.2020	11:20
7	S3B_OL_1_EFR_20200718T083007_0179_041_178	18.07.2020	11:30
8	S3A_OL_1_EFR_20210101T083935_0179_067_007	01.01.2021	11:39
9	S3A_OL_1_EFR_20210209T082826_0179_068_178	09.02.2021	11:28
10	S3B_OL_1_EFR_20210307T081509_0179_050_021	07.03.2021	11:15
11	S3A_OL_1_EFR_20210424T080947_0180_071_078	24.04.2021	11:09
12	S3B_OL_1_EFR_20210515T082625_0179_052_235	15.05.2021	11:26
13	S3B_OL_1_EFR_20210611T082630_0179_053_235	11.06.2021	11:26
14	S3A_OL_1_EFR_20210718T080604_0179_074_135	18.07.2021	11:06
15	S3B_OL_1_EFR_20210820T081136_0179_056_078	20.08.2021	11:20
16	S3A_OL_1_EFR_20210929T081331_0180_077_021	29.09.2021	11:13
17	S3B_OL_1_EFR_20211021T080400_0179_058_192	21.10.2021	11:04
18	S3B_OL_1_EFR_20211121T080019_0179_059_249	21.11.2021	11:00
19	S3B_OL_1_EFR_20211202T081516_0179_060_021	02.12.2021	11:15

3.4. Description of eutrophication analysis methodology using of satellite images

3.4.1. Satellite image selection requirements

Having mastered the methodology of space images processing with the SNAP-C2RCC algorithm and based on practical work and studies of the available from the literature examples of space images use to determine the concentration of chlorophyll in water bodies, we formulated the following requirements for selection of satellite images, which made it possible to assess the representativeness of the chlorophyll concentrations received using the *in situ* data:

- space image resolution should be high enough to identify the field of reliable chlorophyll concentrations all over the area of a studied water body or, in special cases, a part of the water body, where the *in situ* chlorophyll measurements have been performed,

- absence of clouds or haze in the studied area,

- time difference between sampling and a satellite pass over the sampling area should stay within ±2.5-3.0 hours,

- the frequency of satellite passes over the studied areas should be at least twice a month.

Based on the above requirements and in accordance with the recommendations from our Greek partners, Sentinel-2, Landsat 8 and Sentinel-3 images were used fro the further work. At that, for the small water bodies (e.g. the Bile Lake) the Sentinel-2 and Landsat 8 images with resolution 10 and 30 m respectively were used, while for the big water bodies (e.g. the Dniester Estuary) we also used the Sentinel-3 images with resolution 300 m.

3.4.2. Satellite Data Processing and Chlorophyll-a concentration calculation Algorithms

The basis for the chlorophyll concentration in water calculation from satellite images in the automatic mode of the SNAP platform of the ESA's Sentinel Applications Platform (SNAP) [https://sentinels.copernicus.eu/web/sentinel/-/esa-releases-new-and-improved-version-of-snap/1.2] using the C2RCC processor built in as a tool to work with different types of snapshots. The C2RCC processor makes it possible to calculate chlorophyll concentrations and other characteristics of the aquatic environment of both marine and freshwater bodies with complex optical characteristics.

SNAP has been accelerating Earth observation innovation since 2014 by helping the growing global community of data users to process and analyse imagery from numerous international missions. The platform provides access to imagery from Sentinel-1, Sentinel-2 and Sentinel-3 of the European Union's Copernicus Programme, as well as ESA Earth Explorer missions, such as SMOS. SNAP includes an easy-to-use graphical interface and can also be operated from the command line. As a result, it is accessible to people with little experience of coding and programming, as well as experts in data analysis. These features support a wide variety of analysis and processing activities, facilitating scientific research, education and training, and the development of innovative applications across society. The tool's popularity has continued to expand since it was created eight years ago, reflecting the increasing demand for open-access Earth observation data and processing tools.

During the last years, many researchers [Ansper, Alikas, 2018, Voronova, 2020] pointed out that the SNAP – C2RCC calculations for the shallow water bodies and estuaries result at significant mistakes in chlorophyll determination, which often requires empirical algorithms development that can take into account the optical peculiarities of aquatic environment of rivers, lakes and reservoirs. The examples of such empirical algorithms are desctibed in the works [O'Reilly J. E. et al. 1998; Dall'Olmo, G., & Gitelson A., 2005; Gitelson A. et al., 2007; Gitelson A. et al. 2011; Kopelevich O.V. et al., 2015; Tikhomirov O.A. et al. 2016; Watanabe F. et al. 2018].

3.4.2.1. Algorithm of chlorophyll extraction from satellite images using the Sentinel Application Platform (SNAP)

To calculate the values of chlorophyll concentration in the water bodies of the UA2 pilot area (the Dniester Estuary and the Bile Lake) we used at the first stage the algorithm of Chlorophyll extraction from satellite images Sentinel-2, Landsat 8 and Sentinel-3 using the Sentinel Application Platform (SNAP), which was based on the C2RCC (Case 2 Regional CoastColour) processor that helps to calculate the Chl-a concentration in the surface layer of water bodies (Fig. 3.5). The processor operation is based on the use of neural network algorithms (C2RCC and C2X) for calculating the five main bio-optical components of light absorption and scattering by particles in the aquatic environment: absorption by detritus, yellow matter and phytoplankton pigments; scattering by "white particles" and "typical sediment" (Brockmann et al., 2016). At that, salinity and temperature were set as the input parameters for the aquatic environment, and pressure and ozone content - for the atmosphere.

The Inherent Optical Properties (IOP) are used in the SNAP to calculate the of chlorophyll *a* (Chl) and total suspended matter (TSM) concentration. The Inherent Optical Properties (absorption and scattering of the particles in-water) are calculated based on the following. Mean phytoplankton absorption spectrum was derived from the NOMAD data set (NOMAD, 2008). For this purpose, pigment absorption was calculated as the difference apig = ap – ad, where ap is the absorption by particles, and ad - by detritus. All absorptions were normalized to the absorption at 443 nm.

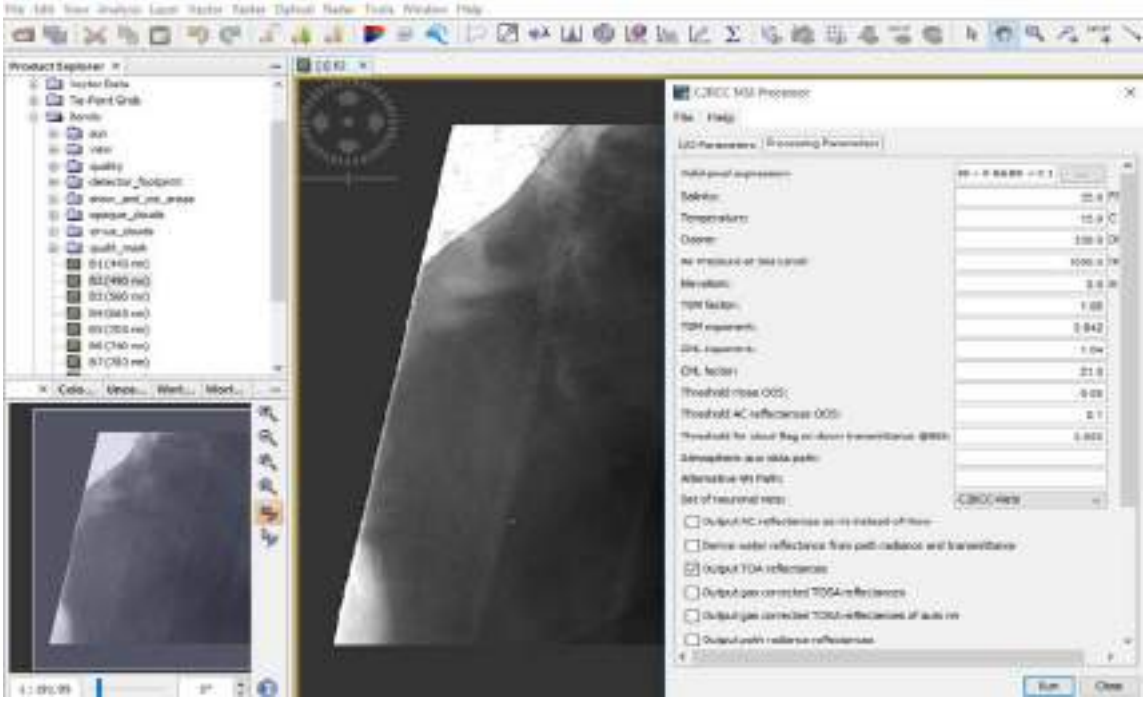

Figure 3.5. Processor MSI C2RCC of SNAP interface

The SNAP contains equations to convert from IOPs to chlorophyll *a* and TSM concentrations:

$Chl = 21.0 * a\_pig(443)^{1.04}$; $TSM = 1.06 * (bp+bw)^{0.942}$.

The factors and exponents of these equations were derived based on the NOMAD database that contains large quantity of marine date. For shallow marine and fresh water the *in situ* data from the studied area should be used; this helps to develop the equations, which ensure the required quality of calculation. Lack of the *in situ* data and use of the standard NOMAD database on marine areas bring down the quality of chlorophyll concentration calculations for freshwater bodies using the SNAP.

To determine the level of reliability of the Chl concentration calculation using SNAP-C2RCC algorithm and the in situ data we processed the Sentinel-2 space images for the Bile Lake and the Dniester Estuary areas. The results are presented in Fig. 3.8-3.12 and 3.13-3.24 respectively.

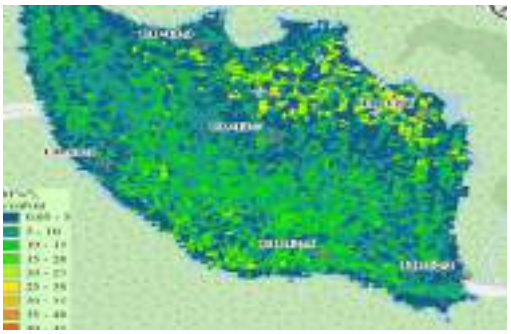

Fig. 3.8. 22 April 2021 (The image S2A_MSIL1C_20210422T085551_N0300_R007)

Fig.3.9. 11 June 2021 (The image S2A_MSIL1C_20210611T085601_N0300_R007)

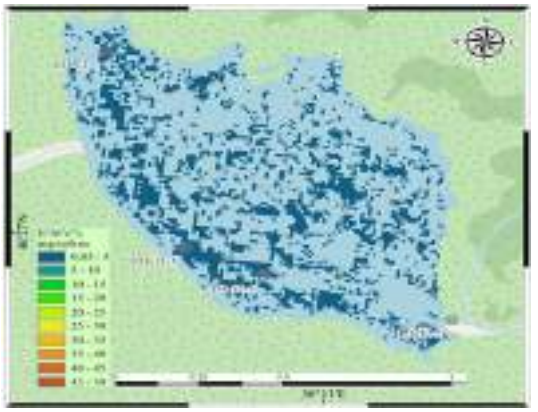

Fig 3.10. 26 July 2021 (The image S2B_MSIL1C_20210726T085559_N0301_R007)

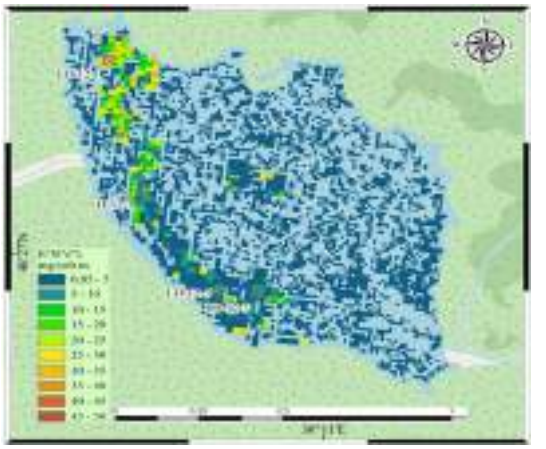

Fig.3.11. 09 September 202) (The image S2A_MSIL1C_20210909T085601_N0301_R007)

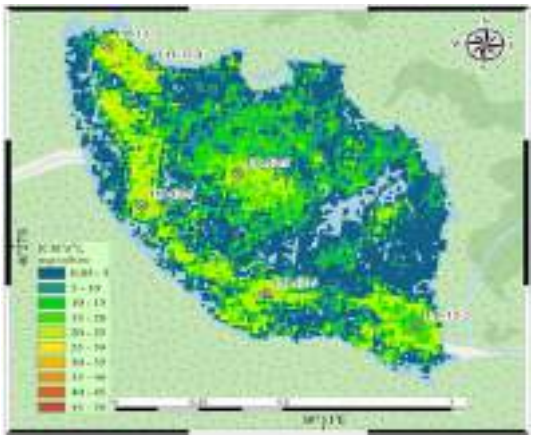

Fig.3.12. 04 October 2021 (The image S2B_MSIL1C_20211004T085729_N0301_R007)

Figure 3.8-3.12. Evolution of Chl-a concentration by SNAP S2 calculation in the Bile Lake in 2021

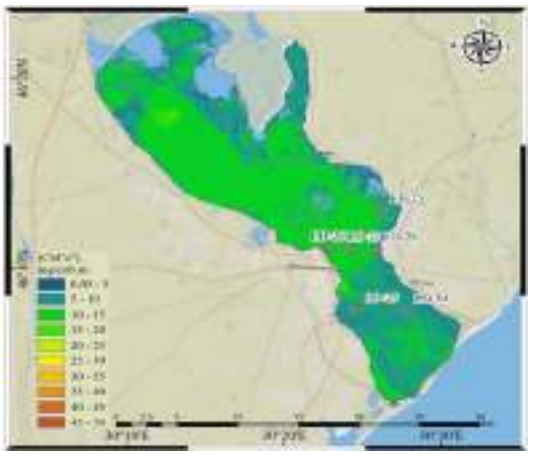

Fig. 3.13. 17 July 2017 (The image S2B_MSIL1C_20170717T090019_N0205_R007)

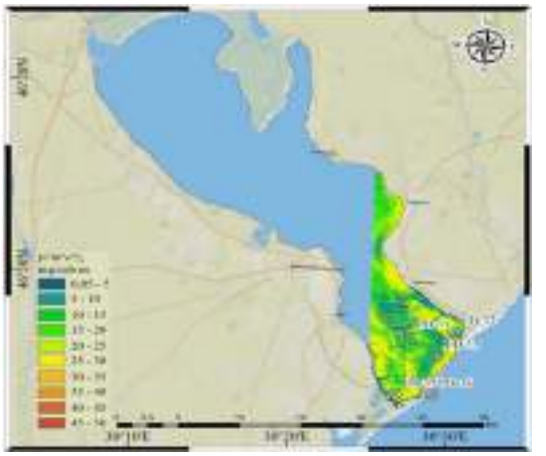

Fig. 3.14. 14 July 2018 (The image S2A_MSIL1C_20180714T084601_N0206_R107)

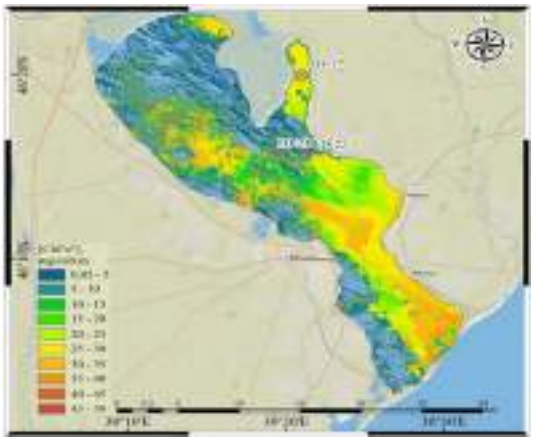

Fig.3.15. 17 July 2018 (The image S2A_MSIL1C_20180717T085601_N0206_R007)

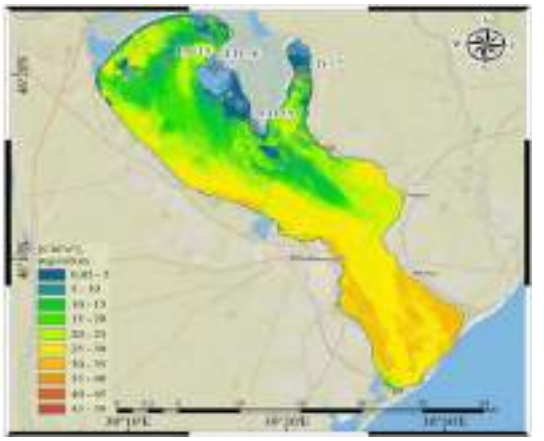

Fig. 3.16. 12 July 2019 (The image S2A_MSIL1C_20190712T085601_N0208_R007)

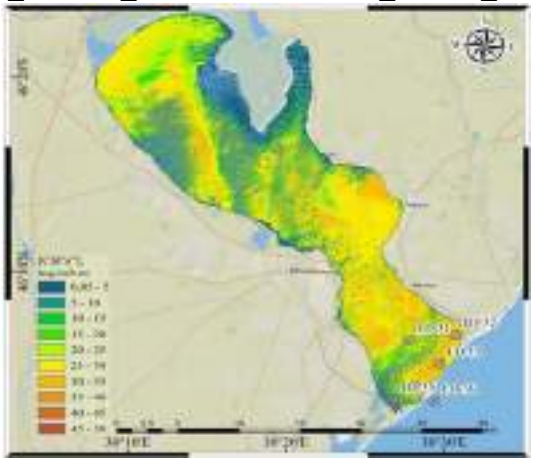

Fig.3.17. 16 July 2020 (The image S2A_MSIL1C_20200716T085601_N0209_R007)

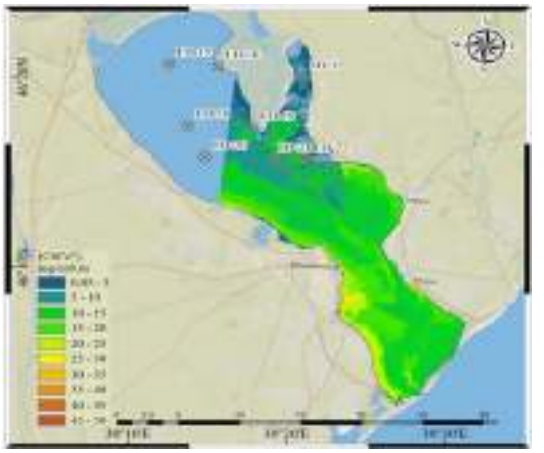

Fig. 3.18. 18 July 2020 (The image S2B_MSIL1C_20200718T084559_N0209_R107)

Figure 3.13-3.18. Evolution of Chl-a concentration (SNAP S2 calculation) in Dniester estuary in 2017-2020

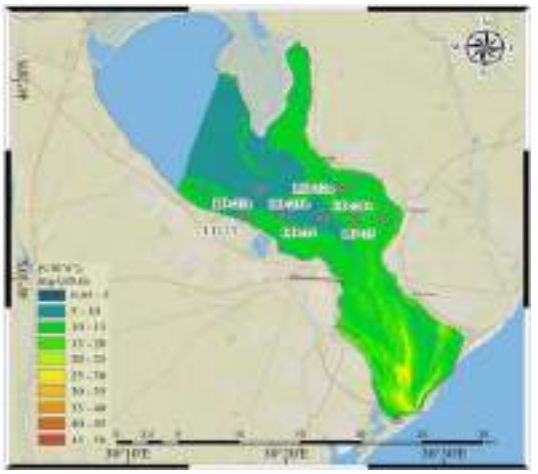

Fig. 3.19. 24 April 2021 (The image S2B_MSIL1C_20210424T084559_N0300_R107)

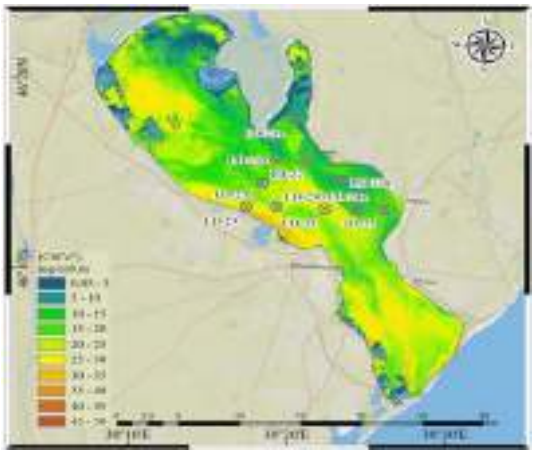

Fig. 3.20. 11 June 2021 (The image S2A_MSIL1C_20210611T085601_N0300_R007)

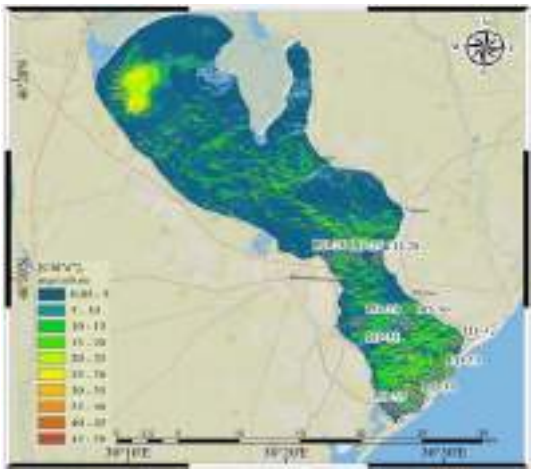

Fig.3.21. 16 July 2021 (The image S2B_MSIL1C_20210716T085559_N0301_R007)

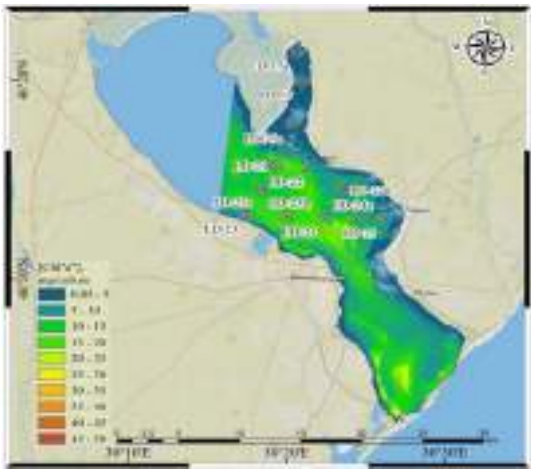

Fig.3.22. 18 July 2021 (The image S2A_MSIL1C_20210718T084601_N0301_R107)

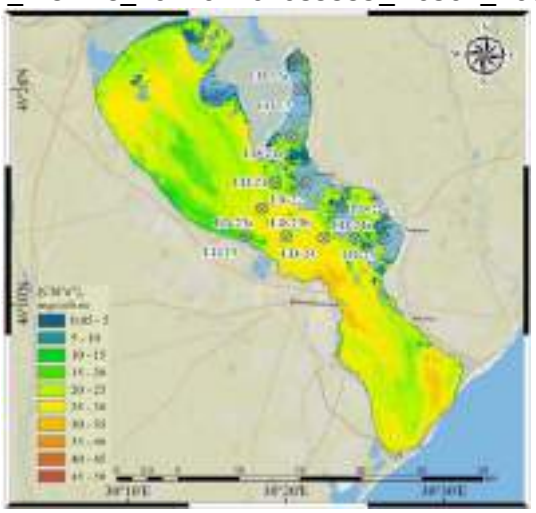

Fig.3.23. 20 August 2021 (The image S2A_MSIL1C_20210820T085601_N0301_R007)

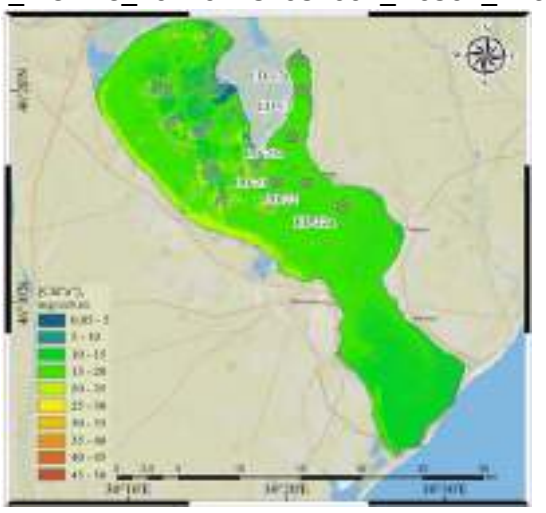

Fig.3.24. 29 September 2021 (The image S2A_MSIL1C_20210929T085751_N0301_R007)

Figure 3.19-3.24. Evolution of Chl-a concentration (SNAP S2 calculation) in the Dniester Estuary in 2021

Comparison of our experimental data on chlorophyll content in the Bile Lake and the Dniester Estuary surface water with those calculated by the above SNAP-C2RCC algorithm (Table 3.7) using Sentinel-2 satellite images showed that for both the lake and the estuary the real coefficients of determination between the series of satellite and *in situ* data were at the levels characterized as insignificant, which allows us to conclude that it is impossible to use data obtained from the satellite images using the SNAP-C2RCC algorithm for the Sentinel-2 satellite in our further practical work.

Based on these results it was recommended to consider other empirical algorithms of images processing and chlorophyll concentration calculation where the data on the Top of Atmosphere radiance (ToA) intensity or Bottom of Atmosphere (BoA) radiation intensity can be used as arguments.

Table 3.7. Statistical characteristics of comparison between the *in situ* and calculated data on Chl concentration from the Sentinel-2 images using the data selection where all the questionable results were discarded

Pilot water body	Number of determinations	Real coefficient of determination	Real coefficient of correlation	Pearson's significance level (p=0.05)	Strength of correlation
Bile Lake	9 (28)	0.55 (0.09)	0.74 (0.30)	0,67 (0.38)	High (insignificant)
Dniester Estuary	46 (78)	0.03(002)	0.17 (0.14)	0.30 (0.23)	Insignificant

Note: In brackets are the data on the whole selection.

To determine the level of reliability of the results of chlorophyll concentrations calculation using the SNAP-C2RCC algorithm we also processed Landsat 8 satellite images for the Bile Lake and the Dniester Estuary. The results are shown in Fig. 3.25-3.27 and 3.28-3.30 respectively.

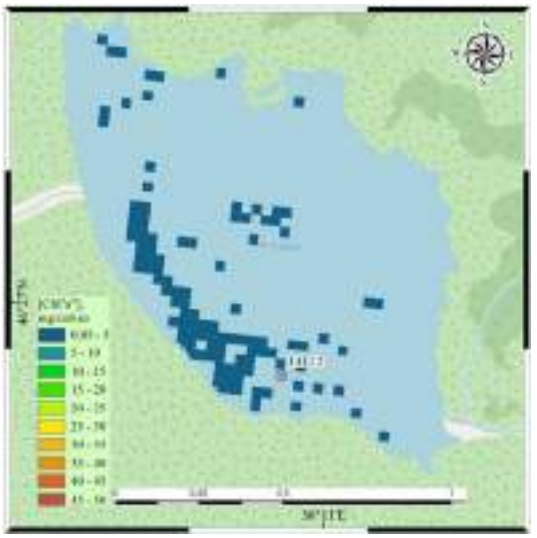

Fig. 3.25. 19 July 2018 (The image LC08_L1TP_181028_20180719)

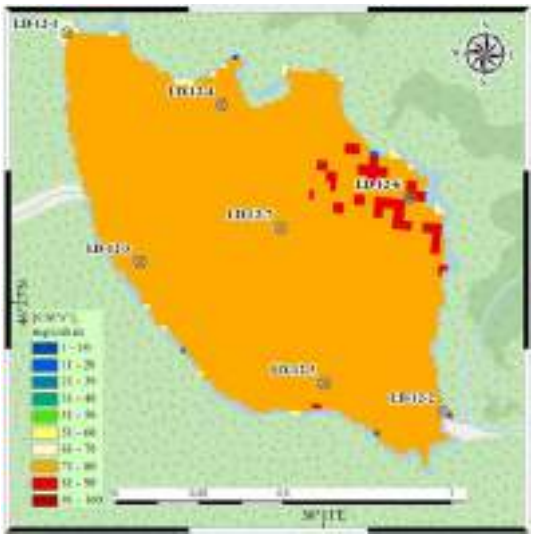

Fig. 3.26. 22 April 2021 (The image LC08_L1TP_181028_20210422)

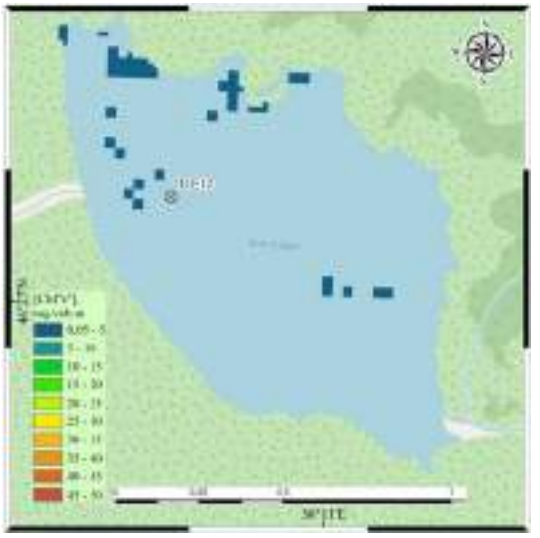

Fi. 3.27. 20 July 2021 (The image LC08_L1TP_180028_20210720)

Figure 3.25-3.27. Evolution of Chl-a concentration by SNAP LandSat 8 calculation in Bile lake in 2021

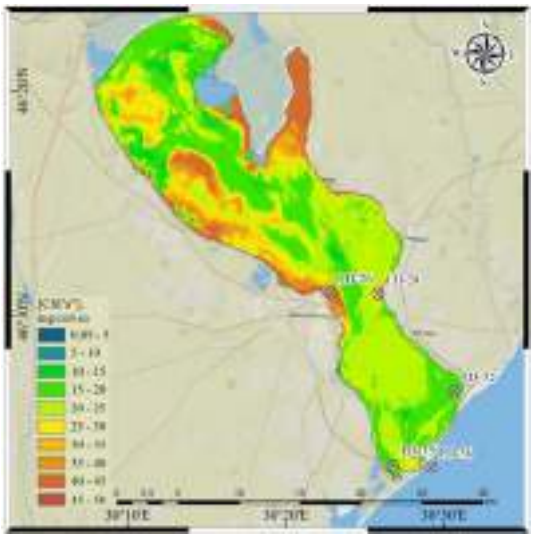

Fig. 3.28. 22 July 2016 (The image LC81800282016204LGN00)

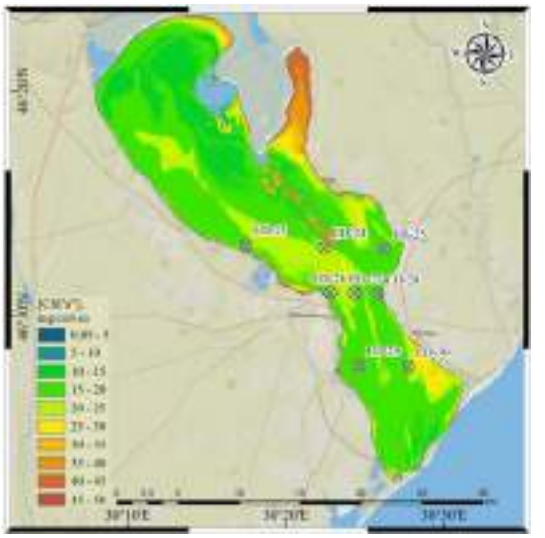

Fig. 3.29. 17 July 2020 (The image LC08_L1TP_180028_20200717)

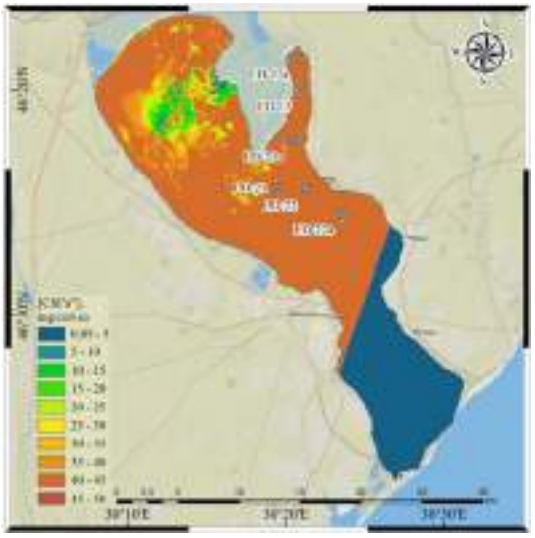

Fig. 3.30. 29 September 2021 (The image LC08_L1TP_181028_20210929)

Figure 3.28-3.30. Evolution of Chl-a concentration (SNAP S2 calculation) in the Dniester Estuary in 2017-2020

Comparison of our experimental data on the chlorophyll content in the surface waters of the Bile Lake and the Dniester Estuary with those calculated using the above SNAP-C2RCC algorithm (Table 3.8) from the Landsat 8 images showed that the real coefficient of determination between the series of satellite and experimental data was at an insignificant level for the Bile Lake, while for the Dniester Estuary the significant coefficient of determination was more than 0.8 and the possible correlation relationship was characterized as high.

Table 3.8. Statistical characteristics of comparison between the *in situ* and calculated data on Chl concentration from the Landsat 8 images using the data selection where all the questionable results were discarded

Pilot water body	Number of determinations	Real coefficient of determination	Real coefficient of correlation	Pearson's significance level (p=0.05)	Strength of correlation
Bile Lake	9 (9)	0.40 (0.40)	0.63 (0.63)	0.67 (0.67)	Insignificant
Dniester Estuary	21 (43)	0.65 (0.0003)	0.81 (0.02)	0.43 (0.30)	High

Note: In brackets are the data on the whole selection.

Based on these results we have made the conclusion that the calculated data of the SNAP-C2RCC algorithm for Landsat-8 images can be used in our further work with mandatory correction after the results of search for the most effective empirical algorithm, where the SNAP-C2RCC data can be used as an argument. At that, it was recommended to consider other empirical algorithms where the data on the Top of Atmosphere radiance (ToA) intensity or Bottom of Atmosphere (BoA) radiation intensity can be used as arguments too.

To determine a level of reliability of the Chl concentration calculation using the SNAP-C2RCC algorithm we processed the Sentinel-3 images for the Dniester Estuary only. The results are presented in Fig. 3.31-3.46.

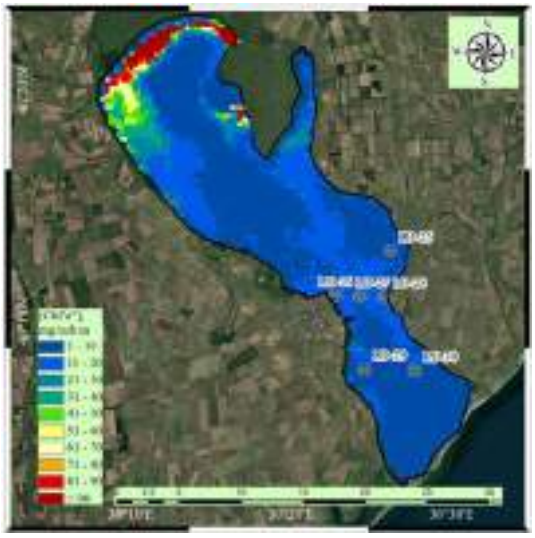

17 July 2017 (The image S3A_OL_1_EFR_20170717T080927)

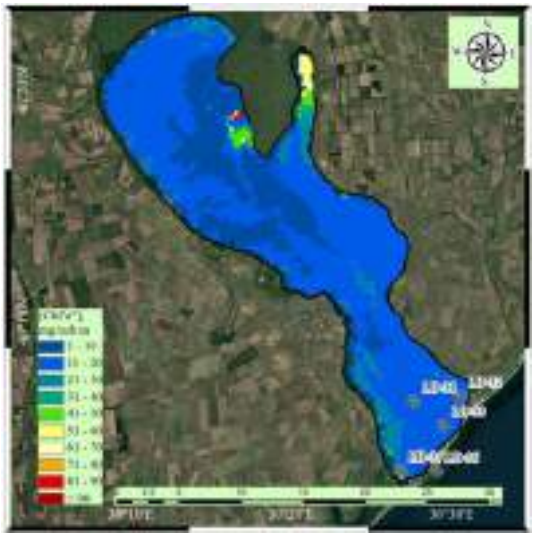

14 July 2018 (The image S3B_OL_1_EFR_20180714T082403)

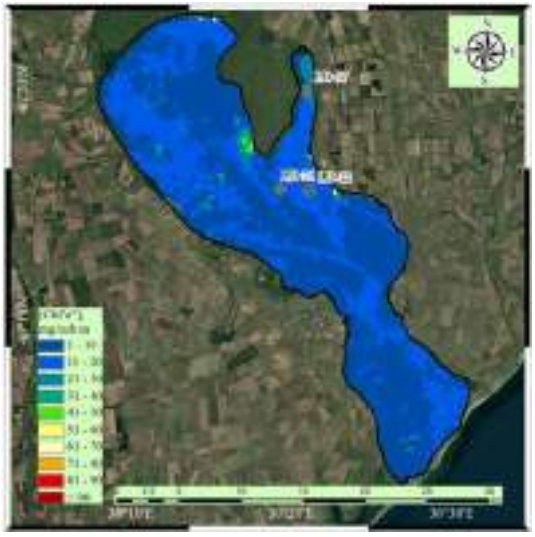

17 July 2018 (The image S3B_OL_1_EFR_20180717T084630)

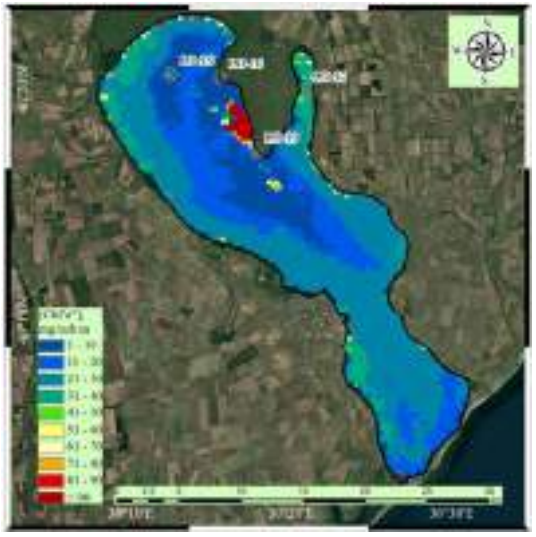

12 July 2019 (The image S3A_OL_1_EFR_20190712T081324)

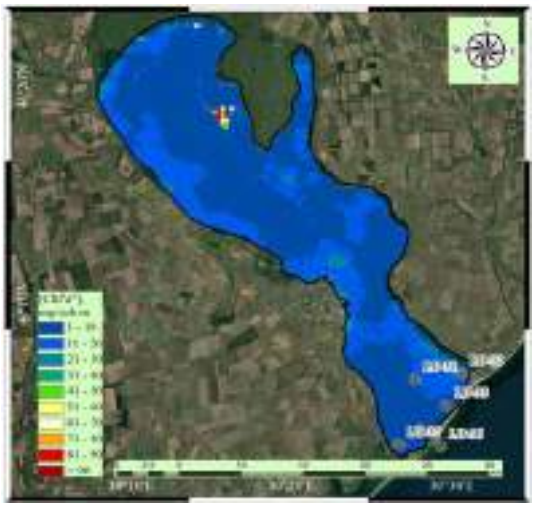

16 July 2020 (The image S3A_OL_1_EFR_20200716T082056)

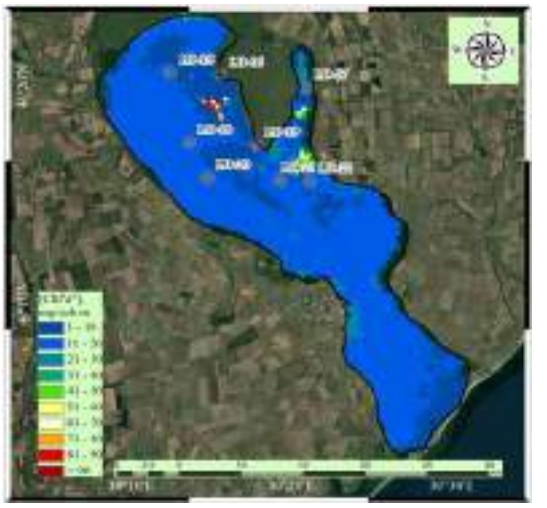

18 July 2020 (The image S3B_OL_1_EFR_20200718T083007)

Figure 3.31-3.36. Evolution of Chl-a concentration (SNAP S3 calculation) in the Dniester Estuary in 2017-2020

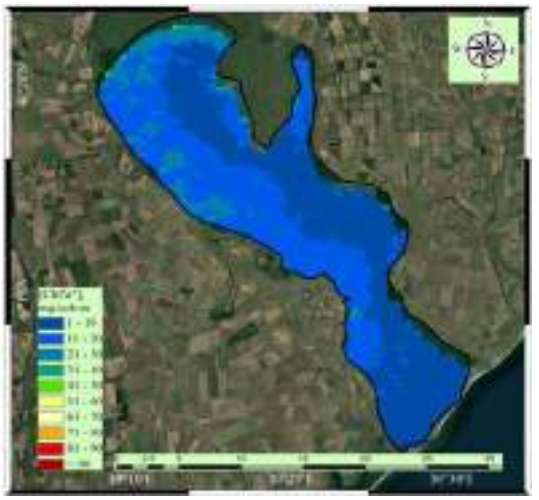

07 March 2021 (The image S3B_OL_1_EFR_20210307T081509)

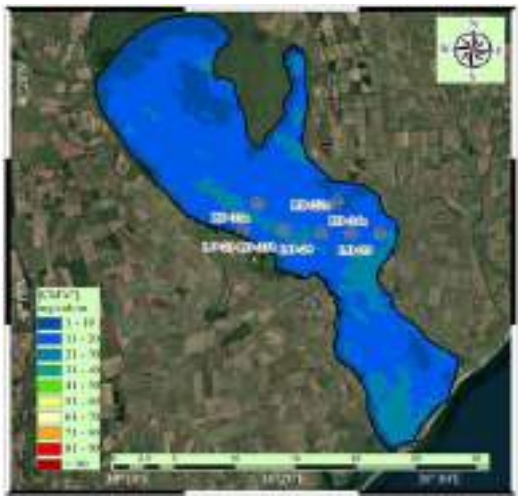

24 April 2021 (The image S3A_OL_1_EFR_20210424T080947)

15 May 2021 (The image S3B_OL_1_EFR_20210515T082625)

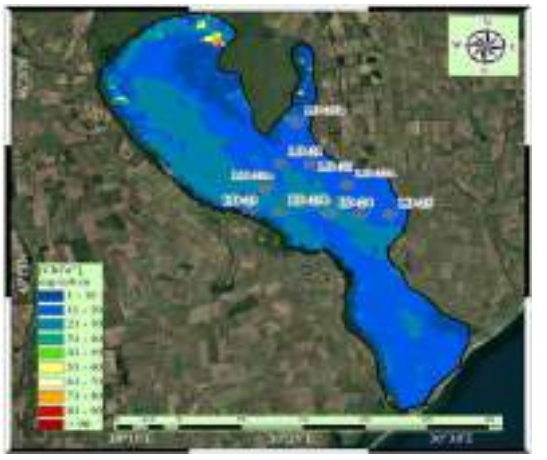

11 June 2021 (The image S3B_OL_1_EFR_20210611T082630)

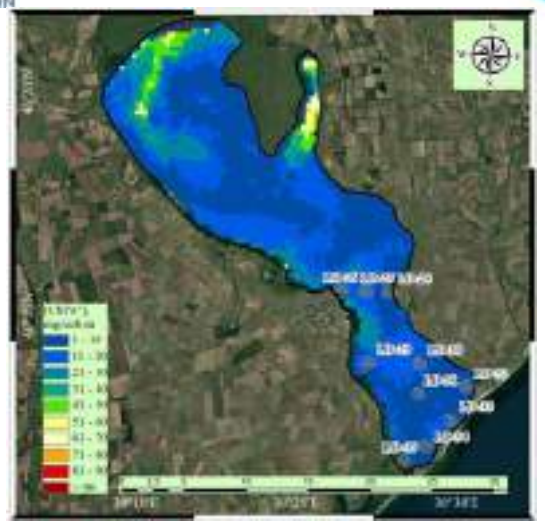

16 July 2021 (The image S3B_OL_1_EFR_20210716T081903)

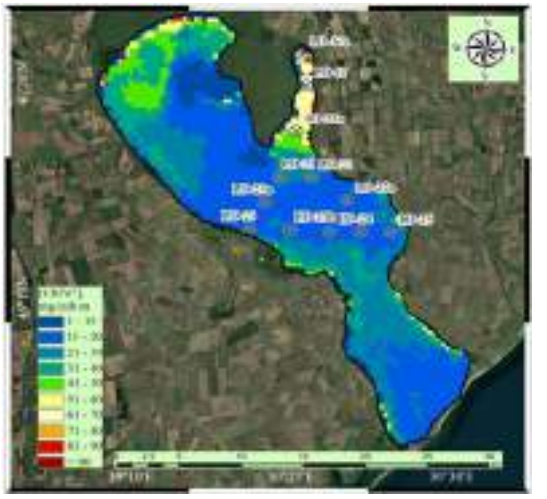

18 July 2021 (The image S3A_OL_1_EFR_20210718T080604)

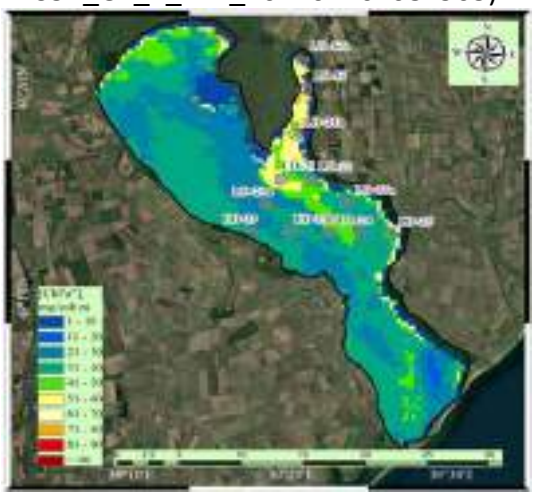

20 August 2021 (The image S3B_OL_1_EFR_20210820T081136)

29 September 2021 (The image S3A_OL_1_EFR_20210929T081331)

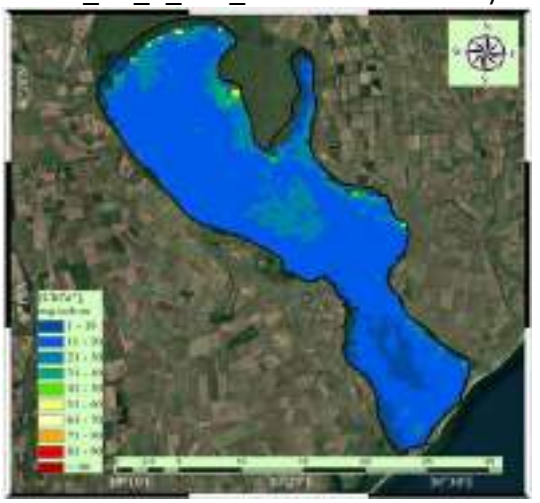

21 October 2021 (The image S3B_OL_1_EFR_20211021T080400)

21 November 2021 (The image S3B_OL_1_EFR_20211121T080019)

Figure 3.37-3.46. Evolution of Chl-a concentration (SNAP S3 calculation) in the Dniester Estuary in 2021

Comparison of our *in situ* Chl concentration measurement in the surface water of the Dniester Estuary only with the calculated SNAP-C2RCC algorithm (Table 3.9) from the Landsat 8 images has shown that the significant coefficient of determination for the Dniester Estuary was under 0.5 and characterised the possible correlative relationship as medium.

Table 3.9. Statistical characteristics of comparison between the *in situ* and calculated data on Chl concentration from the Sentinel-3 images using the data selection where all the questionable results were discarded

Pilot water body	Number of determinations	Real coefficient of determination	Real coefficient of correlation	Pearson's significance level (p=0.05)	Strength of correlation
Dniester Estuary	70 (150)	0.47(0.38)	0.69 (0.62)	0.23 (0.16)	Medium (Medium)

Note: In brackets are the data on the whole selection.

Based on this result it was recommended not to use the calculated results of the SNAP-C2RCC algorithm for Chl concentration in the Dniester Estuary surface water from the Sentinel 3 images in our further work and to concentrate at finding an effective empirical algorithm where where the data on the Top of Atmosphere radiance (ToA) intensity or Bottom of Atmosphere (BoA) radiation intensity can be used as arguments.

Thus, we can conclude that the direct SNAP-C2RCC determinations cannot be used for space images from all three satellites. It is recommended to test other empirical algorithms for calculating chlorophyll concentrations, which we consider in the next section.

3.4.2.2. Improvement of chlorophyll concentrations calculation procedures and algorithms

After the non-satisfactory result of the SNAP-C2RCC algorithm testing (Chapter 3.4.2.1) we were looking for the most effective algorithms of chlorophyll concentrations calculation to use it further on for the pilot objects – the Bile Lake and the Dniester Estuary. For this purpose we used the results of studies performed by such authors as [O'Reilly J. E. et al. 1998; Dall'Olmo, G., & Gitelson A., 2005; Kneubühler, M. et al, 2005; Gitelson A. et al., 2007; Gilerson, A et al, 2010; Gitelson A. et al. 2011; Kopelevich O.V. et al., 2015; Brockmann C. et al, 2016; Tikhomirov O.A. et al. 2016; Ogashawara I. et al, 2017; Mishra D. R., Gitelson A. A., 2017; Watanabe F. et al., 2018; Ansper A. and Alikas K., 2019; Cairo C. et al, 2020; Wang G. & Moisan

J., 2021], who were looking for empirical algorithms on the ToA and BoA radiances values that take into account the level of optical and infrared regions of the spectrum absorption by chlorophyll (Fig. 3.47).

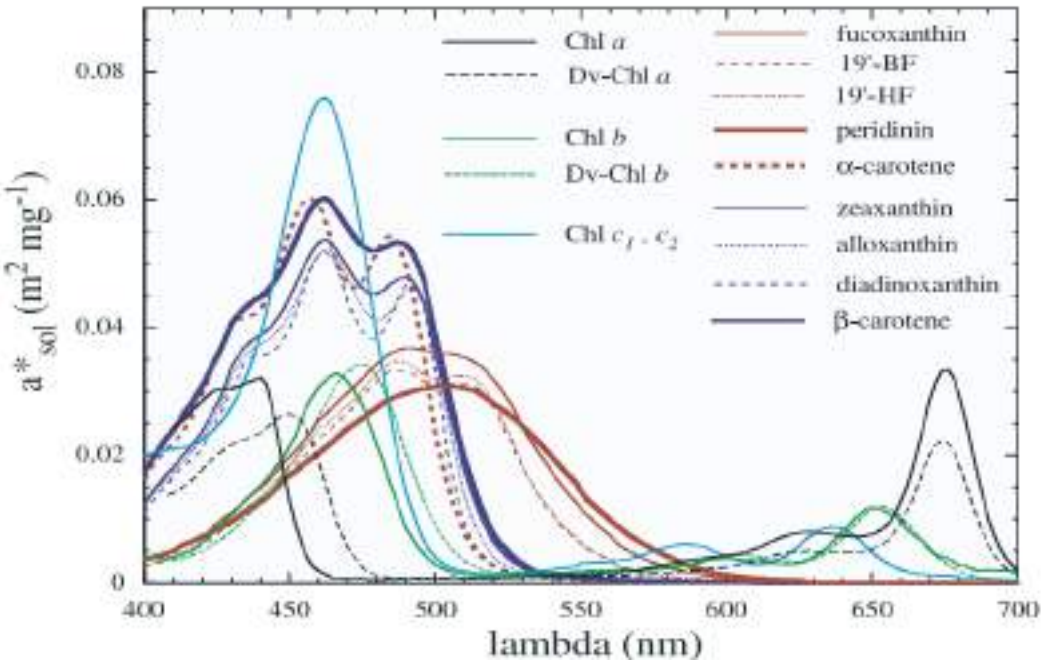

Figure 3.47. Assumed in vivo weight-specific absorption spectra of the main pigments, as derived from absorption spectra of individual pigments in solvent (Bricaud et al., 2004)

Three main features of chl-a are important for the concentration estimation using spectral reflectance (Gitelson A. et al., 2011). First, chl-a has a strong absorption band around 670 nm, forming a trough in the reflectance spectrum. The magnitude of reflectance around 670 nm (R670) is related to chl-a concentration, but chl-a absorption is often not the sole factor controlling R670, and it alone cannot be used for a reliable estimation of chl-a concentration. A peak due to solar-induced chl-a fluorescence near 685 nm is the second significant spectral feature in the red region. However, the accuracy of this approach is limited by the varying fluorescence efficiencies of different phytoplankton populations and changes in water absorption and the use of chl-a fluorescence at 685 nm seems to be useful and effective for the estimation only of low and stabile chl-a concentrations. The third reflectance feature specific to chl-a is a peak in the Near Infrared (NIR) reflectance spectrum area (400-2500nm) with values around 700 nm. The magnitude of the peak, as well as its position, depends on the chl-a concentration but is also affected by absorption and scattering by other constituents.

In the process of obtaining chlorophyll a (Chl-a) concentrations the most effort has focused on empirical algorithms, not only because of the simplicity, but also the effectiveness. The empirical methods or algorithms estimate pigments from satellite derived remote sensing reflectance (Rrs(λ)) through regression of pigment concentrations against band ratios or band differences (Wang & Moisan, 2021). These methods account for regional variabilities in water properties and Rrs(λ) input errors through tuning of the empirical coefficients. The spectrally dependent errors to a large extent could be compensated through the band ratio or band difference used in empirical approaches.

For remote sensing of accessory pigments Pan et al. (Pan, X., et al. 2010) proposed to retrieve 17 different phytoplankton pigments from satellite remote sensing data using empirical methods and applied the information to phytoplankton group identification (Pan, X., et al. 2011). This method simply used empirical relationships between pigment concentrations with the ratio of two remote sensing reflectance bands (488 or 490 to 547 or 555 nm). However, same as Chl-a, in optically complicated coastal and inland waters, higher uncertainties could be introduced by the large influences from coloured detrital matters (CDM) in coastal waters.

To obtain empirical equations we analysed both the values of a calculated using the SNAP-C2RCC algorithm and the values of Inherent Optical Properties (IOP's), Top of Atmosphere (ToA) and Bottom of Atmosphere (BoA) radiances immediately from the files of the space images primary processing – for each spectral channel of the Sentinel-2, LandSat 8 and Sentinel 3 images in each cell of raster image of the respective image (Fig. 3.48).

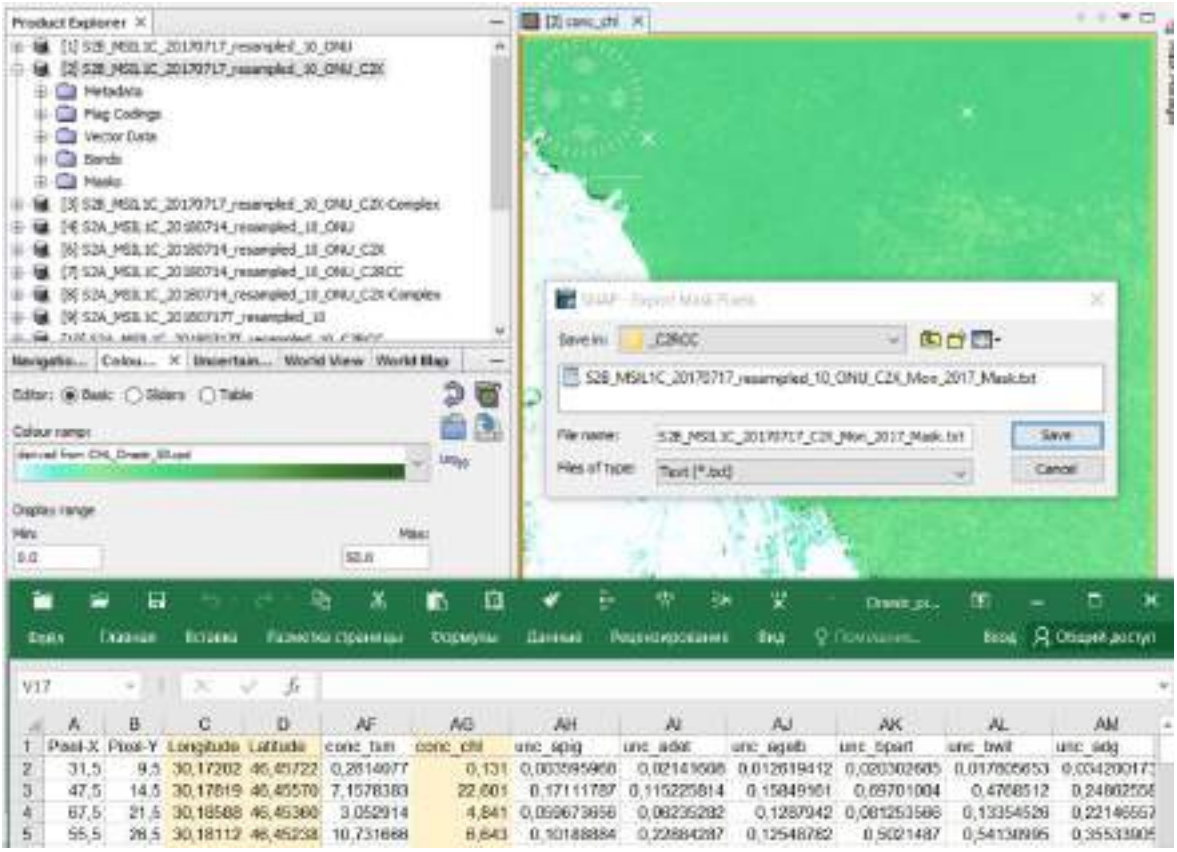

Figure 3.48. An example of extraction of results of the IOPs, concentrations of TSM and chlorophyll and other characteristics' calculation including the values of the ToA and BoA radiances of spectral channels in SNAP-C2RCC.

Using the results of the above procedure we collected for the images from each of the satellites (Sentinel 2, Landsat 8 and Sentinel 3) the massifs of IOPs values (first of all ToA and BoA) for the spectral channels recommended by the authors of the studies [O'Reilly J. E. et al. 1998; Dall'Olmo, G., & Gitelson A., 2005; Kneubühler, M. et al, 2005; Gitelson A. et al., 2007; Gilerson, A et al, 2010; Gitelson A. et al., 2011; Kopelevich O.V. et al., 2015; Brockmann C. et al, 2016; Tikhomirov O.A. et al., 2016; Ogashawara I. et al, 2017; Mishra D. R., Gitelson A. A., 2017;

Watanabe F. et al., 2018, Ansper A. and Alikas K., 2019; Cairo C. et al, 2020; Wang G. & Moisan J., 2021] in order to calculate special indices, which were further used as an argument of X dependence

$$C_{Chla}=F(X)$$

where C_{Chla} is chlorophyll concentration and X is an argument of the empirical function, which was preliminary calculated using the real data of the values of the selected kinds of spectral channels' radiances for the studied point (cell).

We chose the form and kind of the F(X) function based on the results of regression analysis between the experimental values of chlorophyll concentrations in samples from the surface water layer with the values of the used argument X.

At the same time, coefficient of determination and correlation were calculated for each of the probable variants of the empirical algorithm. Tables 3.10 - 3.13 show all the dependences of other authors that we used, for which we obtained high and significant, at the level of 0.95, values of determination (R2) and correlation (r) coefficients obtained by us for the Sentinel 2, Landsat 8 and Sentinel 3 images for the Dniester Estuary and the Bile Lake.

Table 3.10. High and significant empirical dependencies of concentration of the experimentally determined chlorophyll concentrations on X index for the Sentinel-2 space images (number of observations is 46) for the Dniester Estuary

Nos.	X Index	Author	Regression Equation	R^2	r
1	$R_{740}*(1/R_{665}-1/R_{705})$	Dall'Olmo & Gitelson, 2005	$C_{Chla}= 11.5200*\exp(5.2157*(R_{665}^{-1}-R_{705}^{-1})*R_{740})$	0.83	0.91
2	$[35.75*R_{708}/R_{665}-19.30]^{1.124}$	Gilerson et al., 2010	$C_{Chla}= 1.69*([35.75*R_{708}/R_{665}-19.30]^{1.124}) – 29.94$	0.71	0.84
3	R_{720}/R_{670}	Gitelson & Schalles, 2007	$C_{Chla}= 104.34*R_{708}/R_{665} – 95.83$	0.71	0.84
4	$452.88*\ln(R_{702}/R_{672})+4.5279$	Kneubühler et al., 2005	$C_{Chla}= 0.32*(452.88*\ln(R_{705}/R_{665})+4.5279) – 9.30$	0.68	0.82

Note: R(λ) - Remote-sensing reflectance for different band of satellites' sensors; λ - electromagnetic wavelength.

Table 3.11. High and significant empirical dependencies of concentration of the experimentally determined chlorophyll concentrations on X index for the Sentinel-2 space images (number of observations is 9) for the Bile Lake

Nos.	X Index	Author	Regression Equation	R^2	r
1	$(35.75*R_{708}/R_{665}-19.30)^{1.124}$	Gilerson et al., 2010	$C_{Chla} = 1.02* (35.75*R_{708}/R_{665}-19.30)^{1.124} – 29.07$	0.82	0.91
2	$452.88*\ln(R_{702}/R_{672})+4.5279$	Kneubühler et al., 2005	$C_{Chla}= 0.17* (452.88*\ln(R_{705}/R_{665})+4.5279) – 7.21$	0.78	0.88
3	R_{720}/R_{670}	Gitelson & Schalles, 2007	$C_{Chla}= 61.18* R_{708}/R_{665} – 66.67$	0.71	0.90
4	$R_{740}*(1/R_{665}-1/R_{705})$	Dall'Olmo & Gitelson, 2005	$C_{Chla}= 0.461* \exp(12.4179*(R_{665}^{-1}-R_{705}^{-1})*R_{740})$	0.67	0.82

Note: R(λ) - Remote-sensing reflectance for different band of satellites' sensors; λ - electromagnetic wavelength.

Table 3.12. High and significant empirical dependencies of concentration of the experimentally determined chlorophyll concentrations on X index for the Landsat 8 space images (number of observations is 21) for the Dniester Estuary

Nos.	X Index	Author	Regression Equation	R^2	r
1	$21.0*a_{pig}(443)^{1.04}$	C2RCC [Brockmann et.al., 2016]	C_{Chla}= 1.8104* $(21.0*a_{pig}(443)^{1.04})$	0.67	0.82
2	R_{720}/R_{670}	Gitelson & Schalles, 2007	C_{Chla}= 371.89* R_{865}/R_{655} – 67.898	0.40	0.63

Note: R(λ) - Remote-sensing reflectance for different band of satellites' sensors; λ - electromagnetic wavelength. a_{pig} - Pigment absorption calculated as difference $a_{pig} = a_p – a_d$, where a_p is the absorption by particles, and a_d - by detritus.

Table 3.13. High and significant empirical dependencies of concentration of the experimentally determined chlorophyll concentrations on X index for the Sentinel-3 space images (number of observations is 70) for the Dniester Estuary

Nos.	X Index	Author	Regression Equation	R^2	r
1	R_{708}/R_{665}	Gitelson & Schalles, 2007	C_{Chla} = 37.3483* $(R_{708.75}/R_{665})^{5.6002}$	0.79	0.89
2	$[35.75*R_{708}/R_{665}-19.30]^{1.124}$	Gilerson et al., 2010	C_{Chla}= 4.55* $([35.75*R_{708.75}/R_{665}-19.30]^{1.124})$ – 58.20	0.72	0.85
3	$452.88*\ln(R_{702}/R_{672})$ +4.5279	Kneubühler et al., 2005	C_{Chla}= 0.56* $(452.88*\ln(R_{708.75}/R_{665})$ +4.5279) + 47.95	0.67	0.82
4	$R_{740}*(1/R_{665}-1/R_{705})$	Dall'Olmo & Gitelson, 2005	C_{Chla}= 34.5435* $\exp(7.27*(R_{665}^{-1}-R_{708.75}^{-1})*R_{753.75})$	0.67	0.82

Note: R(λ) - Remote-sensing reflectance for different band of satellites' sensors; λ - electromagnetic wavelength.

Analysis of the data presented in tables 3.10 - 3.13. has shown that the most effective empirical algorithms to calculate chlorophyll concentrations, which we later used to process the corresponding images, are the following:

a) For the Dniester Estuary the recommended formulas for the implementation of empirical algorithms that depend on the type of a particular satellite, the images of which will be available for research:

- for the Sentinel 2 images – the algorithm based on the recommendations from [Dall'Olmo & Gitelson, 2005]: $C_{Chla} = 11.5200*\exp(5.2157*X)$, where $X=(R_{665}^{-1}-R_{705}^{-1})*R_{740}$)

- for the Sentinel 3 images – the algorithm based on the recommendations from [Gitelson & Schalles, 2007]: $C_{Chla} = 37.3483*X^{5.6002}$, where $X= R_{708}/R_{665}$

- for the Landsat 8 images – the algorithm that uses the SNAP-C2RCC [Brockmann et.al., 2016]: C_{Chla} = 1.8104* X, where X=21.0*$a_{pig}(443)^{1.04}$

b) For the Bile Lake the empirical algorithm of satellite images (refers to Sentinel 2 images only) is based on the recommendations from [Gilerson et al., 2010]: C_{Chla}= 1.02*X, where X=(35.75*R_{708}/R_{665}-19.30)$^{1.124}$ – 29.07.

3.4.3. Evaluation of the chlorophyll eutrophication level

The National (Table 3.14) and International (Table 3.15) classification of water bodies trophic states have been used to assess the environmental status of aquatic ecosystems using simple indicators such as nutrients, chlorophyll and other characteristics of water bodies state [Cardoso et al, 2001; Methodology of surface waters environmental assessment according to respective categories, 1998; OECD, 1982; Toner et al, 2008].

Table 3.14. Ukrainian National Classification of freshwater aquatic systems according to their trophic conditions and limiting values of indicators of various trophic statuses in freshwater bodies

Trophic status indicator		Oligotrophic	Mesotrophic	Eutrophic	Hypertrophic
P_{total}	mkg/l	<10	10-35	35-100	>100
PO_4	mkg/l	<0.015	0.015-0.050	0.051-0.200	>0.200
N_{total}	mkg/l	<350	350-650	650-1200	>1200
NO_3	mkg/l	<0.20	0.20-0.050	0.51-1.00	>1.00
NO_2	mkg/l	<0.002	0.002-0.01	0.011-0.050	>0.05
NH_4	mkg/l	<0.1	0.1-0.30	0.31-1.0	>1.01
Chl *a*	mkg/l	<2.5	2.5-8.0	8.0-25.0	>25.0
Transparency	m	>1.5	0.65-1.50	0.35-0.60	<0.30
B_{phyto}	mg/l	<0.5	0.5-2.0	2.1-50.0	>50
N_{micro}	mln/cm^3	<0.5	0.5-2.5	2.6-10.0	>10
O_2	mg/ dm^3	>8.0	7.1-8.0	5.1-7.0	<5.0

Table 3.15. Final Eutrophication Criteria used for freshwater aquatic systems in the UA2 Ukrainian pilot area according to some National and EU countries recommendations

Trophic status indicator		Greece[1]	Italy[1]	Ukraine[2]	JRC EC[1]	Ireland[3]	OECD[4]	PONTOS UA
P_{total}	mkg/l	>50	>50	>35	-	>35	>35	>35
PO_4	mkg/l		-	>0.051	-	-	-	>0.051
N_{total}	mkg/l	>50	-	>650	-	-	-	>650
NO_3	mkg/l	-	-	>0.51	-	-	-	>0.51
NO_2	mkg/l	-	-	>0.011	-	-	-	>0.011
NH_4	mkg/l	-	-	>0.31	-	-	-	>0.31
Chl *a*	mkg/l	>10	>10	>8.0	>10	>8 (>25)	>8.0	>10.0
Transparency	m	<2.0	-	<0.35	<3	<1.5(<0,7)	<0.7	<0.35
B_{phyto}	mg/l	-	-	>2.1	-	-	-	>2.1 (10)
N_{micro}	mln/cm^3	-	-	>2.6	-	-	-	>2.6
O_2	mg/ dm^3	<4.0	-	<5.1	<4	-	-	<5.1
TRIX						-	-	>5.0
TSI						-	-	>50

Note: 1 – [A.C. Cardoso, J. Duchemin,P. Magoarou, G. Premazzi, 2001. Criteria for the Identification of Freshwaters Subject to Eutrophication. Luxembourg: Office for Official Publications of the European Communities, 2001. 90 P. ISBN 92-894-0947-9],

2 – [Methodology of surface waters environmental assessment according to respective categories. V.D. Romanenk, V.M. Zhukinskyi, O.P. Oksiyuk et al., - K.: SIMVOL-T, 1998. - 28 p.] (In Ukrainian).

3 – [P. Toner, J. Bowman, K. Clabby, J. Lucey, M. McGarrigle, C. Concannon, C. Clenaghan, P. Cunningham, J. Delaney, S. O'Boyle, M. MacCárthaigh, M. Craig and R. Quinn Water Quality in Ireland 2001-2003. Ireland Environmental Protection Agency. 2005. - 233p.],

4 – [OECD (Organisation for Economic Cooperation and Development), 1982. Eutrophication of Waters, Monitoring, Assessment and Control. Paris, OECD. – 145p.]

Usually aquatic systems are classified into oligotrophic, lower mesotrophic, higher mesotrophic and eutrophic, and ranges are given per parameter. Nutrient concentrations are given in mg/l, phytoplankton cells number and biomass in cells/l in mg/l and chlorophyll in µg/l.

More objective and more accurate but more complicated and effective trophic state of water bodies assessments methods are using trophic indexes, such as TRIX and TSI, based on on nutrients (total phosphorus and total nitrogen or phosphate, nitrate, ammonium), chlorophyll ***a***, dissolved oxygen and water transparency [Carlson,1977, Vollenweider R.A.,1998, Kovalova N.V. and Medinets V.I., 2012].

Keeping in mind the approaches to standardisation of the freshwater bodies eutrophication existing in the European countries [OECD, JRC, WFD, TRIX, TSI] we have partially used in the PONTOS Project the normative limiting values of trophic status indicators shown in Table 3.15

Taking into account the fact that chlorophyll concentration and biomass are the direct indicators of a water body eutrophication, we have taken the average annual chlorophyll concentration level exceeding 10 mkg/l for a signal of the water body's eutrophication. Other characteristics presented in Table 3.15 are indirect eutrophication indicators that can be used to assess the risk of eutrophication effects emerging in biological component and their role is outside the scope of the present overview. It should, however, be noted that such abiotic factors as temperature, transparency and illumination are, together with nitrogen and phosphorus compounds content, the main factors determining the level of risk of eutrophication development, which causes blooms of microalgae that are the main indicators of phytoplankton biomass explosive growth with further development of hypoxia, death of aquatic organisms and sharp degradation of aquatic environment quality.

4. Study Site Description

4.1. The Ukrainian Pilot area (PONTOS-UA2)

The Ukrainian Pilot area UA2 consists of 2 water bodies that belong to the Dniester Delta area (Dniester Estuary and Bile Lake) which are located in the southern part of Ukraine in Odesa Oblast (**Ошибка! Источник ссылки не найден.**). These 2 water bodies are ecologically important sites as parts of the Lower Dniester National Park and protected by the Convention on Wetlands of International Importance (Ramsar Convention).

Figure 4.1. Pilot water bodies (Dniester Estuary and Bile lake) under study.

4.1.1 Dniester Estuary

The Dniester Estuary is located in Odesa Oblast, Ukraine. It is a bay in the north-western Black Sea, where the Dniester disgorges. The bay cuts 41 km deep inland from south-east to north-west, its area is 373.65 km^2, mean depth 2.6 m (Figure 4.2.). The Dniester Estuary is separated from the sea by a narrow sand spit Bugaz, which is 40 to 500 m wide. In its southern part of the estuary it is connected to the open part of the Black Sea through the cannel named Tsaregradske Gyrlo, which is about 200 m wide, 500 m long and 3.5-5.0 m deep at mean sea level. There are resorts Karolino-Bugaz and Zatoka on the sand spit. The current in the estuary depends on winds and the Dniester floods. The estuary often freezes over in winter. There are ports Bilhorod-Dnistrovskyi and Ovidiopol in the Dniester Estuary. There is a bay in the estuary called the Karagolskyi Bay.

The Estuary basin is used for extensive aquaculture and fishery. The Estuary may be considered as an open ecosystem with freshwater input from the Dniester River, directly from rainfall and through seepage from the adjoining agricultural lands. The Dniester Estuary is a very important fishery water body and is an ecologically important ecosystem. The northern part of the Dniester Estuary is included into the Lower Dniester National Park.

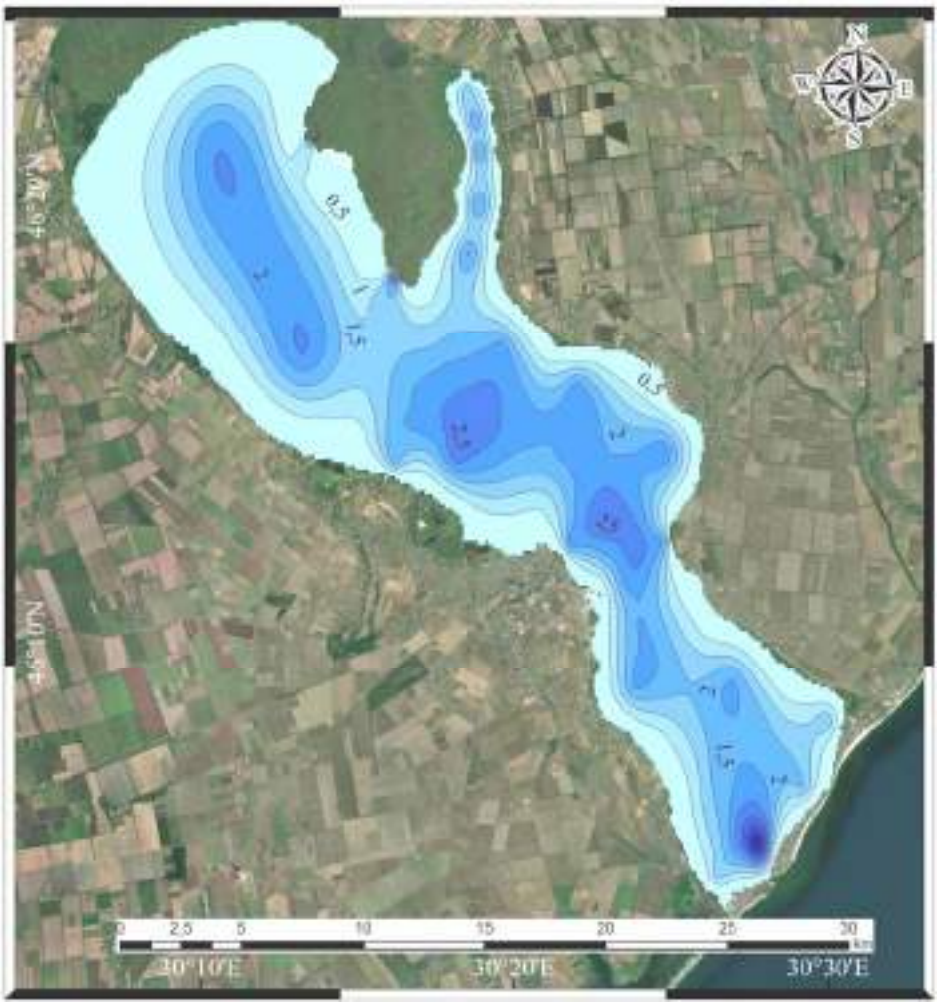

Figure 4.2. Dniester Estuary bathymetry map

4.1.2 Bile Lake

Bile is a small lake covering approximately 1.036 km^2. Its length is about 1.7 km, width – 0.8-0.9 km and its perimeter is 4.58 km (Figure 4.3 Bile Lake bathymetry map3). It is situated in Bilyaivka Region of Odesa Oblast in the Dniester Delta. The mean depth of the lagoon is 0.9 m and the maximum depth 1.4 m. Bile is a running-water lake. Water enters it from the Turunchuk River and flows into the Dniester through small channels. All economic activities in the lake are prohibited as the Bile is located in the central part of the Lower Dniester National Park. Of special importance are aquatic and coastal plants (ca. 65 species), most of which are entered into the Red Data Bool of Ukraine.

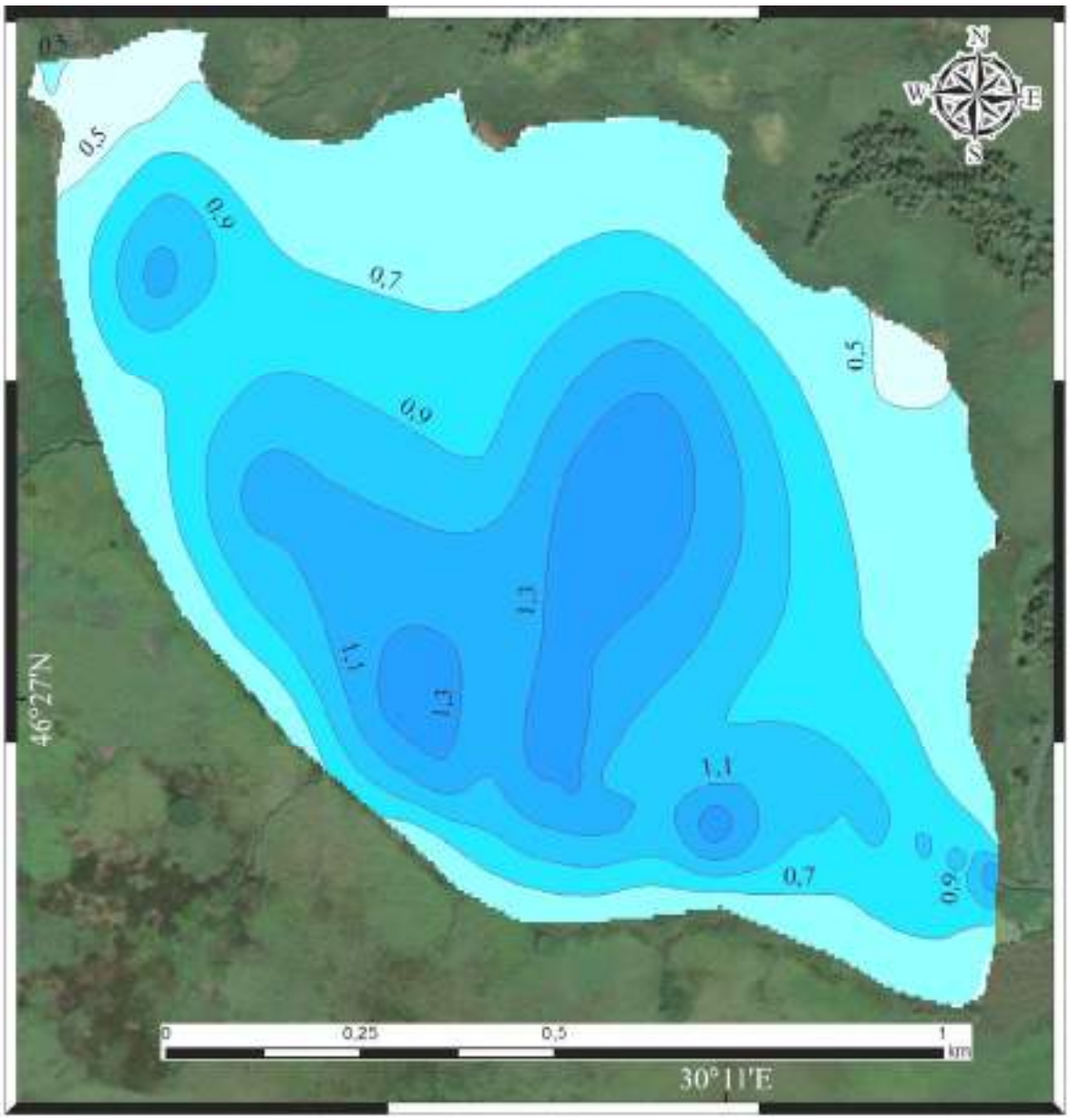

Figure 4.3 Bile Lake bathymetry map

The geometric and hydrologic parameters of the discussed water bodies are presented in Table 4.2.

Table 4.2. Study sites and their geometric and hydrologic characteristics

Water object	Geographical boundaries	Surface area, km^2	Mean water depth, m	Water volume (km^3)	Perimeter, km
Bile lake	30.171-30.188°E 46.446-46.458°N	1.036	0.9	0.93×10^{-3}	4.58
Dniester Estuary	30.101-30.511°E 46.065-46.398°N	373.650	2.0	0.73	143.83

5. Results

5.1. Spatial Chlorophyll analysis

During the first stage of the study, chlorophyll spatial distribution in the pilot water bodies (Dniester Estuary and Bile Lake) was assessed based on the results of space images Sentinel 2 (18 images), Sentinel 3 (11 images) and Landsat 8 (3 images) processing using the empirical algorithms, which we have established for each type of the images (see Chapter 3).

5.1.1. Dniester Estuary

The examples of chlorophyll spatial distribution in the Dniester Estuary according to the results of Sentinel 2, Landsat 8 and Sentinel 3 images processing for the period 2017-2021 are presented in Figures 5.1-5.12, 5.13-5.15 and 5.16-5.25 respectively

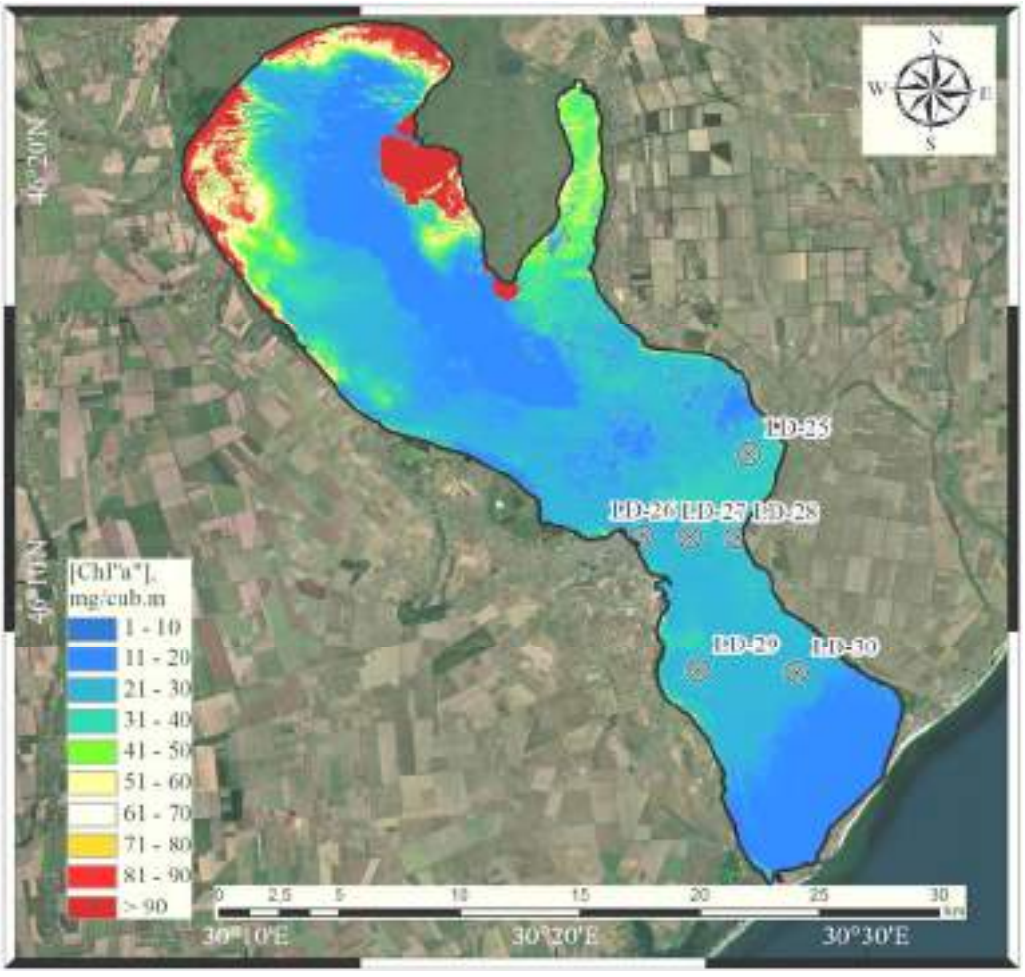

Figure 5.1. Chl-a concentration (S2-ONU calculation) in Dniester estuary for 17 July 2017

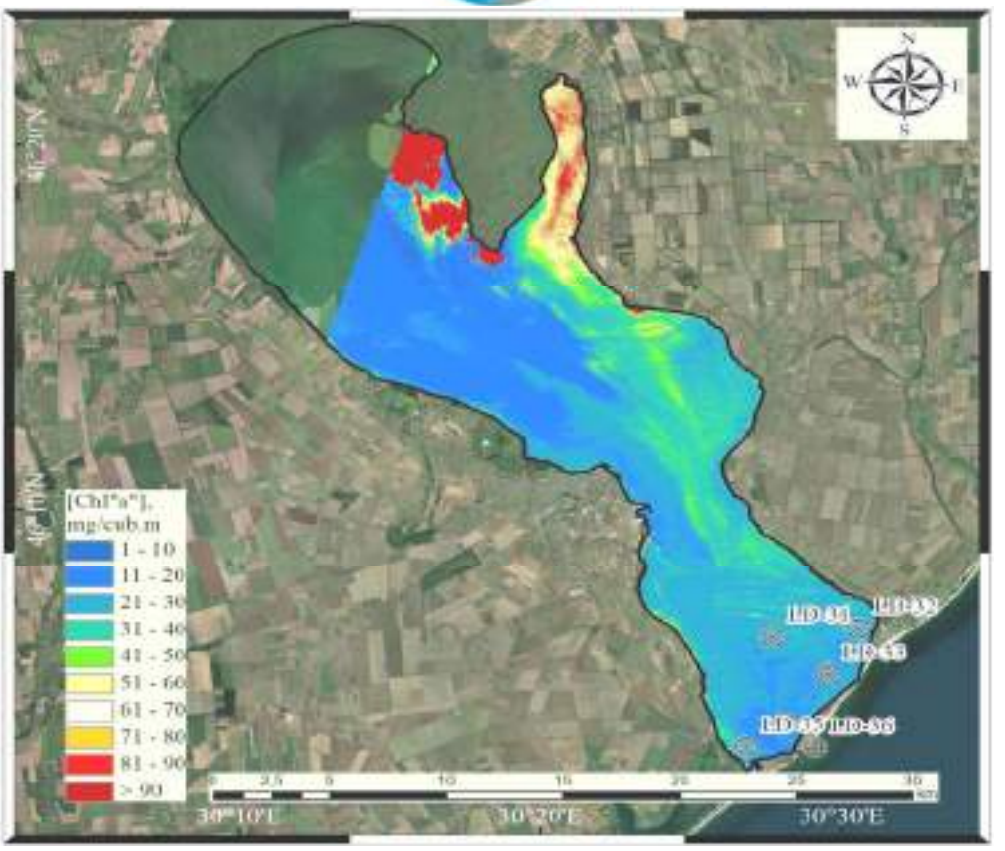

Figure 5.2. Chl-a concentration (S2-ONU calculation) in Dniester estuary for 14 July 2018

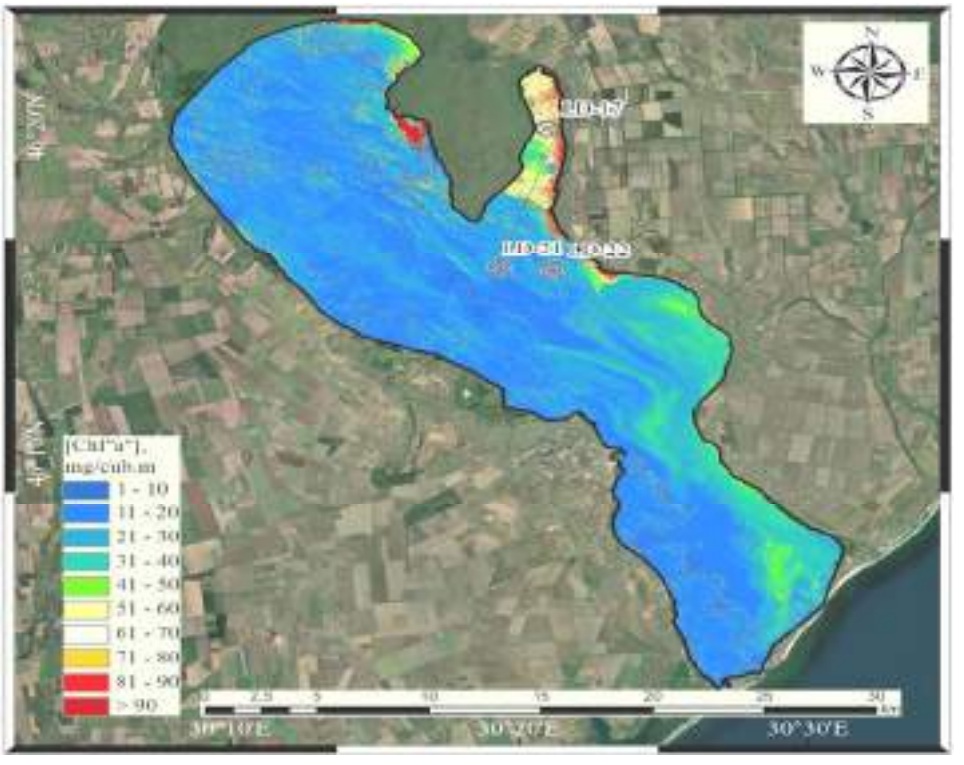

Figure 5.3. Chl-a concentration (S2-ONU calculation) in Dniester estuary for 17 July 2018

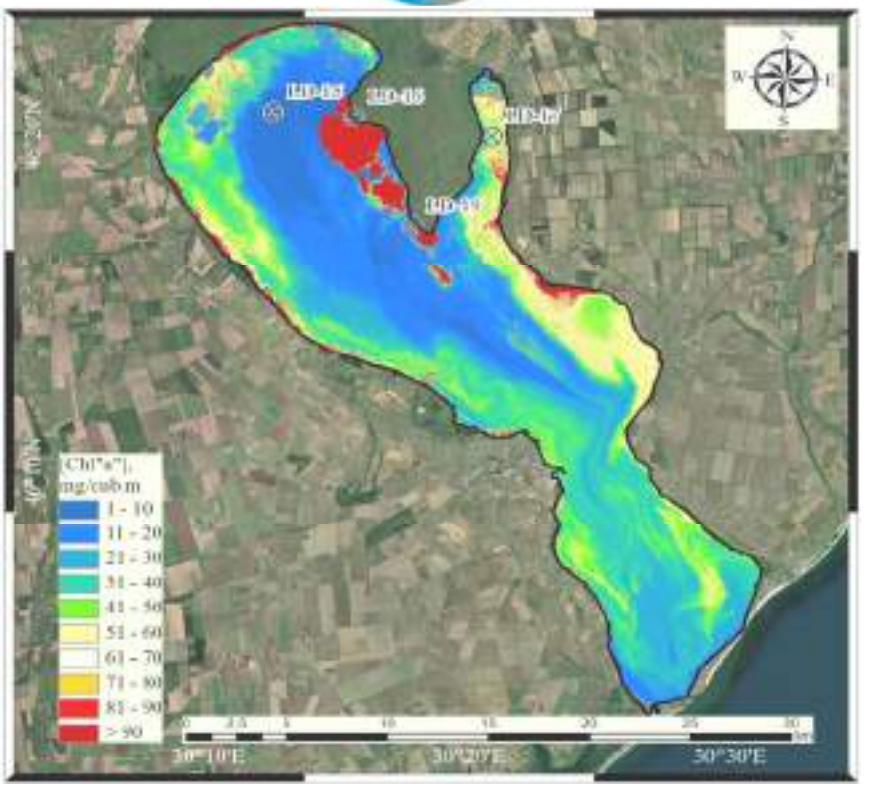

Figure 5.4. Chl-a concentration (S2-ONU calculation) in Dniester estuary for 12 July 2019

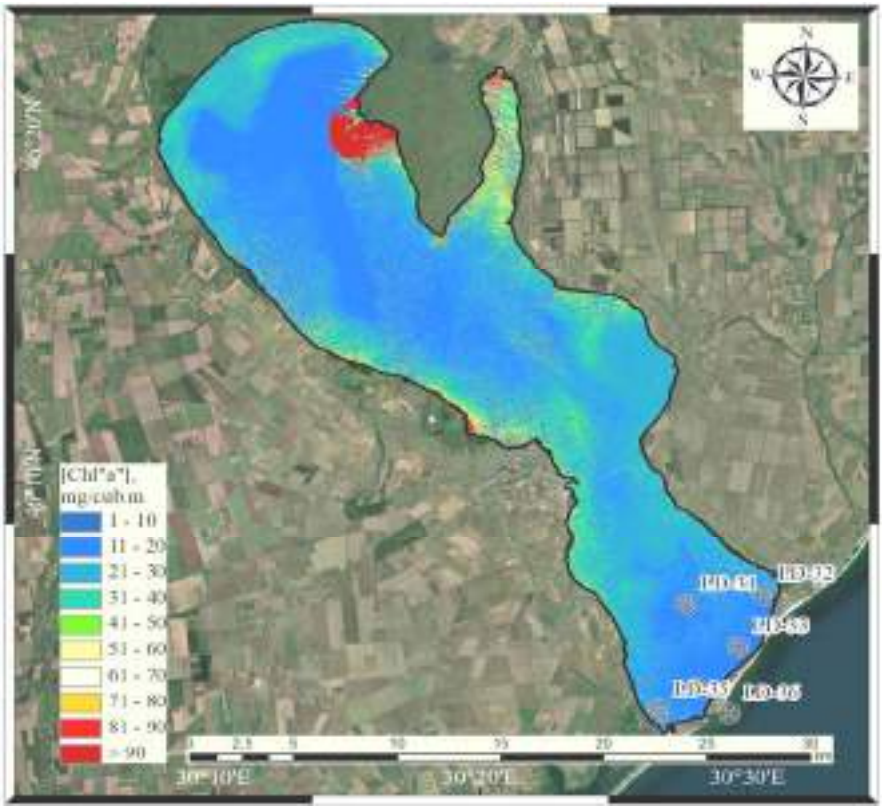

Figure 5.5. Chl-a concentration (S2-ONU calculation) in Dniester estuary for 16 July 2020

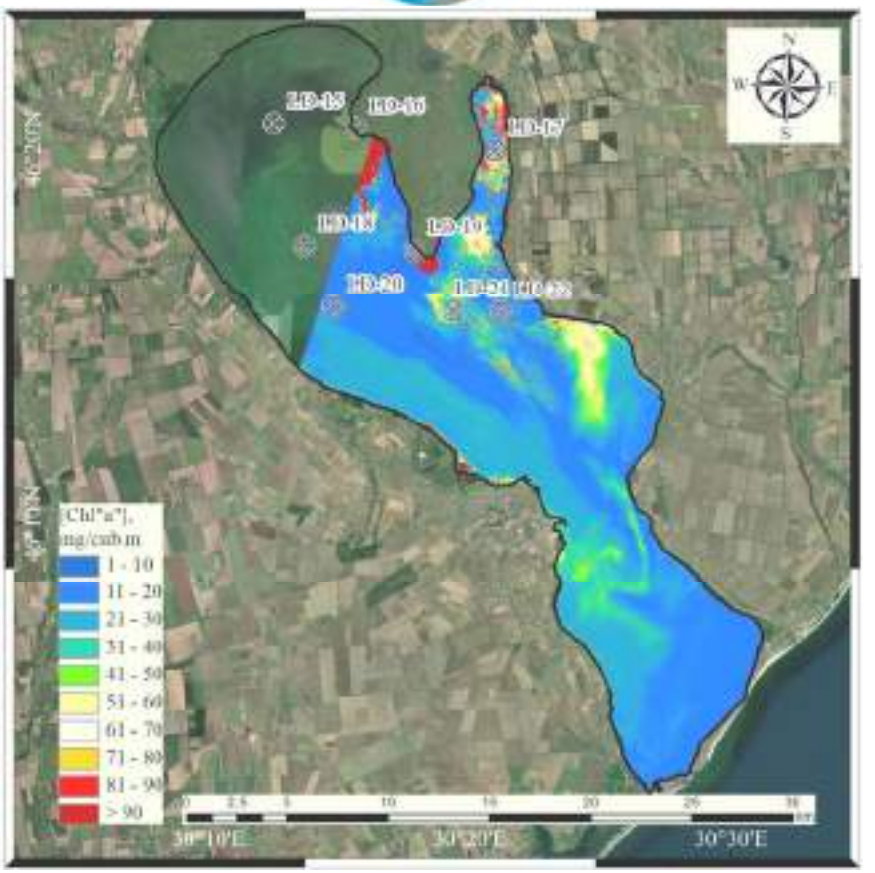

Figure 5.6. Chl-a concentration (S2-ONU calculation) in Dniester estuary for 18 July 2020

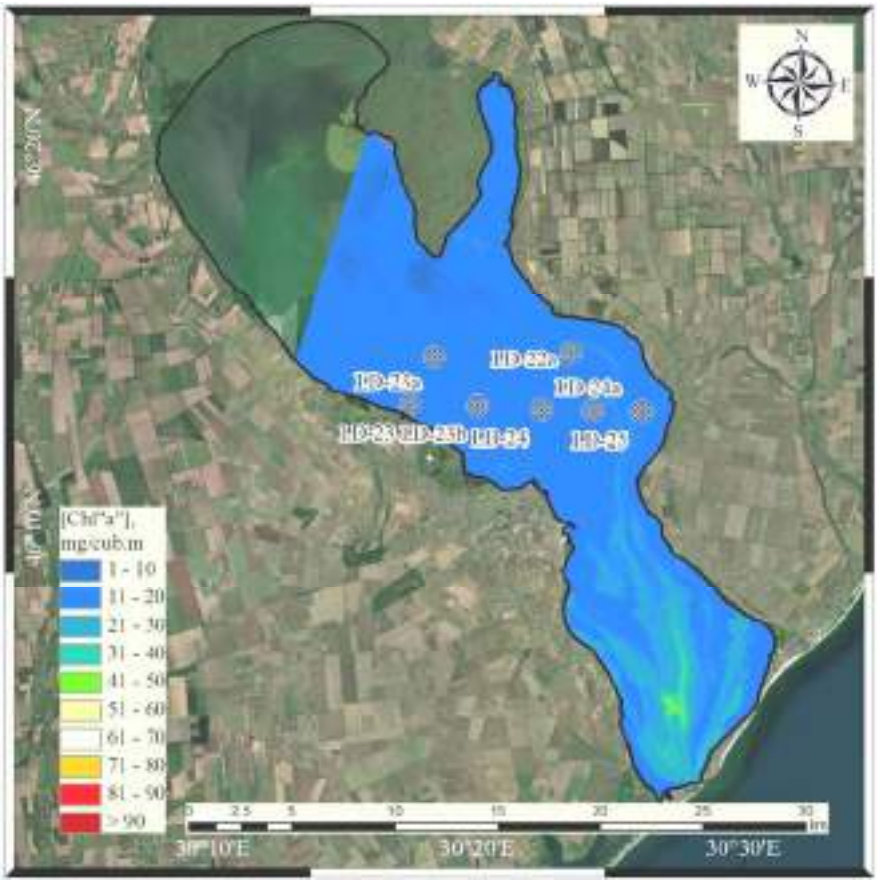

Figure 5.7. Chl-a concentration (S2-ONU calculation) in Dniester estuary for 24 April 2021

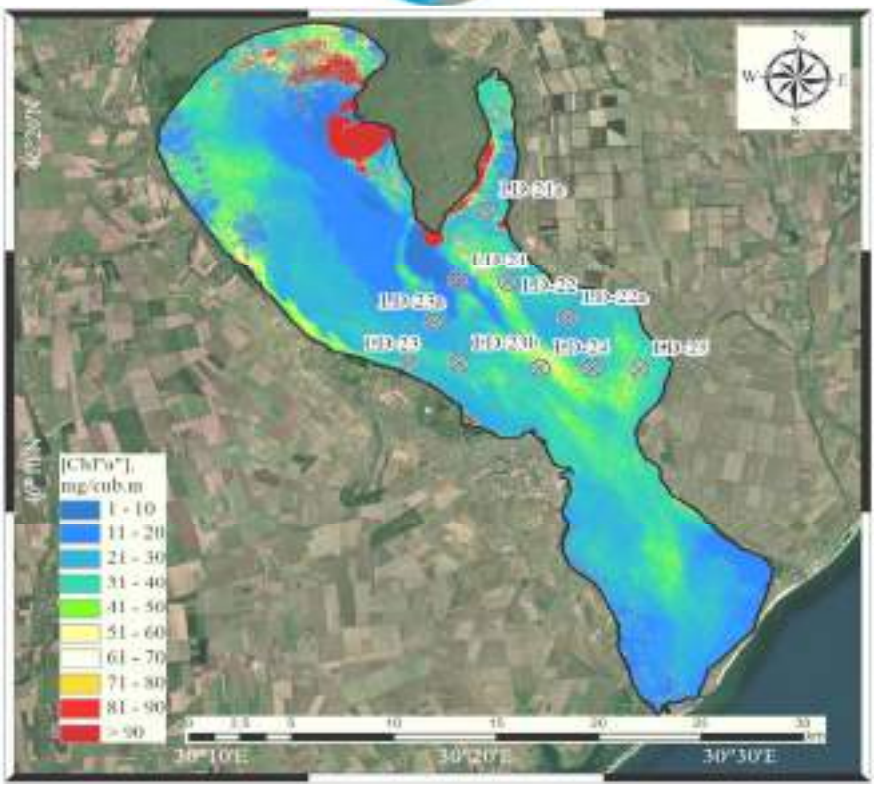

Figure 5.8. Chl-a concentration (S2-ONU calculation) in Dniester estuary for 11 June 2021

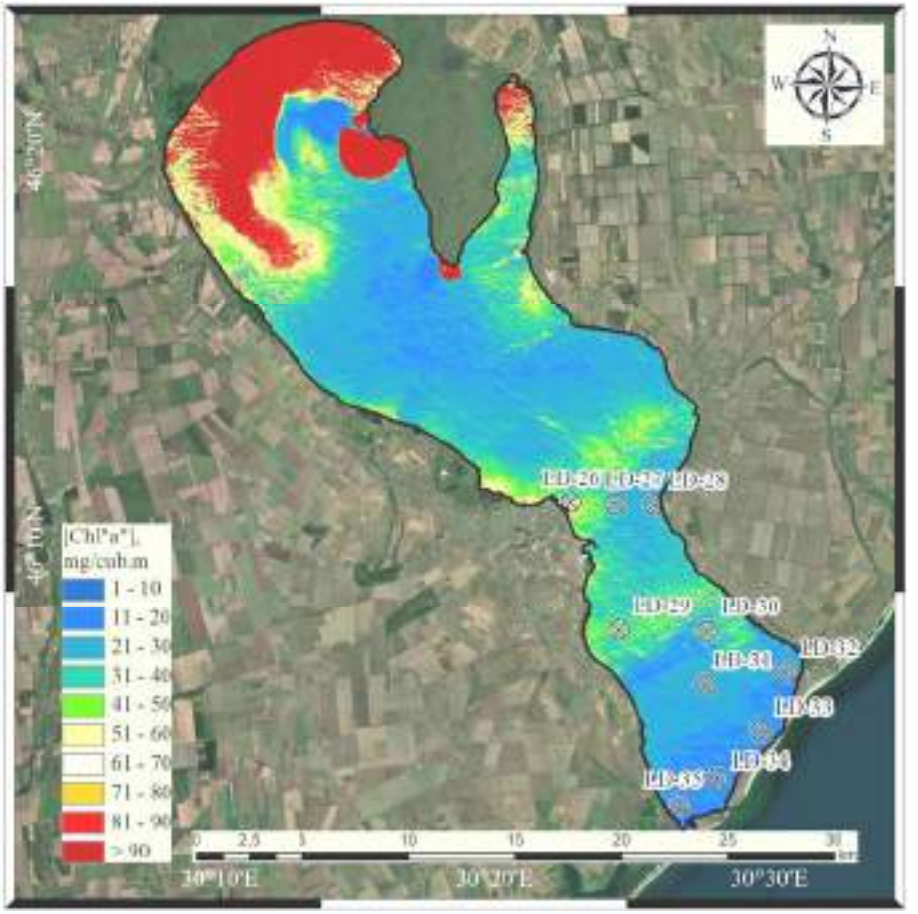

Figure 5.9. Chl-a concentration (S2 - ONU calculation) in Dniester estuary for 16 July 2021 (black line – the border of water pond)

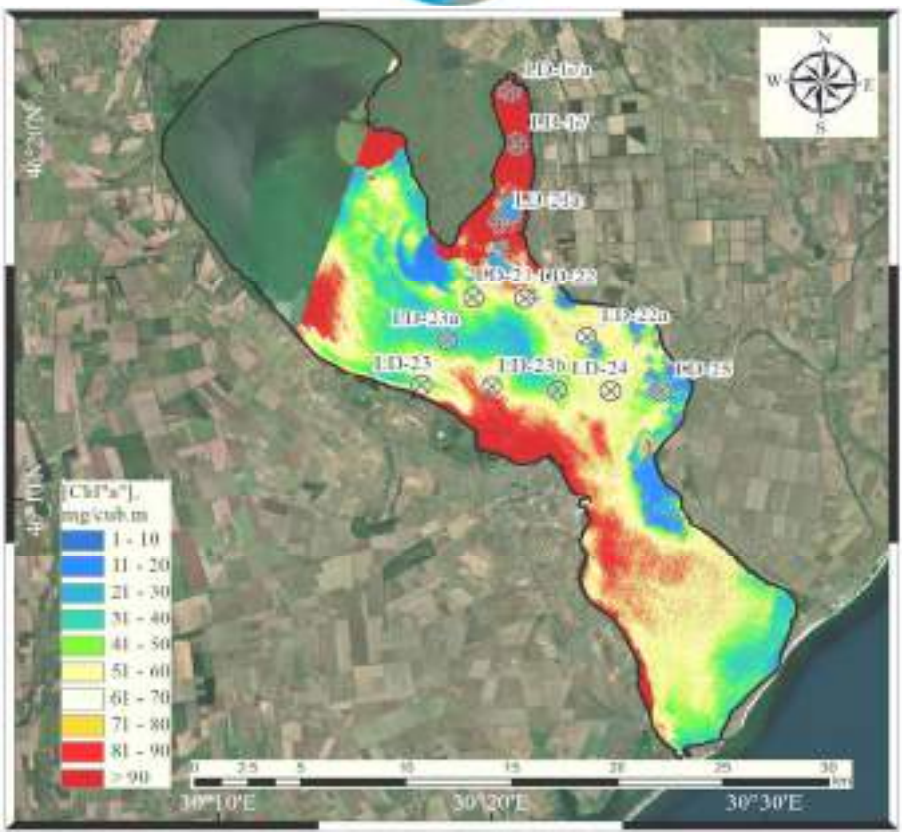

Figure 5.10. Chl-a concentration (S2 - ONU calculation) in Dniester estuary for 18 July 2021 (black line – the border of water pond)

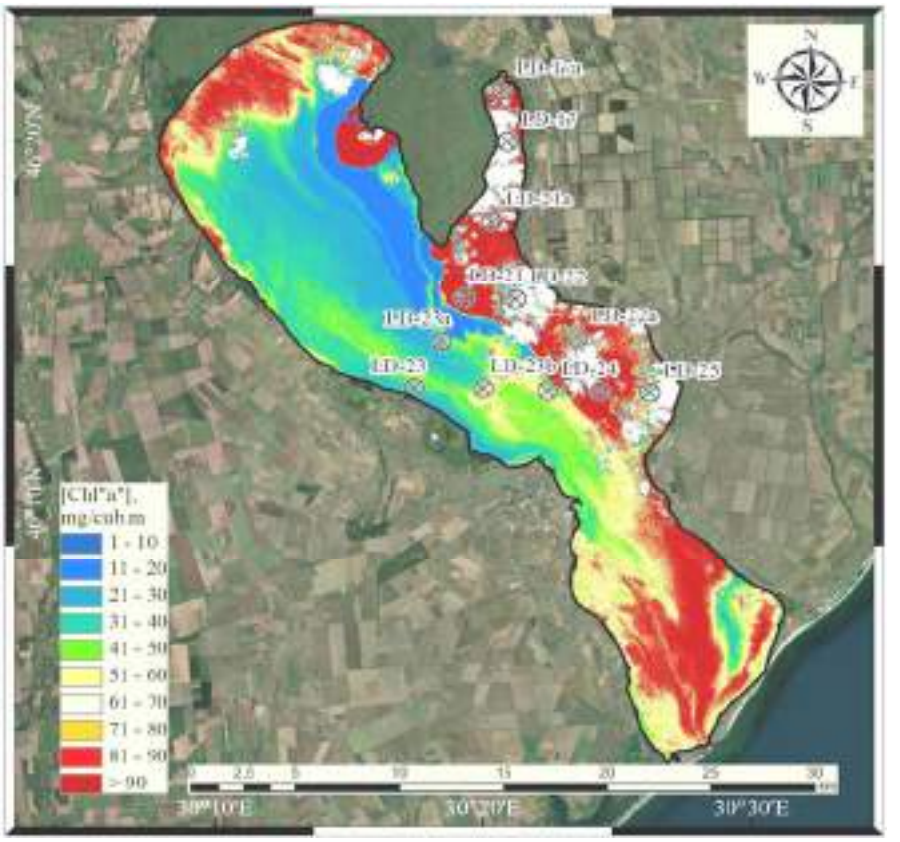

Figure 5.11. Chl-a concentration (S2-ONU calculation) in Dniester estuary for 20 August 2021

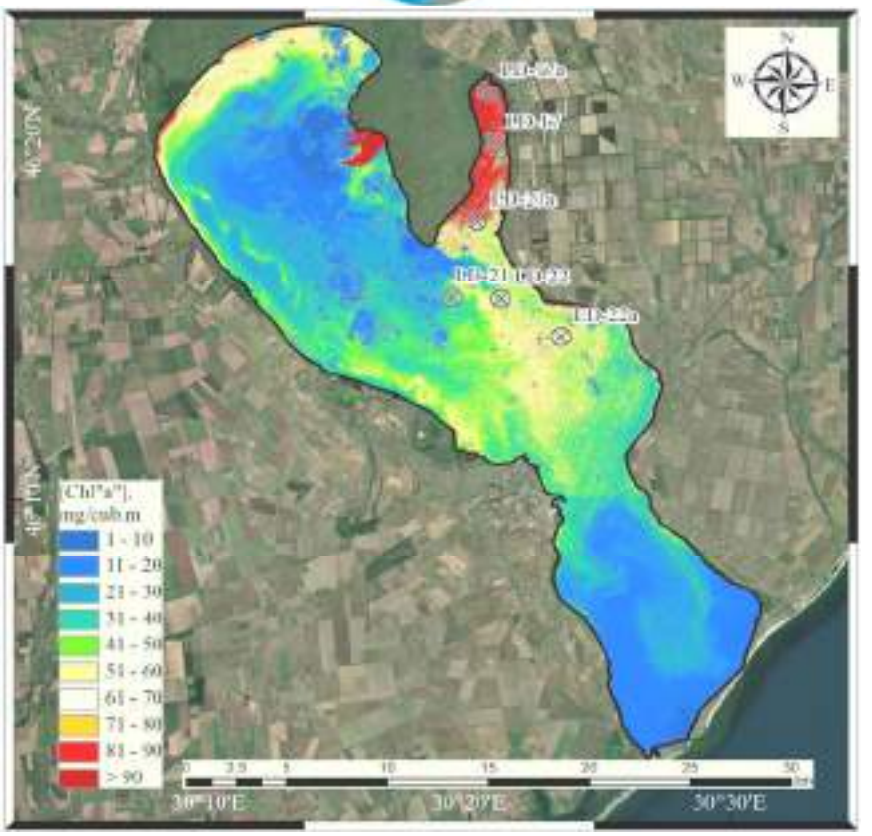

Figure 5.12. Chl-a concentration (S2-ONU calculation) in Dniester estuary for 29 September 2021

Analysis of chlorophyll concentration spatial distribution from Sentinel 2 images for summer periods of 2017-2021 (Fig. 5.1-5.12) has shown the following.

Maximal concentrations were observed in all years in the shallow areas of the Dniester Estuary northern part and the Karagol Bay, while minimal were found in the relatively deep central and southern parts of the estuary. At that, the maximal concentrations were observed all over the estuary during summer periods.

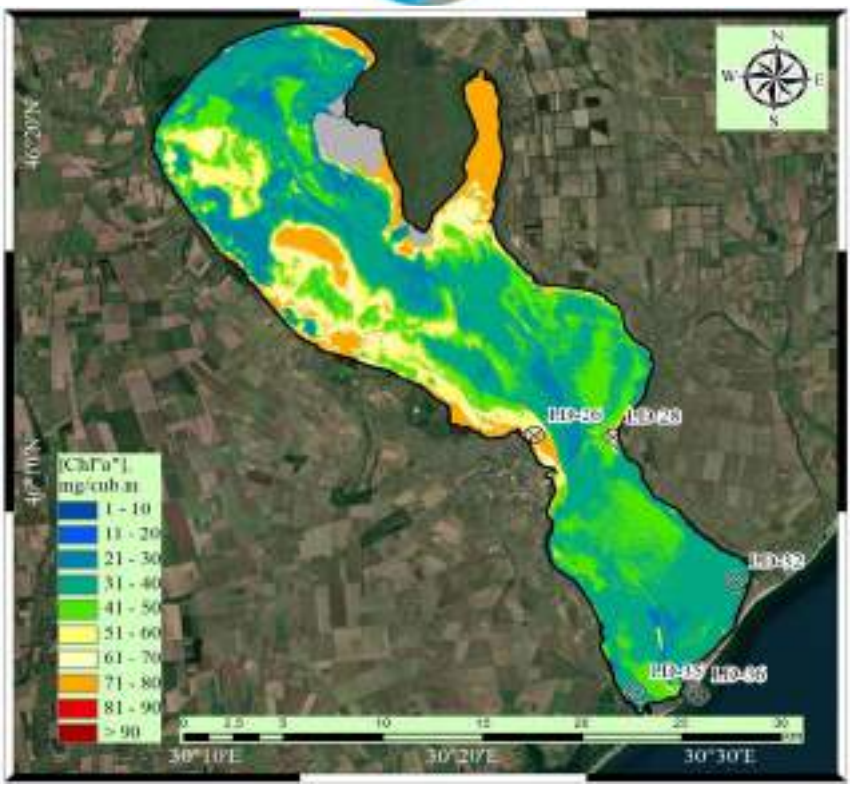

Figure 5.13. Chl-a concentration (L8-ONU calculation) in Dniester estuary for 22 July 2016 (grey colour – floating water vegetation)

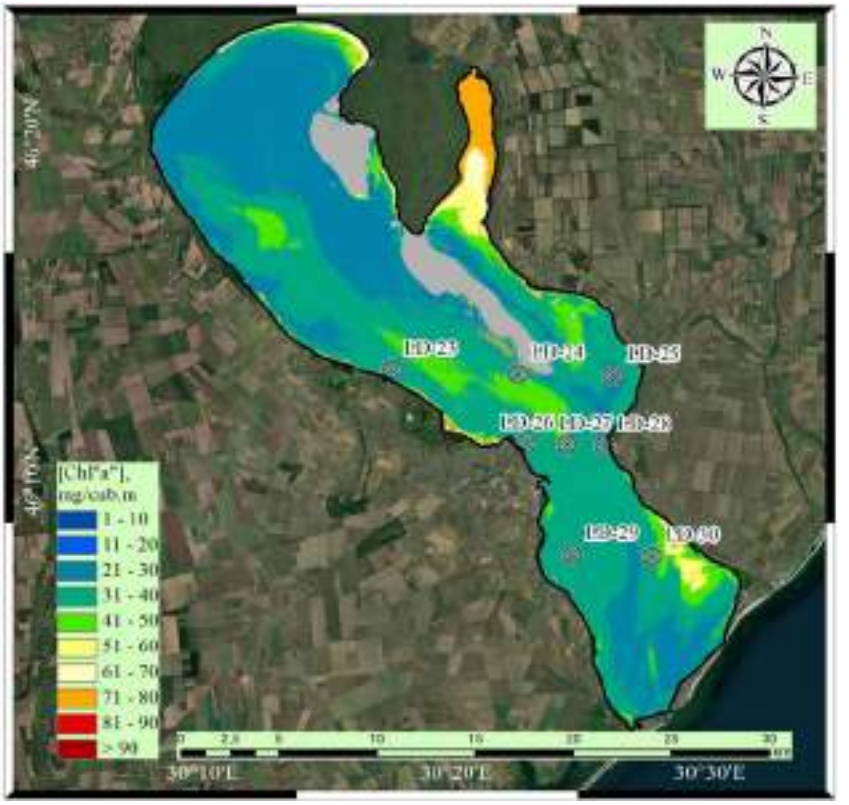

Figure 5.14. Chl-a concentration (LS8 – ONU calculatioon) in Dniester estuary for 17 July 2020 (grey colour – floating water vegetation)

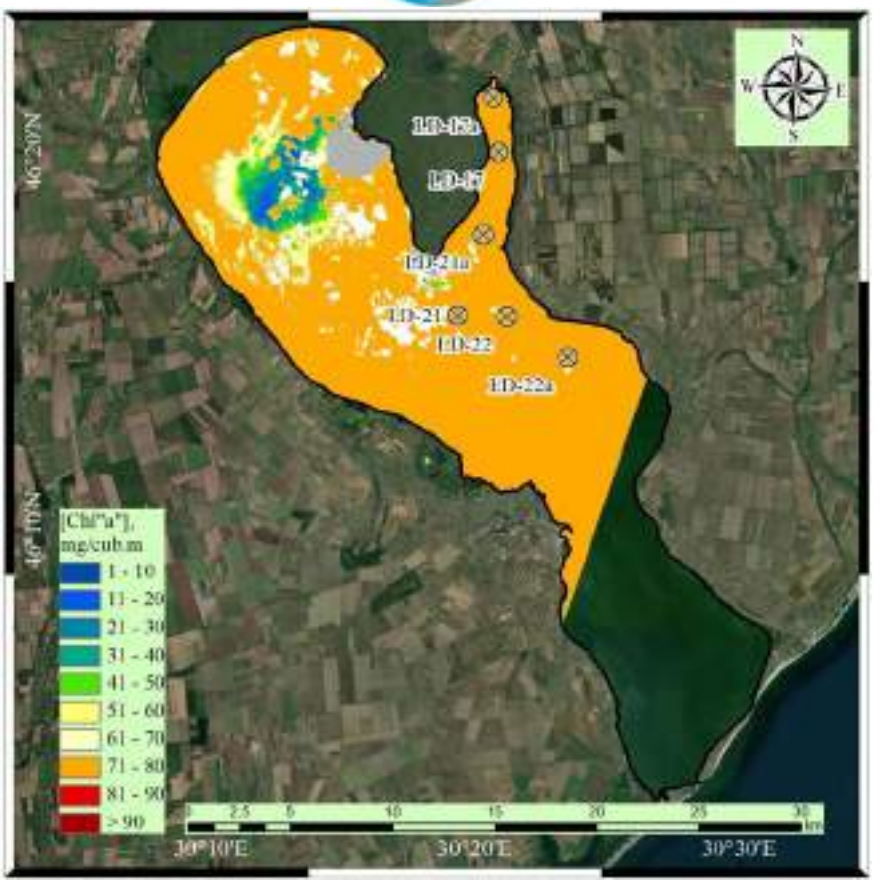

Figure 5.15. Chl-a concentration (LS8 – ONU calculation) in Dniester estuary for 29 September 2021 (grey colour – floating water vegetation)

Analysis of chlorophyll concentrations spatial distribution from the Landsat 8 images for summer periods of 2016-2021 (Fig. 5.13-5.15) has shown similar distribution of concentrations in the estuary. It has though to be mentioned that the maximal concentrations for the period considered were registered in September 2021.

It should be pointed out that trying to study chlorophyll concentrations' seasonal variation using the data from Sentinel 2 and Landsat 8 images we encountered lack of representative images (without clouds, covering the whole area of the estuary) for some months, as the frequency of the Sentinel 2 and Landsat 8 satellites passages (4-5 days and 14 days) was not enough to find good quality satellite imagery covering the entire estuary for some month in the period from January to December. That made us use the Sentinel 3 images to study the seasonal variation; the examples are presented in Fig. 5.16-5.24.

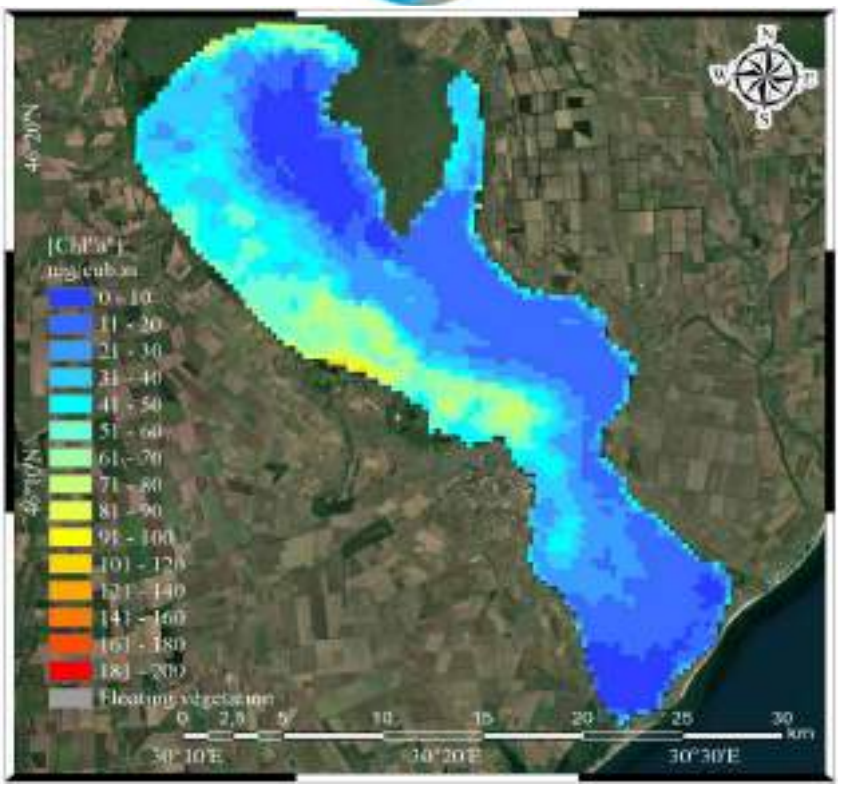

Figure 5.16. Chl"a" concentration (S3 bands - ONU calculation) in Dniester estuary for 07 March 2021

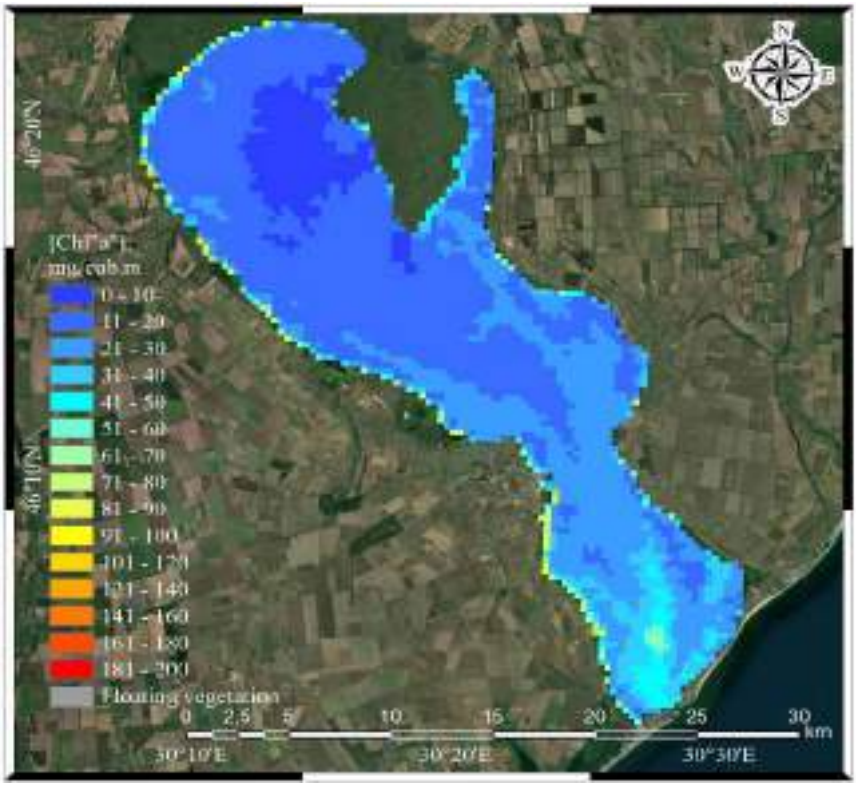

Figure 5.17. Chl"a" concentration (S3 bands - ONU calculation) in Dniester estuary for 24 April 2021

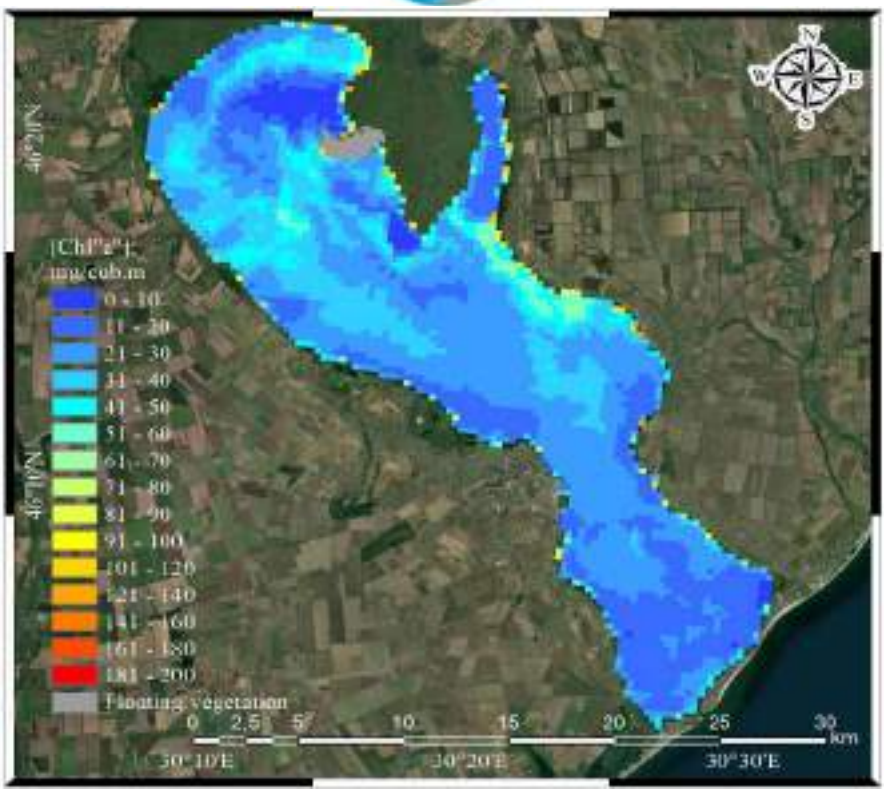

Figure 5.18. Chl"a" concentration (S3 bands - ONU calculation) in Dniester estuary for 15 May 2021

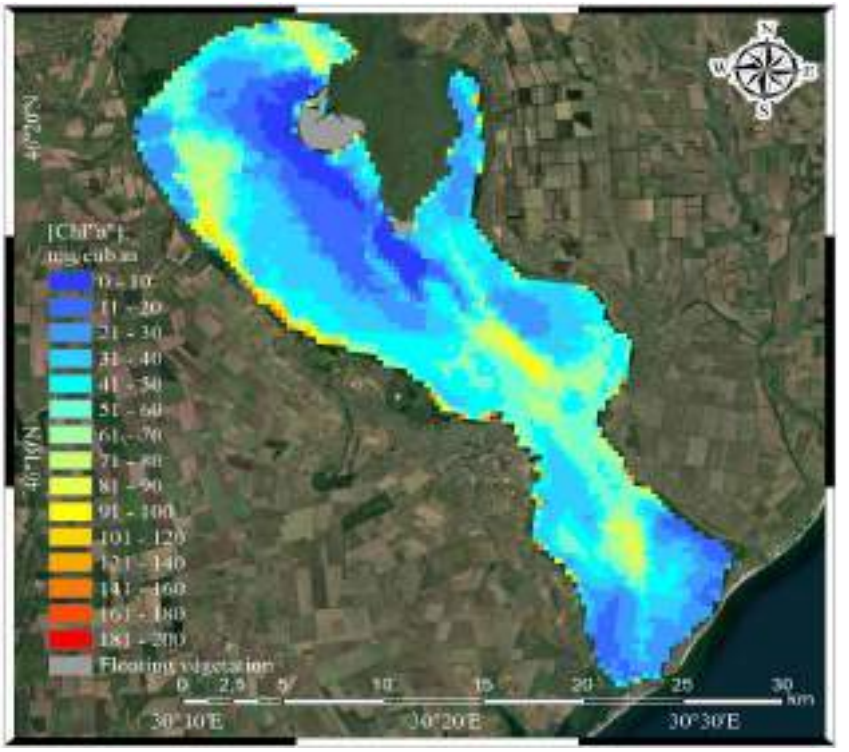

Figure 5.19. Chl"a" concentration (S3 bands - ONU calculation) in Dniester estuary for 11 June 2021

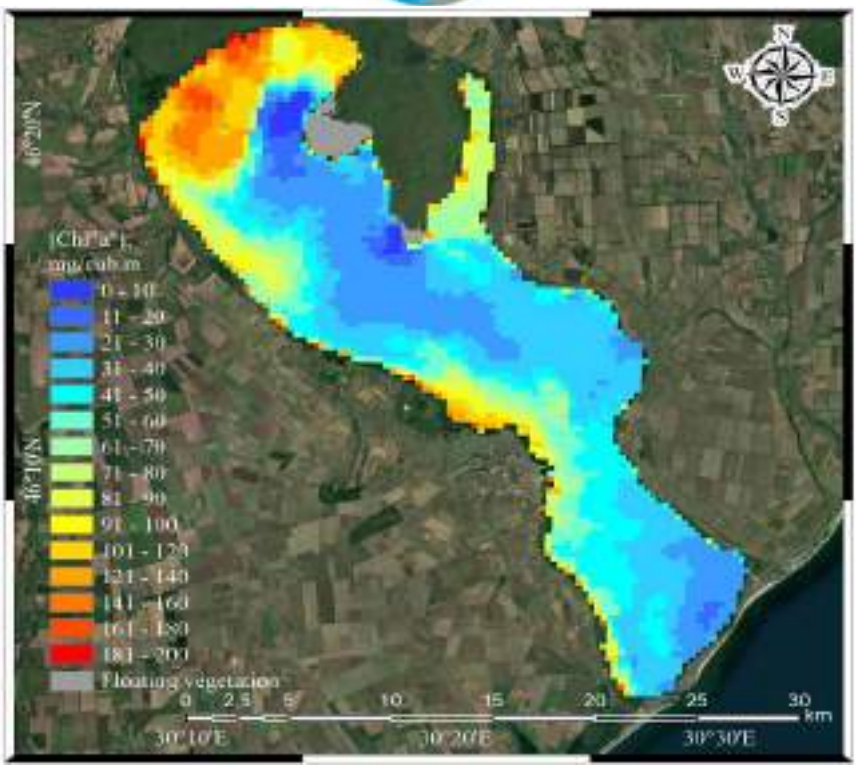

Figure 5.20. Chl"a" concentration (S3 bands - ONU calculation) in Dniester estuary for 18 July 2021

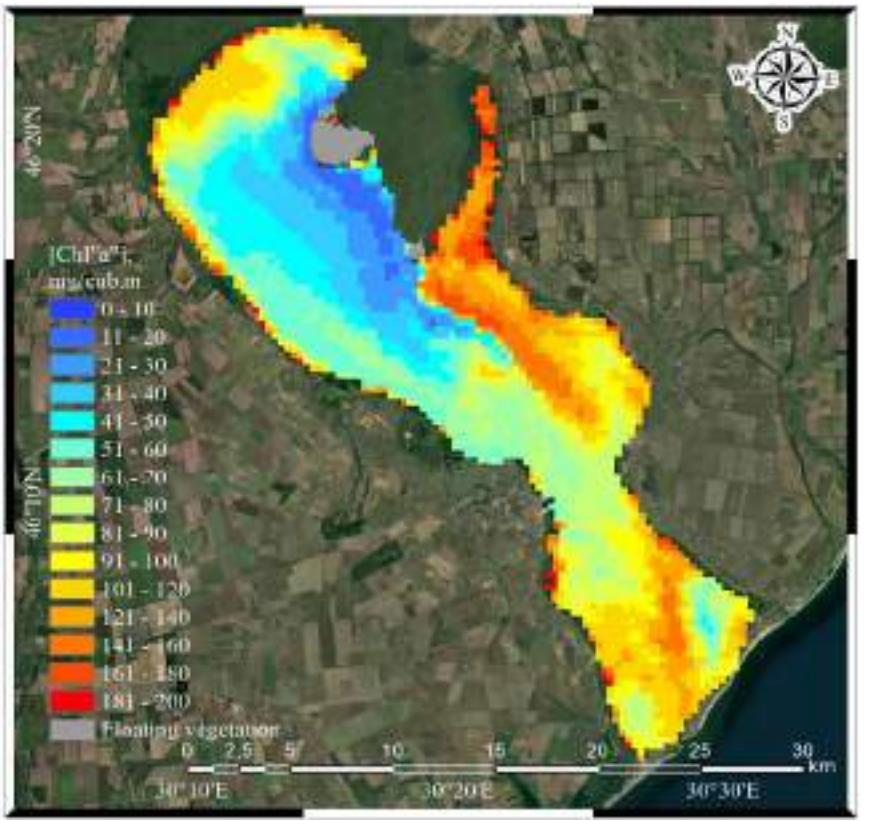

Figure 5.21. Chl"a" concentration (S3 bands - ONU calculation) in Dniester estuary for 20 August 2021

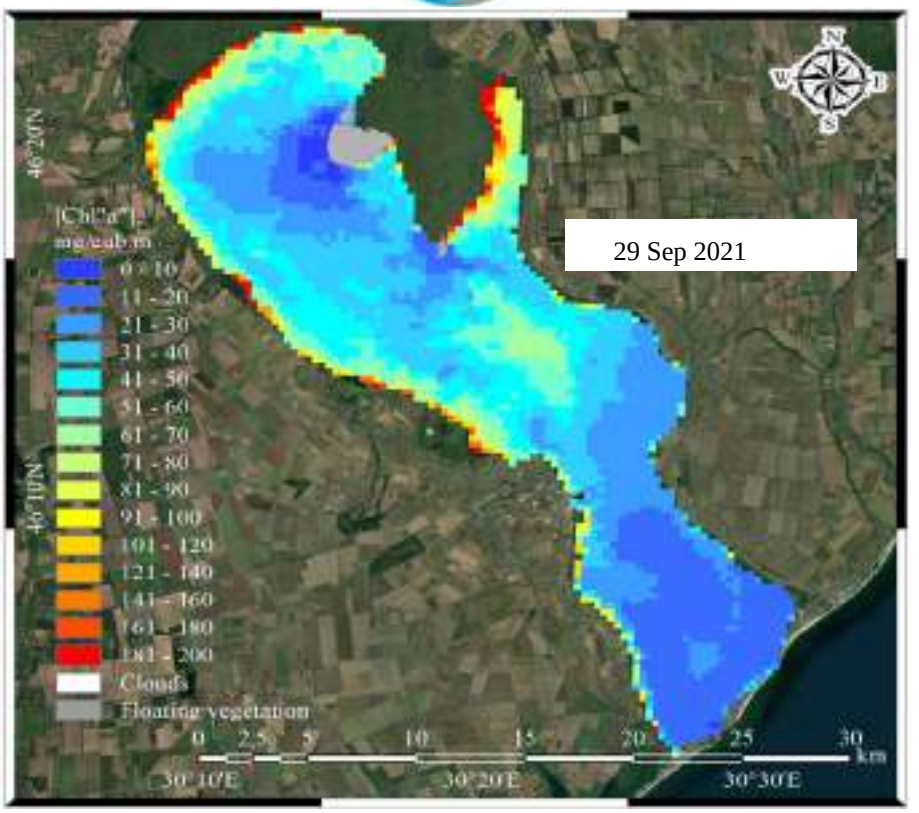

Figure 5.22. Chl"a" concentration (S3 bands - ONU calculation) in Dniester estuary for 29 September 2021

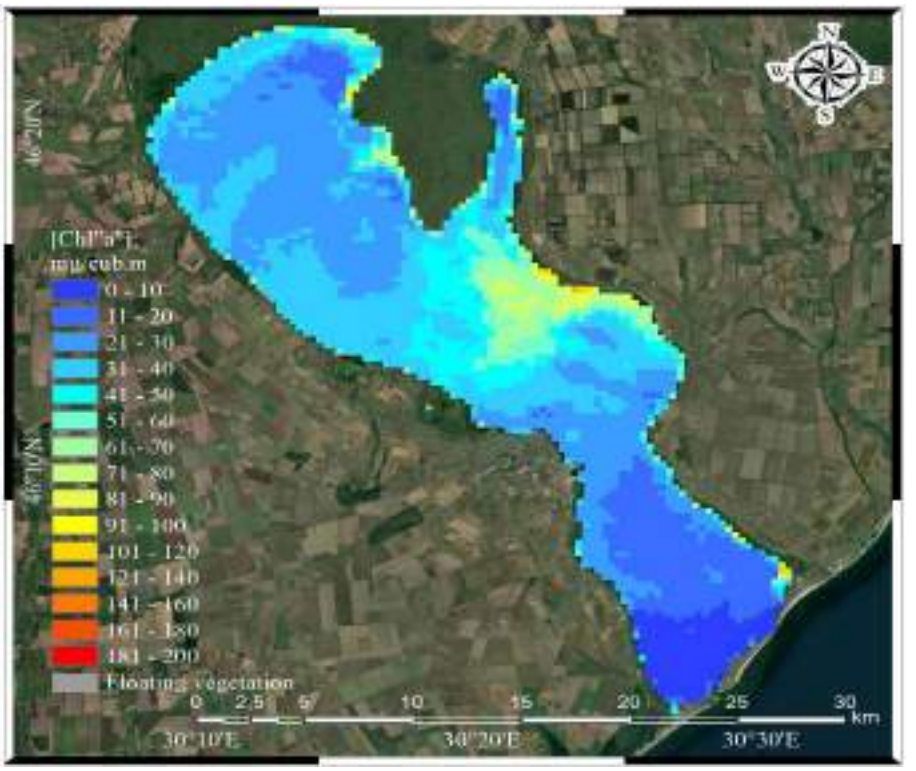

Figure 5.23. Chl"a" concentration (S3 bands - ONU calculation) in Dniester estuary for 21 October 2021

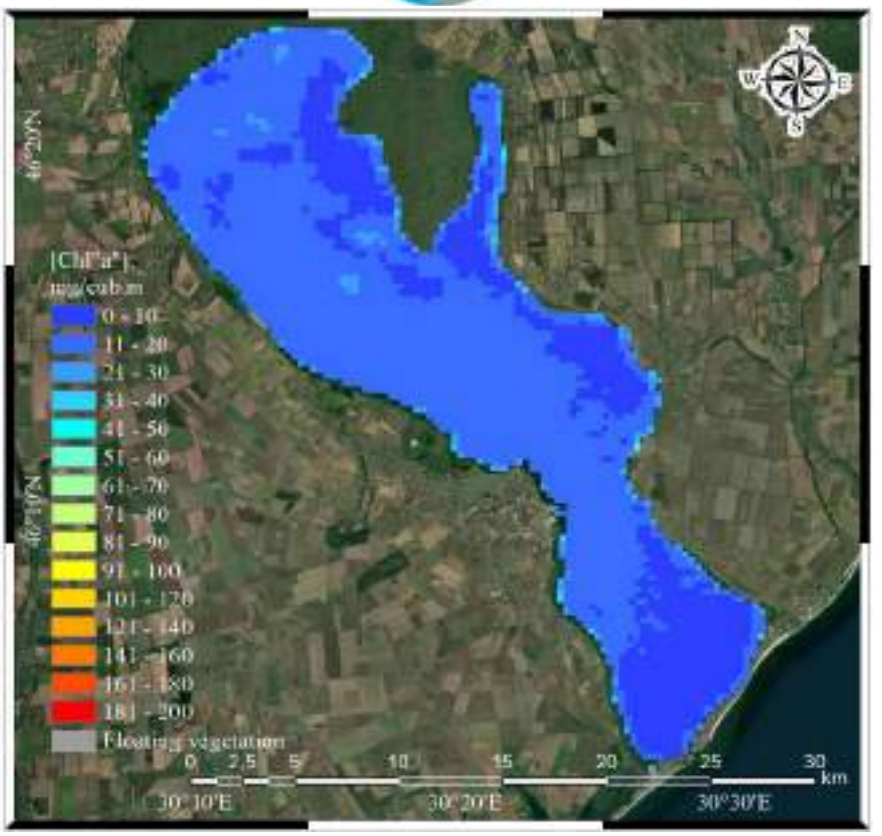

Figure 5.24. Chl"a" concentration (S3 bands - ONU calculation) in Dniester estuary for 21 November 2021

Analysis of the figures mentioned above showed that the chlorophyll concentrations' distribution in the estuary had a strongly-pronounced seasonal variation with maximal concentrations in July-August. At that the maxima of concentration in July were observed in the shallow northern part of the estuary, while in August they moved to the middle and southern parts reaching annual maximum in the Karagol Bay and the southern part of the estuary during August-September. Further on the concentration of chlorophyll was going down reaching its minimal values in November (Fig. 5.24).

5.1.2. Bile lake

Analysis of the chlorophyll concentrations distribution maps shown in Figures 5.25-5.27 showed that a sharp increase in chlorophyll concentration took place in the Bile Lake from April to July 2021.

The parallel studies of aquatic vegetation performed in 2021 showed that the areas with maximal chlorophyll concentrations, which we had identified in the most part of the lake, were not representative as they coincided with the areas covered with floating vegetation that we established using the aerial images taken by UAV to map the aquatic vegetation boundaries (Fig. 5.28)

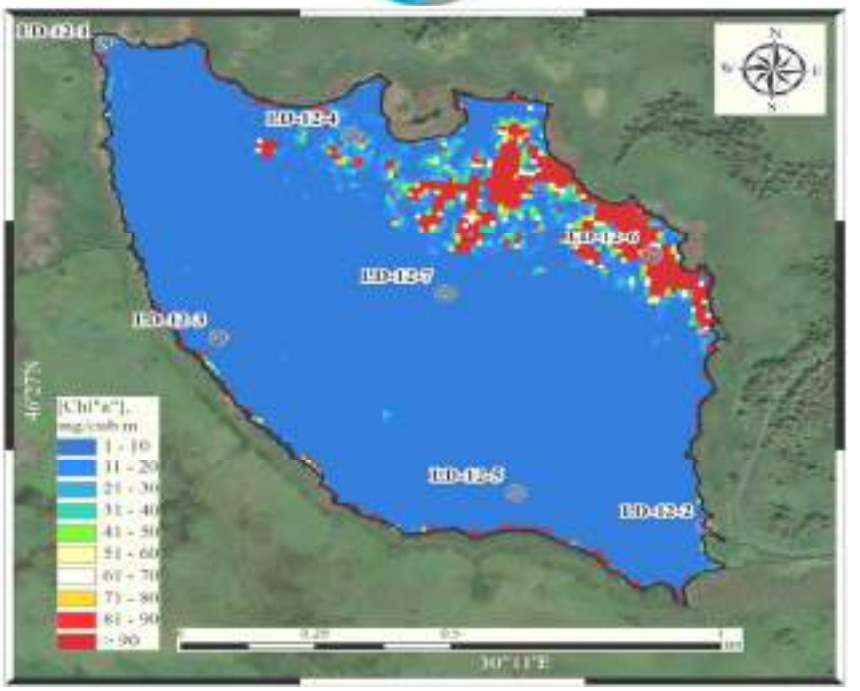

Figure 5.25. Chl-a concentration (S2 – ONU calculation) in Bile lake for 22 April 2021 (black line – the border of water pond)

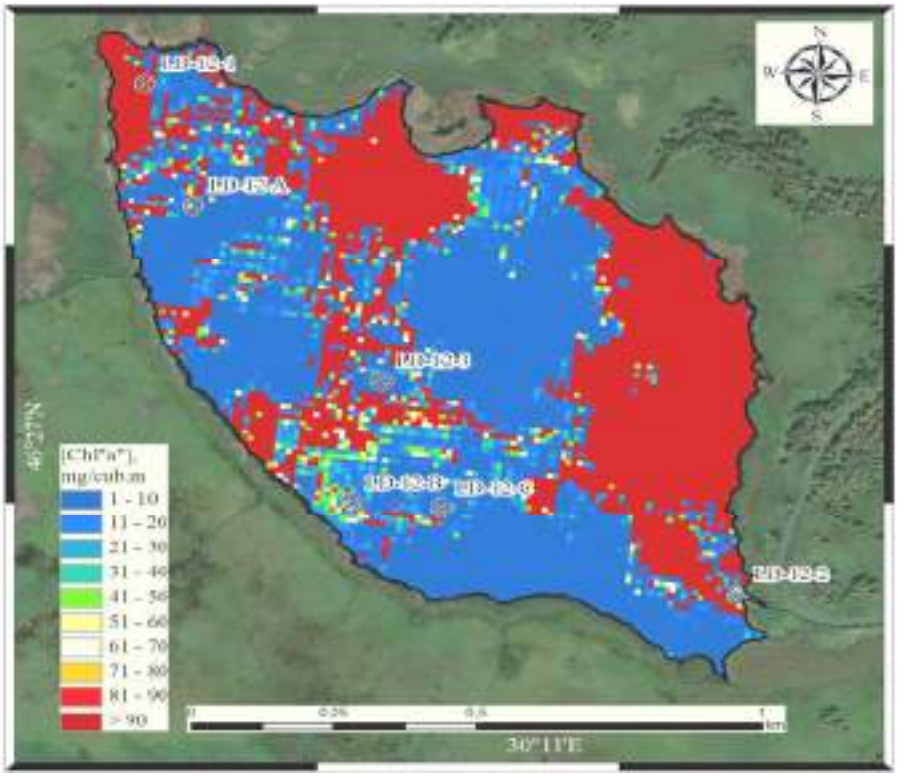

Figure 5.26. Chl-a concentration (S2 - ONU calculation) in Bile lake for 11 June 2021 (black line – the border of water pond)

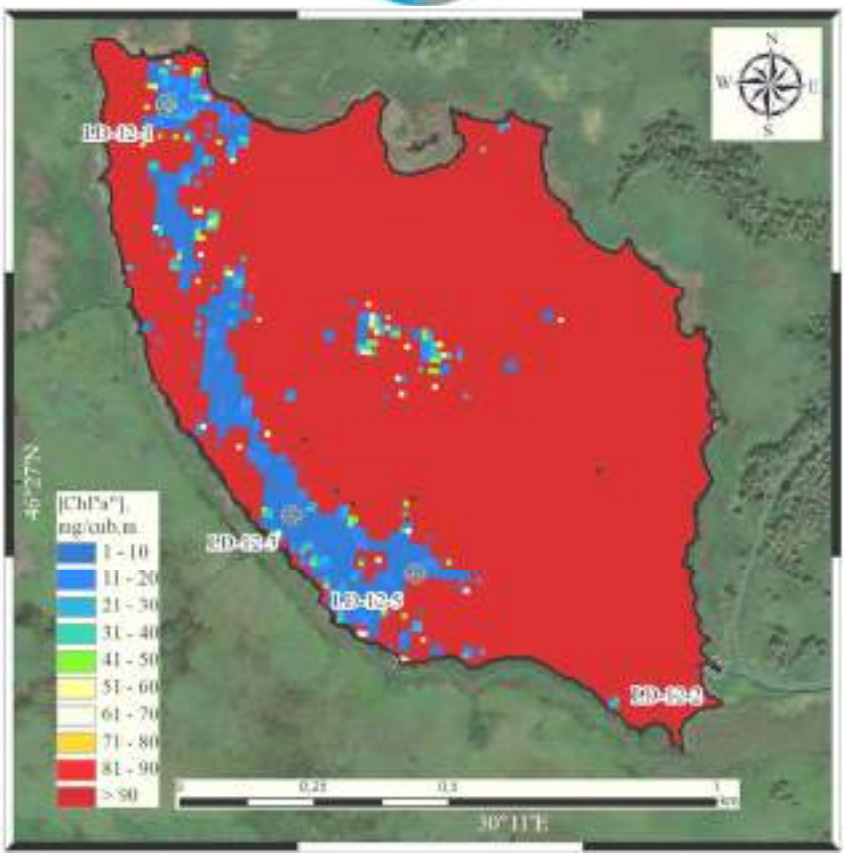

Figure 5.27. Chl-a concentration (S2 - ONU calculation) in Bile lake for 26 July 2021 (black line – the border of water pond)

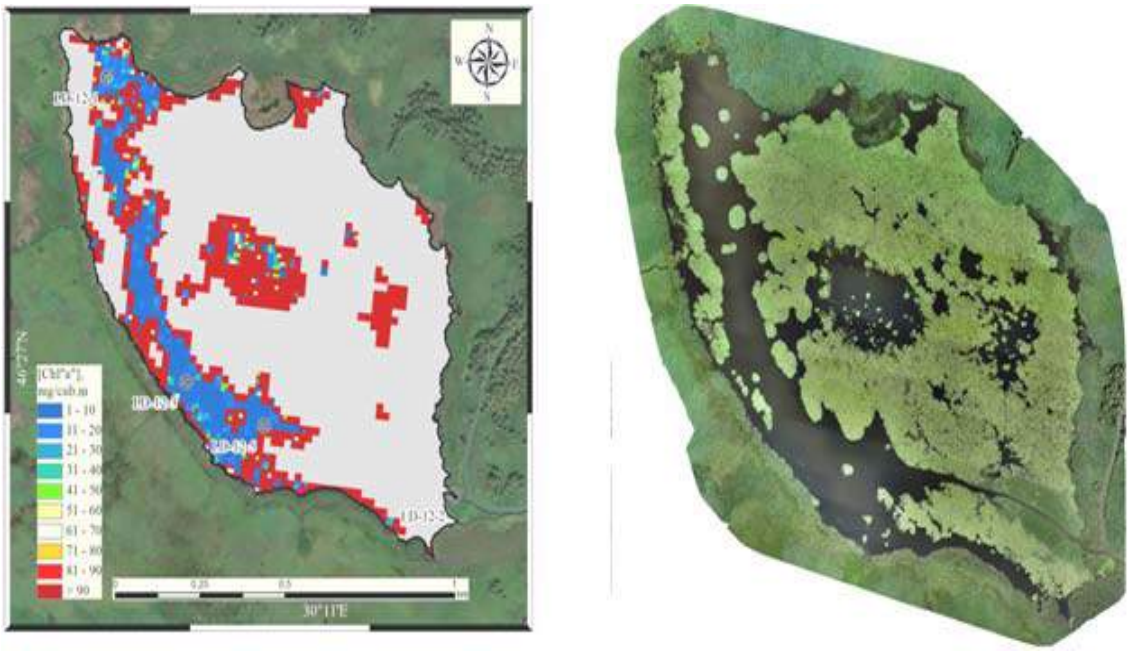

Figure 5.28. Real Chl-a concentration (S2 – ONU calculation left) after correction using floating vegetation mapping (right) in Bile lake for 26 July 2021 (grey colour – floating vegetation

At that, after the end of the aquatic plants vegetation period (Figures 5.29 and 5.30) the lake surface is clearing from the residues of aquatic vegetation and the chlorophyll concentration data obtained using the space images become representative again and the chlorophyll concentration decreases sharply to reach its minimal values.

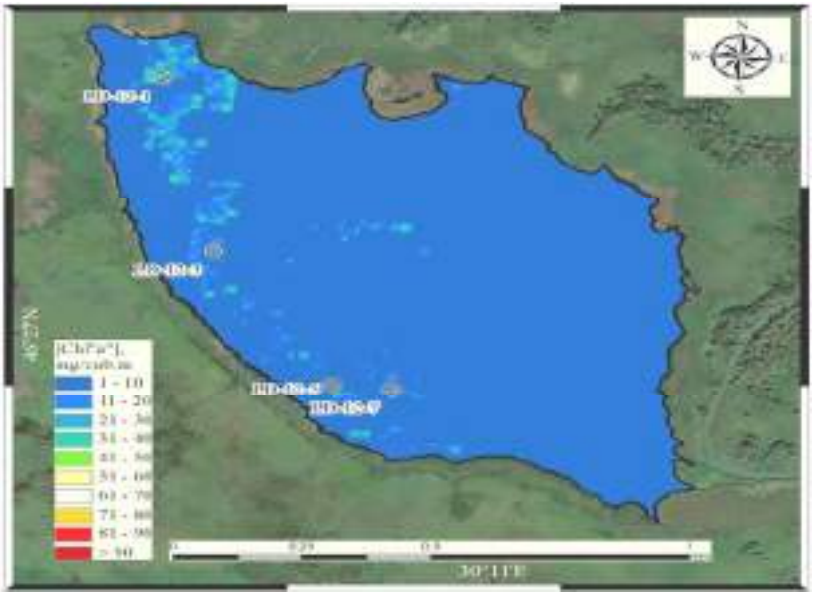

Figure 5.29. Chl-a concentration (S2 - ONU calculation) in Bile lake for 09 September 2021

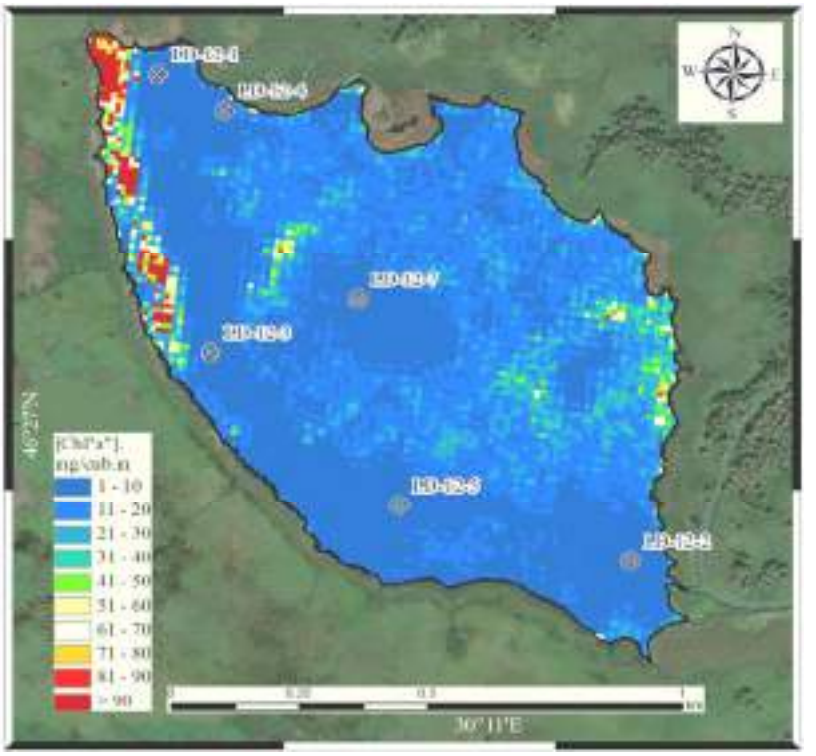

Figure 5.30. Chl-a concentration (S2 - ONU calculation) in Bile lake for 04 October 2021 (black line – the border of water pond)

To implement the approach consisting in exclusion of the water body areas covered with aquatic vegetation we had to change the final methodology of space images processing. We entered a mandatory recommendation for all the water bodies to have an obligatory preparation stage – mapping of the floating vegetation boundaries, and the areas covered with the vegetation should be excluded from consideration and analysis. After that we used this approach for all the water bodies under research, especially for studies of seasonal changes in chlorophyll concentration fields.

5.2. Seasonal changes of chlorophyll concentration fields in the Dniester Estuary

Study results and their discussion. The chlorophyll ***a*** concentrations for March – November 2021, calculated using the empirical algorithms for the LandSat 8, Sentinel-2 and Sentinel-3 space images described in Chapter 3, are presented in Figures 5.31 and 5.32.

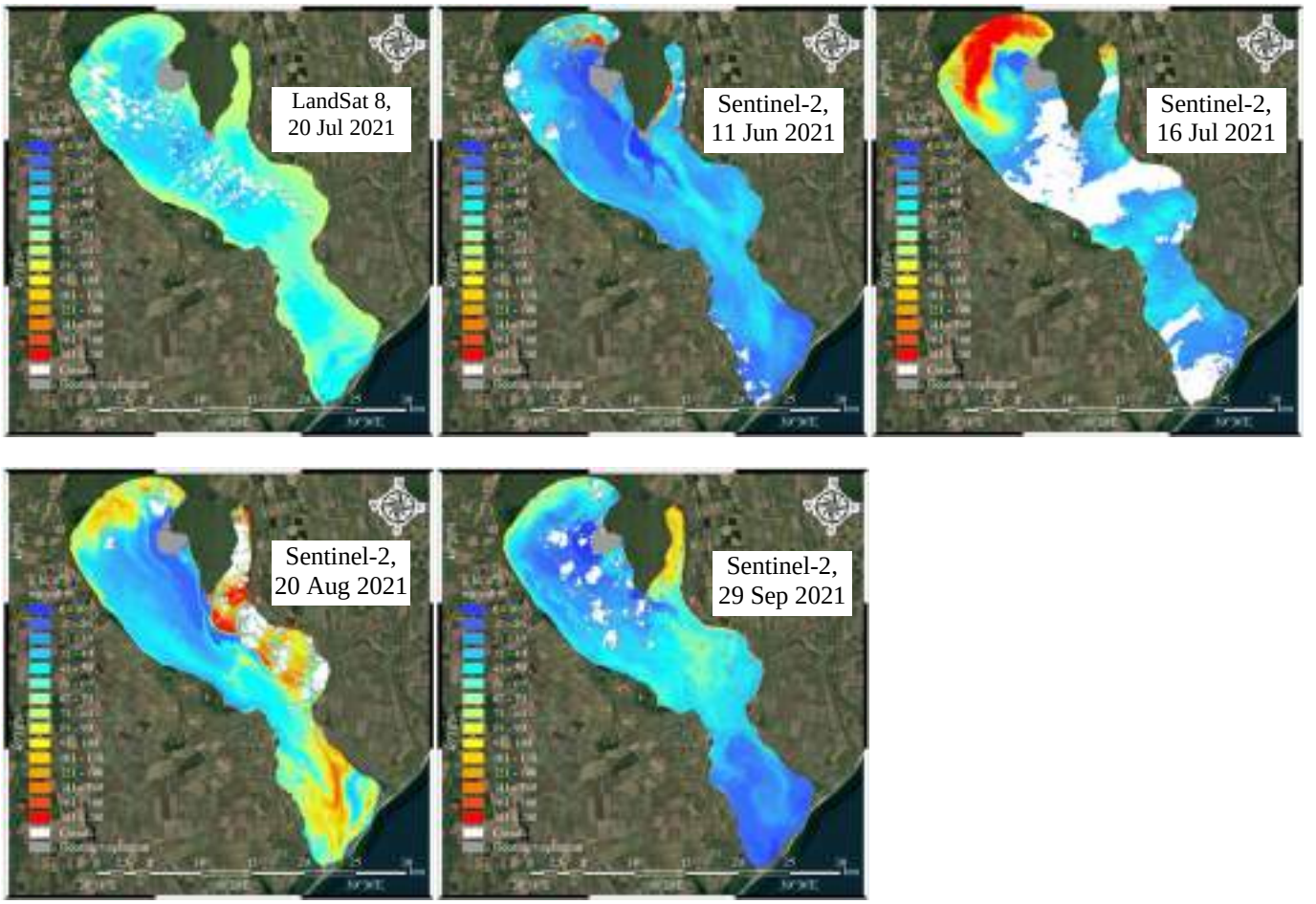

Figure 5.31. Seasonal spatial distribution of Chl"a" concentration in the Dniester estuary in 2021 using LandSat 8 and Sentinel-2 data (white color – clouds; grey color – floating vegetation)

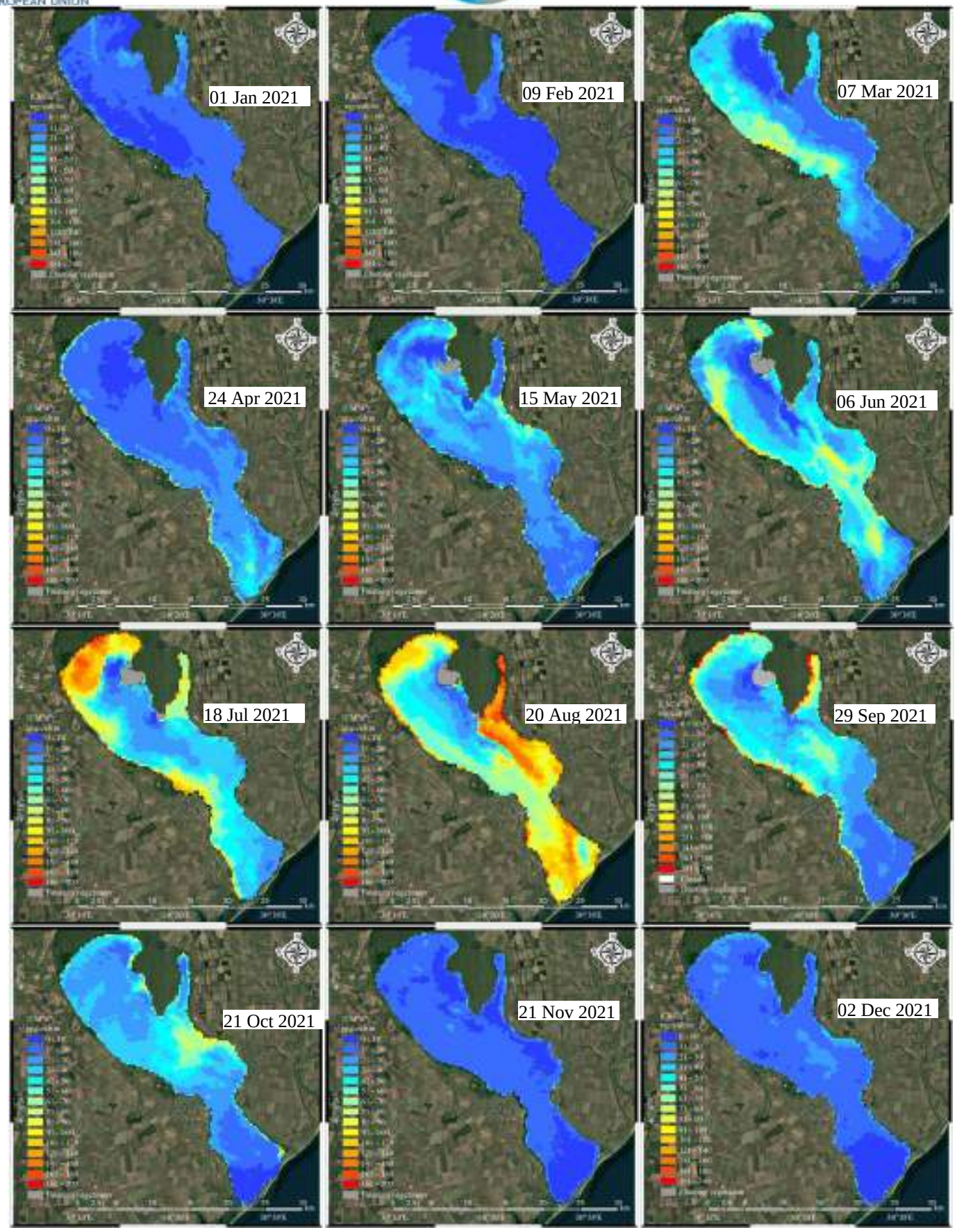

Figure 5.32. Seasonal spatial distribution of Chl"a" concentration in the Dniester estuary in 2021 usung Sentinel-3 data (grey color – floating vegetation)

Analysis of the chlorophyll ***a*** concentration maps presented above showed that the concentration variations in the Dniester Estuary water area in 2021 had a strongly-pronounced seasonal heterogeneity

Visual analysis of the maps of chlorophyll concentration distribution showed that minimal concentration was practically always registered near the zones where the river water mixed with estuarine (the mouth areas of the Dniester and Turunchuk Rivers), as well as near the areas where estuarine water was mixing with the Black Sea water that had higher salinity (southern part of the estuary). Zones of chlorophyll ***a*** maximal concentrations were registered in the summer period in the northern part of the estuary, near the banks in its middle part and in the vicinity of the deep (~ 4.5 m) navigable channel from Bilgorod-Dnistrovskyi Port to the Tsaregradske Arm and the adjacent part of the Black Sea (in April).

Qualitative estimation of mean chlorophyll ***a*** concentrations in the Dniester Estuary as a whole (Table 5.1) has shown the following.

Table 5.1. Average Statistical Characteristics of Chlorophyll ***a*** (mg/m^3) distribution in the Dniester Estuary Water in 2021

Date	Image	MINIMUM	MAXIMUM	MEAN	STDDEV
01.01.2021	S3A_OL_1_EFR_20210101T0839	5.38	45.17	13.24	4.50
09.02.2021	S3A_OL_1_EFR_20210209T0828	4.72	35.29	10.28	4.17
07.03.2021	S3B_OL_1_EFR_20210307T0815	5.14	107.31	30.01	18.43
24.04.2021	S3A_OL_1_EFR_20210424T0809	7.8	118.17	20.79	11.85
15.05.2021	S3B_OL_1_EFR_20210515T0826	6.22	129.22	27.39	13.13
11.06.2021	S2A_MSIL2A_20210611T0856	2.63	199.35	30.71	18.03
11.06.2021	S3B_OL_1_EFR_20210611T0826	4.74	155.25	40.64	20.6
16.07.2021	S2B_MSIL2A_20210716T0855	4.56	199.89	48.46	37.40
18.07.2021	S3A_OL_1_EFR_20210718T0806	7.67	199.11	55.41	35.75
20.07.2021	LC08_L1TP_180028_20210720	0,1	81.23	49.73	16.36
20.08.2021	S2A_MSIL2A_20210820T0856	3.8	199.96	59.46	36.35
20.08.2021	S3B_OL_1_EFR_20210820T0811	11.31	198.72	81.06	39.2
29.09.2021	S2A_MSIL2A_20210929T0857	3.11	198.78	36.77	21.96
29.09.2021	S3A_OL_1_EFR_20210929T0813	7.35	197.72	39.04	24.48
21.10.2021	S3B_OL_1_EFR_20211021T0804	4.93	129.15	31.38	15.29
21.11.2021	S3B_OL_1_EFR_20211121T0800	5.46	50.24	12.92	4.33
02.12.2021	S3B_OL_1_EFR_20211202T0815	3.67	53.38	14.55	5.92

The minimal values of chlorophyll concentration averaged for the entire estuary were within the limits from 10.28 to 14.55 mg /m^3 and registered in winter period (January - February, end of November – December 2021) with absolute minimum (10.28 mg/m^3) in February 2021. High values of the averaged

for the whole estuary chlorophyll ***a*** concentration (36.77 – 81.06 mg/m^3) were typical of the summer-autumn period (June - September) with absolute maximum (81.06 mg/m^3) in August 20221.

Keeping in mind that the cloud-covered areas of different size were found on practically all the Sentinel 2 and Landsat 8 images, the data on which were presented in Table 5.1 and Fig. 5.32, we excluded those images from the further consideration and analysis.

For the purpose of comparison of the data obtained as the result of the images processing with our historical data collected in 2003-2020 we applied the method of the estuary water area division into three parts: northern, central and southern, as we did in our previous studies (Fig. 5.33). The method was based on the difference in hydrological and hydrochemical processes that formed the main hydromorphological, hydrophysical and hydrochemical conditions in those estuarine areas.

Figure 5.33. Historical sampling and observations stations network during 2003-2021 and borders of three (northern. middle and southern) parts of Dnietsr Estiary .

The analysis of average statistical characteristics of chlorophyll concentration's spatiotemporal distribution performed separately for the northern, middle and southern parts of the estuary (Tables 5.2 – 5.5. and Fig. 5.34) has shown the following.

Table 5.2. Statistical characteristics of the chlorophyll ***a*** concentrations (mg/m^3) averaged for the entire Dniester Estuary water area using the Sentinel-3 space images for 2021

Date	Image	MINIMUM	MAXIMUM	MEAN	STDDEV	Area without floating vegetation, sq.km	Total water area of Dniester liman, sq.km
01.01.2021	S3A_OL_1_EFR_20210101T0839	5,38	45,17	13,24	4,50	358,48	358,48
09.02.2021	S3A_OL_1_EFR_20210209T0828	4,72	35,29	10,28	4,17	357,88	357,88
07.03.2021	S3B_OL_1_EFR_20210307T0815	5,14	107,31	30,01	18,43	371,19	371,19
24.04.2021	S3A_OL_1_EFR_20210424T0809	7,8	118,17	20,79	11,85	371,04	371,04
15.05.2021	S3B_OL_1_EFR_20210515T0826	6,22	129,22	27,39	13,13	363,67	367,15
11.06.2021	S3B_OL_1_EFR_20210611T0826	4,74	155,25	40,64	20,6	349,27	355,98
18.07.2021	S3A_OL_1_EFR_20210718T0806	7,67	199,11	55,41	35,75	348,68	355,83
20.08.2021	S3B_OL_1_EFR_20210820T0811	11,31	198,72	81,06	39,2	342,17	348,16
29.09.2021	S3A_OL_1_EFR_20210929T0813	7,35	197,72	39,04	24,48	357,77	363,39
21.10.2021	S3B_OL_1_EFR_20211021T0804	4,93	129,15	31,38	15,29	358,17	358,17
21.11.2021	S3B_OL_1_EFR_20211121T0800	5,46	50,24	12,92	4,33	358,10	358,10
02.12.2021	S3B_OL_1_EFR_20211202T0815	3,67	53,38	14,55	5,92	372,10	372,10
Annual average value		6,20	118,23	31,39	16,47	359,04	361,46

Table 5.3. Statistical characteristics of the chlorophyll ***a*** concentrations (mg/m^3) averaged for the northern part of the entire Dniester Estuary water area using the Sentinel-3 space images for 2021

Date	Image	MINIMUM	MAXIMUM	MEAN	STDDEV	Area without floating vegetation, sq.km	Total water area, sq.km
01.01.2021	S3A_OL_1_EFR_20210101T0839	5,38	38,98	14,32	5,51	141,81	141,81
09.02.2021	S3A_OL_1_EFR_20210209T0828	4,72	33,76	11,91	5,29	140,98	140,98
07.03.2021	S3B_OL_1_EFR_20210307T0815	6,68	78,54	28,18	15,87	148,48	148,48
24.04.2021	S3A_OL_1_EFR_20210424T0809	7,80	118,17	16,08	10,76	146,71	146,71
15.05.2021	S3B_OL_1_EFR_20210515T0826	6,22	129,22	29,81	15,69	143,65	147,13
11.06.2021	S3B_OL_1_EFR_20210611T0826	4,74	119,87	35,36	20,68	133,19	139,90
18.07.2021	S3A_OL_1_EFR_20210718T0806	7,67	197,49	72,92	45,37	134,26	141,41
20.08.2021	S3B_OL_1_EFR_20210820T0811	11,31	198,72	69,94	44,76	125,73	131,73
29.09.2021	S3A_OL_1_EFR_20210929T0813	7,36	197,72	43,71	28,51	135,76	141,76
21.10.2021	S3B_OL_1_EFR_20211021T0804	15,70	93,43	31,37	11,15	139,33	139,33
21.11.2021	S3B_OL_1_EFR_20211121T0800	6,51	37,47	12,70	4,26	142,20	142,20
02.12.2021	S3B_OL_1_EFR_20211202T0815	5,65	48,98	16,12	5,07	150,33	150,33
Annual average value		7,48	107,7	31,87	17,74	140,20	142,65

Table 5.4 Statistical characteristics of the chlorophyll ***a*** concentrations (mg/m^3) averaged for the meddle part of the entire Dniester Estuary water area using the Sentinel-3 space images for 2021

Date	Image	MINIMUM	MAXIMUM	MEAN	STDDEV	Water area without floating vegetation, sq.km	Total water area, sq,km
01.01.2021	S3A_OL_1_EFR_20210101T0839	6,80	45,17	12,08	3,97	140,57	140,57
09.02.2021	S3A_OL_1_EFR_20210209T0828	6,13	30,62	9,67	2,86	140,58	140,58
07.03.2021	S3B_OL_1_EFR_20210307T0815	10,26	107,31	38,19	20,57	143,61	143,61
24.04.2021	S3A_OL_1_EFR_20210424T0809	9,86	118,09	19,85	9,02	144,27	144,27
15.05.2021	S3B_OL_1_EFR_20210515T0826	11,66	128,61	28,25	10,33	141,67	141,67

Date	Image	MINIMUM	MAXIMUM	MEAN	STDDEV	Water area without floating vegetation, sq,km	Total water area, sq,km
11.06.2021	S3B_OL_1_EFR_20210611T0826	5,70	155,25	46,53	20,12	139,21	139,21
18.07.2021	S3A_OL_1_EFR_20210718T0806	14,23	199,11	46,04	23,74	138,68	138,68
20.08.2021	S3B_OL_1_EFR_20210820T0811	18,57	198,53	80,40	36,18	139,52	139,52
29.09.2021	S3A_OL_1_EFR_20210929T0813	20,33	187,02	43,36	18,05	142,80	142,80
21.10.2021	S3B_OL_1_EFR_20211021T0804	16,96	129,15	39,46	14,74	141,42	141,42
21.11.2021	S3B_OL_1_EFR_20211121T0800	7,36	50,24	14,41	3,75	139,36	139,36
02.12.2021	S3B_OL_1_EFR_20211202T0815	7,97	49,01	15,45	5,03	142,26	142,26
Annual average value		11,32	116,51	32,81	14,03	141,16	141,16

Table 5.5. Statistical characteristics of the calculated rasters of chlorophyll ***a*** concentration (mg/m^3) in the southern part of the Dniester Estuary from the Sentinel-3 space images for 2021

Date	Image	MINIMUM	MAXIMUM	MEAN	STDDEV	Water area without floating vegetation, sq,km	Total water area, sq,km
01.01.2021	S3A_OL_1_EFR_20210101T0839	5,93	25,35	13,30	2,12	76,09	76,09
09.02.2021	S3A_OL_1_EFR_20210209T0828	5,25	35,29	8,42	2,37	76,31	76,31
07.03.2021	S3B_OL_1_EFR_20210307T0815	5,14	47,16	18,14	9,13	79,10	79,10
24.04.2021	S3A_OL_1_EFR_20210424T0809	16,10	109,84	31,03	12,01	80,05	80,05
15.05.2021	S3B_OL_1_EFR_20210515T0826	8,65	73,57	20,42	6,60	78,35	78,35
11.06.2021	S3B_OL_1_EFR_20210611T0826	14,82	152,63	39,11	18,44	76,87	76,87
18.07.2021	S3A_OL_1_EFR_20210718T0806	18,88	167,71	42,04	18,73	75,74	75,74
20.08.2021	S3B_OL_1_EFR_20210820T0811	49,05	191,46	100,34	24,90	76,91	76,91
29.09.2021	S3A_OL_1_EFR_20210929T0813	9,80	189,18	21,80	15,75	79,05	79,05
21.10.2021	S3B_OL_1_EFR_20211021T0804	4,93	106,33	16,52	10,86	77,42	77,42
21.11.2021	S3B_OL_1_EFR_20211121T0800	5,46	35,39	10,41	3,85	76,54	76,54
02.12.2021	S3B_OL_1_EFR_20211202T0815	3,67	39,37	9,42	5,40	79,51	79,51
Annual average value		12,31	97,77	27,58	10,85	77,66	77,66

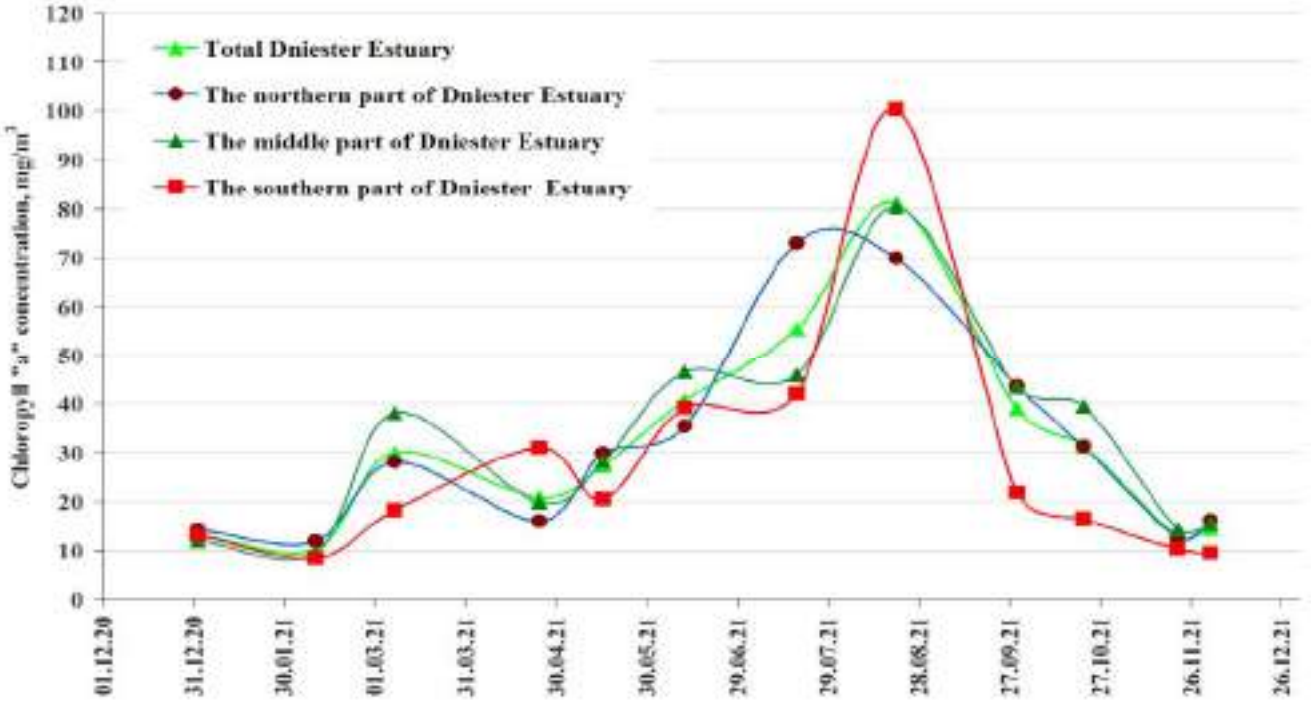

Figure 5.34. *Seasonal distribution of Chl"a" concentration in the Dniester estuary in 2021 calculated with empirical ONU algorithm using of TOA of Sentinel-3*

The minimal values of chlorophyll concentration averaged for the entire estuary (10.28 to 14.55 mg/m^3) were observed in winter period (January - February, end of November – December 2021) with the absolute minimum (10.28 mg/m^3) in February 2021 (Table 5.2 and Fig. 5.35). High values of chlorophyll ***a*** concentration averaged for the entire estuary (36.77 – 81.06 mg/m^3) were typical of summer-autumn period (June - September) with absolute maximum (81.06 mg/m^3) in August 20221. At that, in the period from January to August, a pseudo-monotone increase in the chlorophyll concentration averaged for the entire water area was observed, from 13.2 and 10.28 mg/m^3 in January and February respectively to 81.06 mg/m^3 with subsequent gradual decrease to 12.92 and 14.55 in November and December respectively.

Keeping in mind that water temperature in the estuary was changing similarly, with maximum in August and minimum in January – February, we may conclude that the seasonal changes in water temperature are the main driver of eutrophication processes. Year average chlorophyll ***a*** concentration (averaged for the whole water area of the estuary) made 31.39 mg/m^3, which showed that in general the Dniester Estuary, where the average annual chlorophyll concentration exceeded in all months the established by us eutrophication level of 10 mg/m^3, was eutrophic water body according to all criteria and the chlorophyll concentration during summer periods was reaching the hypertrophic level.

Comparison of the chlorophyll concentrations averaged for the specified parts of the estuary in 2021 (Tables 5.3 – 5.5) showed that they practically coincided with the concentration averaged for the entire estuary (31.39 mg/m^3, see Table 5.2) and made 31.87, 32.81 and 27.58

mg/m^3 for the northern, central and southern parts of the estuary. This evidences that the average annual chlorophyll concentration in all parts of the Dniester Estuary and in all months exceeds the established by us eutrophication level of 10 mg/m^3, which shows that all parts of the estuary are eutrophic, and the level of chlorophyll concentration in summer periods reaches the hypertrophic level in all estuary parts.

Distribution of chlorophyll a concentration in the central part of the estuary (Table 5.4 and Fig. 5.34) was the most similar to distribution of the averaged for the whole Dniester Estuary chlorophyll ***a*** concentration (mg/m^3). Minimal values of the chlorophyll concentration averaged for the Dniester estuary (9.67 to 15.45 mg/m^3) were observed during winter period (January-February, end of November-December 2021) with absolute minimum (9.67 mg/m^3) in February 2021. High values of chlorophyll ***a*** concentration averaged for the entire estuary (39.46 - 80.40 mg/m^3) were typical of summer-autumn period (June-October) with absolute maximum (80.40 mg/m^3) in August 2021.

In the north of the estuary the minimal values of chlorophyll concentrations averaged for this part of the estuary (11.91-16.12 mg/m^3) were registered in winter period (January-February, end of November – December 2021) with absolute maximum (11.91 mg/m^3) in February 2021, which exceeded insignificantly the minimums of concentration in the central part and all over the estuary. High values of chlorophyll ***a*** concentration averaged for the whole estuary (31.37 – 72.24 mg/m^3) were typical of summer-autumn period (June - October) with absolute maximum (72.24 mg/m^3) in July 2021. It should be pointed out that the maximal values of chlorophyll concentration were registered in the northern part of the estuary one month before than in the other parts and in the whole estuary in general.

Both minimal and maximal concentrations of chlorophyll were registered in the southern part of the estuary. The minimal averaged concentration in the southern part (9.42 – 13.30 mg/m^3) were observed in January-February and November-December 2021 with absolute minimum of 9.42 mg/m^3 in February 2021. The maximal averaged for the southern part of the estuary concentration (100.34 mg/m^3) was registered in August 2021. The general picture of chlorophyll concentration seasonal variations in the southern part of the estuary was similar to the concentration variations in other parts of the estuary.

5.3. Eutrophication Dynamics in the Dniester Estuary

To study the eutrophication dynamics (long-term changes) in the northern, middle and southern parts of the Dniester Estuary we used historical data with chlorophyll concentrations from the annual surveys performed by Odessa I.I. Mechnikov University for the period from 2003 to 2020, the main results of which are illustrated in Figure 5.35.

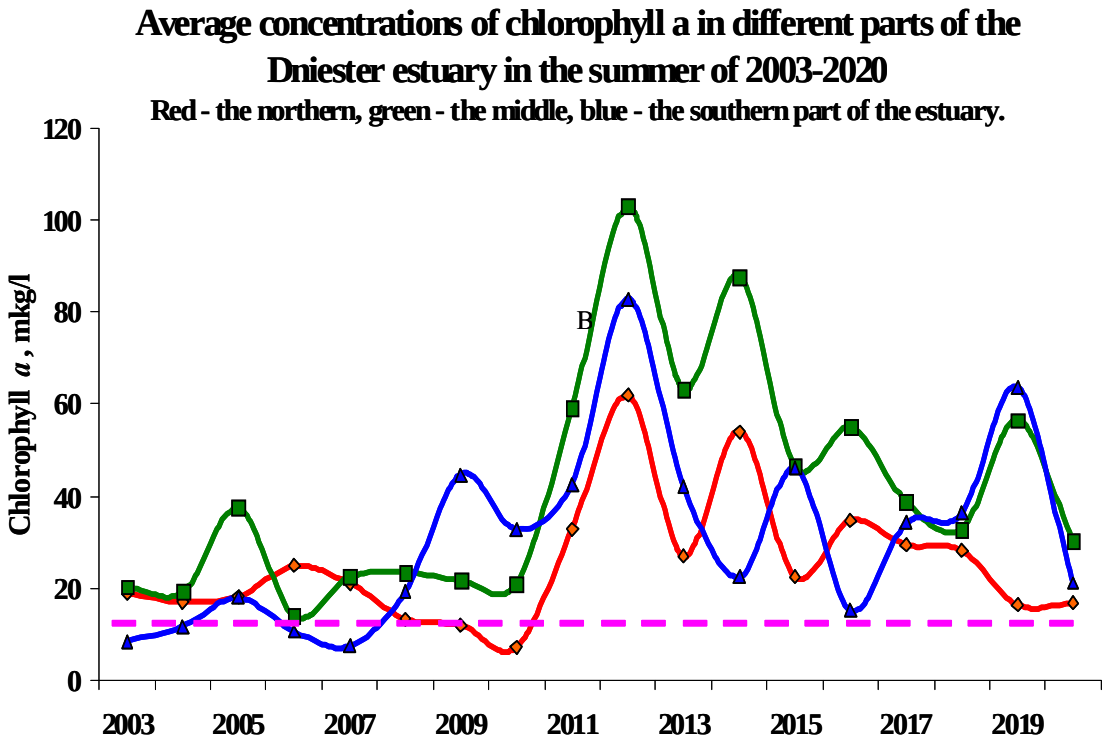

Fugure 5.35. Average concentrations of chlorophyll a in northern. middle and southern parts of Dnister Estuary in 2003-2020 (ONU historical data).
Pink line – level of eutrophication 10 mg/m^3

The dynamics of chlorophyll concentrations in summer periods of 2003-2020 averaged for different parts of the estuary (Fig. 5.35) was characterized as follows.

From 2003 to 2010, the average concentrations of chlorophyll in all parts of the Dniester Estuary varied from 5 to 40 mg. At the same time, in some years the average levels of chlorophyll concentration in certain parts of the estuary were below the level of eutrophication (10 mg/m3): in the southern part - in 2003 and 2007, in the northern part - in 2020.

After the abnormal floods of 2011-2012, the absolute maximum of chlorophyll concentration was observed in 2012, when it reached 100, 80 and 60 mg/m^3 for the middle, southern and northern parts of the estuary respectively. This effect was caused by huge inflow of nutrient-enriched suspended matter washed away from the catchment area during the flood

and deposited in the Dniester Estuary. Then, from 2013 to 2020, the chlorophyll concentration decreased monotonically to the level of 12–60 mg/m^3 in 2020 as the deposited nutrients accumulated during the floods of 2011–2012 were consumed. Comparison between the historical data and our data for July 2021 (Fig. 5.35) showed that the chlorophyll concentrations in the northern (72.92 mg/m^3), in central (46.04 mg/m3) and in southern parts (42.04 mg/m3) of the estuary were slightly higher than in 2020. They were at the level of 2019 and did not exceed the maximum chlorophyll concentrations observed in 2012. However, the average concentrations in all parts of the estuary were above the level of eutrophication (10 mg/m^3).

The dynamics of changes in the average values of phytoplankton biomass in different parts of the Dniester Estuary (Fig. 5.36) in 2003-2020 generally confirms that there are two periods of eutrophication processes development in the estuary: the first - from 2003 to 2010, when the minimum concentrations of phytoplankton biomass in the range from 5 to 50 mg/l were observed, and the second - from 2011 to 2020, when the phytoplankton biomass levels significantly exceeded the eutrophication levels (10 mg/l).

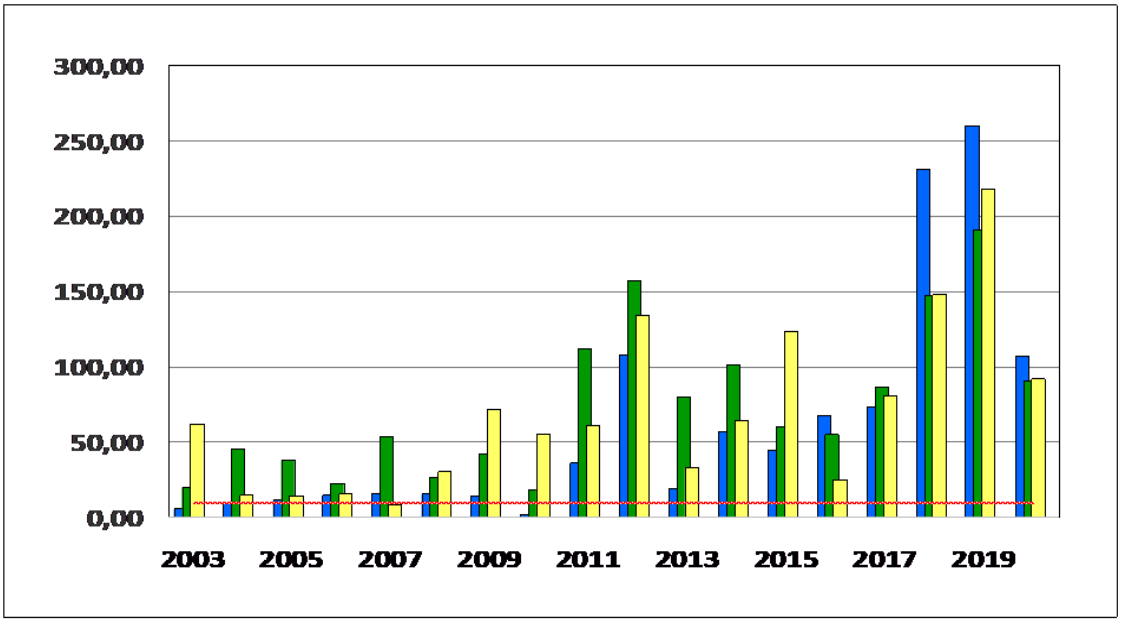

Figure 5.36. Average values of Biomass of phytoplankton (mg/l) in Dniester estuary in 2003-2020. Blue - the northern. green - the middle. yellow - the southern part of the estuary. Red line – level of phytoplankton bloom (10 mg/l)

Moreover, it should be noted that there was a steady increase in phytoplankton biomass during summer time in the second period, reaching the values of 200-250 mg/l in all parts of the estuary in 2019.

In addition, we studied the dynamics of the eutrophic status achieving by the Dniester Estuary water in 2021. We performed the analysis of seasonal dynamics in the Dniester Estuary areas, where the eutrophication exceeded the level of 10 mg/m^3 in 2021. The analysis was based on the results of processing the Sentinel 3 satellite images from January to December 2021 (Fig. 5.37. Table 5.6) and showed the following.

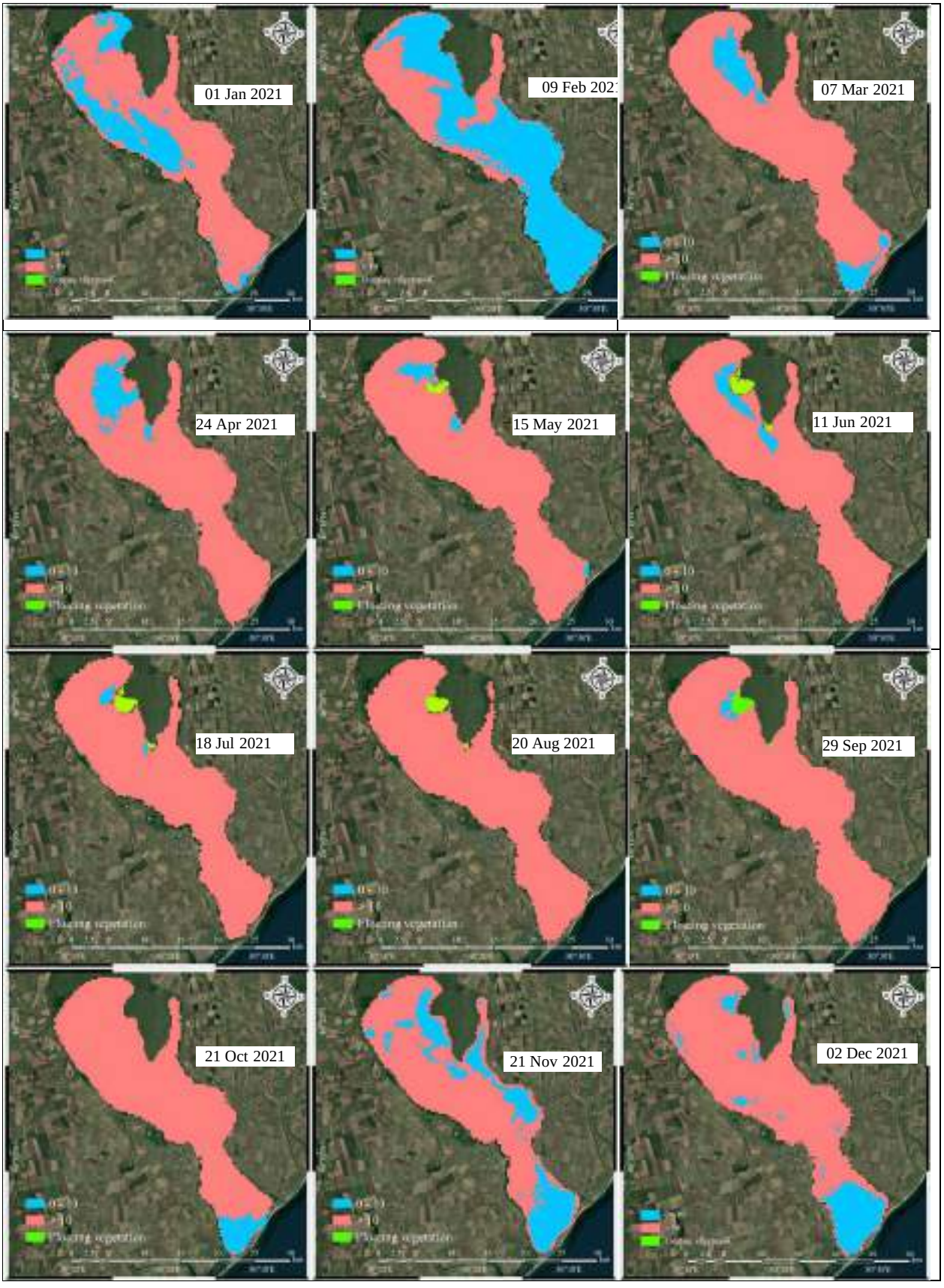

Figure 5.37. Seasonal evolution of the Dniester estuary waters eutrophication in 2021 in accordance to ONU calculation on Sentinel-3 data

Table 5.6. Seasonal dynamics of Dniester Estuary with different levels of eutrophication and squares of water floating vegetation in 2021

№	Date	Image for calculation	Area of clouds over Dniester liman, sq,km	Area of clouds over Dniester liman, %	Area of floating vegetation in Dniester liman, sq,km	Area of floating vegetation in Dniester liman, %	Area of Dniester liman with [Chl"a"] < 10 mg/cub,m,, sq,km	Area of Dniester liman with [Chl"a"] < 10 mg/cub,m,, %	Area of Dniester liman with [Chl"a"] > 10 mg/cub,m,, sq,km	Area of Dniester liman with [Chl"a"] > 10 mg/cub,m,, %	Total area of Dniester liman, sq,km
1	01.01.21	S3A_OL_1_EFR_20210101T0839	-	-	0.00	0.0	86.15	24.0	272.33	76.0	358.48
2	09.02.21	S3A_OL_1_EFR_20210209T0828	-	-	0.00	0.0	233.51	65.2	124.37	34.8	357.88
3	07.03.21	S3B_OL_1_EFR_20210307T0815	-	-	0.00	0.0	41.31	11.1	329.88	88.9	371.19
4	24.04.21	S3A_OL_1_EFR_20210424T0809	-	-	0.00	0.0	32.67	8.8	338.37	91.2	371.04
5	15.05.21	S3B_OL_1_EFR_20210515T0826	-	-	3.48	0.9	10.87	3.0	352.80	96.1	367.15
6	11.06.21	S3B_OL_1_EFR_20210611T0826	-	-	6.71	1.9	16.30	4.6	332.97	93.5	355.98
7	18.07.21	S3A_OL_1_EFR_20210718T0806	-	-	7.15	2.0	4.25	1.2	344.43	96.8	355.83
8	20.08.21	S3B_OL_1_EFR_20210820T0811	-	-	5.99	1.7	0.00	0.0	342.17	98.3	348.16
9	29.09.21	S3A_OL_1_EFR_20210929T0813	-	-	5.62	1.5	4.02	1.1	359.37	98.9	363.39
10	21.10.21	S3B_OL_1_EFR_20211021T0804	-	-	0.00	0.0	20.87	5.8	337.30	94.2	358.17
11	21.11.21	S3B_OL_1_EFR_20211121T0800	-	-	0.00	0.0	94.57	26.4	263.52	73.6	358.10
12	02.12.21	S3B_OL_1_EFR_20211202T0815	-	-	0.00	0.0	60.26	16.2	311.85	83.8	372.10

Waters of two trophic classes were identified in the Dniester estuary during 2021: mesotrophic and eutrophic.

The maximum area of mesotrophic water was observed in February 2021 (65.2% of the total area of the estuary), which then decreased to 0% in August and slightly rised reaching 26.4% in November and 16.2% in December 2021. The increase in the area of mesotrophic water during the cold season of the year indicated the leading role of water temperature in eutrophication processes development. At the same time, mesotrophic waters were observed mainly in the northern part of the estuary in spring period (March - April) and in the southern part of the estuary in autumn and winter (October - December).

The maximum areas of eutrophic waters in the Dniester Estuary were observed in July, August and September 2021 and made 96.8%, 98.3% and 98.9% of the total area respectively, while the minimum was registered in February 2021 (34.8% of the total area). At the same time, in the summer period (July – September) almost 100% of the estuary area was eutrophic, except for the areas covered with the floating aquatic vegetation. The maximum areas of the floating vegetation were observed in July (up to 7.2% of the total area of the estuary).

6. CONCLUSIONS AND RECOMMENDATIONS

During 2021-2022 we collected the data for **in the Ukrainian UA2 pilot site (2 subareas): 16** space images of Sentinel 2 (2017-2021). 7 - of Landsat 8 (2016-2021) and 19 - of Sentinel 3 (2017-2021 and historical data for Chlorophyll concentration and hydrology and hydrochemistry characteristics for 2003-2021. Field program in pilot areas (Dniester Estuary – 12 stations and Bile lake – 8 stations) was curried out in April. June. July. August. September and Octobber 2021 with total number of samples: Chl – 105. Hydrology observations – 200. Nutrients – 200. Oxygen – 200. Phytoplankton – 70. Bacteria – 70. The chlorophyll concentration calculations for pilot area UA2 (Bile lake and in Dniester Estuary) using SNAP platform and space images of Sentinel 2. Landsat 8 and Sentinel 3 was carried out for the period from 2016 to 2021. The concentration of chlorophyll and phytoplankton biomass data in a different parts of the Dniester Estuary were collected and analysed for historical interpretation of eutrophication processes in 2003-2020.

Comparison of SNAP data and experimental data for 2016-2021 showed that for all satellites the differences between values of SNAP and experimental data were very high (50-400%) with low correlations and this required us to find empirical algorithms to have more representative results of using space images data.

Using the data of Digital Numbers of reflectance spectrum bands from SNAP and ONU experimental field (in situ) data which were collected in 2021 we found the empirical algorithms for each type of satellites which were used for real calculations and mapping of chlorophyll concentration in Bile lake and in Dniester Estuary.

The methodology of chlorophyll concentartion dynamic assessment applied to assess the eutrophication intensity in Ukrainian pilot area PONTOS UA2 (in Bile lake and in Dniester Estuary) was based on processing historical satellite images, using remote sensing techniques and values (Digital Numbers) of reflectance spectrum bands from SNAP, developed empirical algorithms and GIS software as using of the SNAP methodology developed for marine areas does not help us receive adequate and reliable results on chlorophyll concentration. In reality, the information from the SNAP results on spectral characteristics of underlying surface can be only partially used for chlorophyll concentration further calculation. Finally we concluded that for each water body preliminary experimental studies should be performed in the days for which space images are available – to find the most effective (close) correlation interrelations between real chlorophyll concentrations and space images' spectral characteristics...

The analysis of Eutrophication intensity in historical retrospective showed that in 2003-2010 average concentrations in Dniester Estuary were in two time less as in the 2011-2020. In the same time periods the Biomass of phytoplankton increased in 7-10 times.

The estimation of chlorophyll concentrations using space images using SNAP intermediate results as Digital Numbers of reflectance spectrum bands and ONU empirical algorithms calculations showed the good convergence with experimental (in-situ) observations and such approach can be recommended for Dniester Estuary and Bile lake. For other water bodies it will be necessary to collect experimental data for recalibration only for concrete water body.

Taking in account the our experience 2021 about eligibility of space images different satellites without clouds which is connected with their frequency observations it was recommended for seasonal analysis of chlorophylls dynamics to use the Sentinel 3 images for Dniester Estuary. .

We recommended to introduce additional obligatory step in methodology of mapping of chlorophylls concentrations using the results the space images processing: it is necessary to exclude from final chlorophylls maps the areas with floating vegetations.

The seasonal analysis of intensity of eutrophication using chlorophyll concentration from space images processing for Dniester Estuary showed that maximal eutrophication was in summer (July – September) and minimal – in winter (January . February< November< December). Practically in all months expect February the concentrations of chlorophyll were more as 10 mg per litre (level of eutrophication).

7. REFERENCES

Ali K.. Witter D.. Ortiz J. (2013) Application of empirical and semi-analytical algorithmsto MERIS data for estimating chlorophyll a in Case 2 waters of Lake Erie // Environ Earth Sci. 2014. V. 71. P. 4209–4220. doi 10.1007 / s12665-013-2814-0

Ansper A.. Alikas K. (2019) Retrieval of Chlorophyll «a» from Sentinel-2 MSI Data for the European Union Water Framework Directive Reporting Purposes // Remote Sensing. 2019. V. 11. Iss. 1. P. 64.

Borum, J. (1996). 'Shallow waters and land/sea boundaries' in *Eutrophication in Coastal Marine Ecosystems. Eds: B.B. Jørgensen and K. Richardson. American Geophysical Union. pp. 179-205*.

Bricaud A. (2004) Natural variability of phytoplanktonic absorption in oceanic waters Influence of the size structure of algal populations // Journal of Geophysical Research. V. 109doi:10.1029/2004JC002419.

Brockmann C., Doerffer R., Peters M., Stelzer K., Embacher S., Ruescas A. (2016) Evolution of the C2RCC neural network for Sentinel 2 and 3 for the retrieval of ocean colour products in normal and extreme optically complex waters // Proc. Living Planet Symp. 2016. ESA-SP. V. 740. P. 54.

Cairo C. et al. (2020) Hybrid chlorophyll-a algorithm for assessing trophic states of a tropical Brazilian reservoir based on MSI/Sentinel-2 Data // Remote Sens. 2020. V. 12. Article No. 40. doi: 10.3390/rs12010040

Cardoso A.C., Duchemin J., Magoarou P., Premazzi G. (2001) Criteria for the Identification of Freshwaters Subject to Eutrophication. Luxembourg: Office for Official Publications of the European Communities, 2001. 90 P. ISBN 92-894-0947-9.

Carlson R.E. (1977) A trofic state index for lakes/Limnology and Oceanography. 1977, 22. P. 361-369.

CoastColour (2022). CoastColour project of the European Space Agency. Internet resource: https://www.coastcolour.org

Dall'Olmo, G., and A. A. Gitelson (2005) Effect of bio-optical parameter variability on the remote estimation of chlorophyll-a concentration in turbid productive waters: Experimental results. Appl. Opt 44:412-22.

Doerffer R., Brockmann C. (2014) Consensus Case 2 Regional Algorithm Protocols. https://www.coastcolour.org/documents/DEL-26_Consensus_Case_2_Regional_Algorithm_Protocols_v1.0.pdf

DUTH (2022). Integrated assessment on chlorophyll concentration and eutrophication dynamics. Deliverable D.T1.2.5. PONTOS-GR (Greece). 163 p.

EEA (2019). Nutrient enrichment and eutrophication in Europe's seas Moving towards a healthy marine environment. EEA Report No 14/2019, European Environment Agency, 2019. 46 p. cm ISBN 978-92-9480-111-1 doi:10.2800/09264

ESA's Sentinel Applications Platform (SNAP) [https://sentinels.copernicus.eu/web/sentinel/-/esa-releases-new-and-improved-version-of-snap/1.2]

Gitelson A. et al. (2007) Remote chlorophyll-a retrieval in turbid, productive estuaries: Chesapeake Bay case study. Rem Sens Environ 109:464-72.

Gilerson, A., Gitelson, A.A., Zhou, J., Gurlin, D., Moses, W., Ioannou, I., Ahmed S.A. (2010) Algorithms for remote estimation of chlorophyll-a in coastal and inland waters using red and near infrared bands: Opt. Express, 18. 2010, p. 24109. 10.1364/oe.18.024109.

Gitelson A. et al. (2011) Remote Estimation of Chlorophyll-a Concentration in Inland. Estuarine. and Coastal Waters // Chapter of Advances in Environmental Remote Sensing. 2011.

Gitelson, A., Schalleset, J. (2007). Remote chlorophyll-a retrieval in turbid, productive estuaries: Chesapeake Bay case study. *Remote Sensing Environment*, 109 : 464-72.

Greenwood N, Devlin MJ, Best M, Fronkova L, Graves CA, Milligan A, Barry J and van Leeuwen SM (2019) Utilizing Eutrophication Assessment Directives From Transitional to Marine Systems in the Thames Estuary and Liverpool Bay, UK. *Front. Mar. Sci.* 6:116. doi: 10.3389/fmars.2019.00116

Hydrobiological regime (1992). Hydrobiological regime of the Dniester and its water bodies / L.A. Sirenko, N.Yu. Evtushenko, F. Komsrovskiy et.al.; Edited by Braginskiy L.P. Kyiv: Naukova Dumka, 1992. 356 p. (In Russian).

Kneubühler, M., Gemperli, Ch., Schläpfer, D., Zah, R., Itten, K. (2005). Determination of water quality parameters in Indian ponds using remote sensing methods. In: 4th EARsel workshop on Imaging Spectroscopy, Warsaw, Poland, 27 April 2005 - 30 April 2005. s.n., 301-315.

Kopelevich O.V. et al. (2015) Seasonal and interannual variability of the bio-optical characteristics of the waters of the surface layer of the Barents, White, Black and Caspian seas according to satellite data // Fundamentalnaya i prikladnaya gidrofizika. 2015. V. 8. No. 1. P. 7–16 (in Russian)

Kovalova N.V., Medinets V.I. (2012) Assessment of modern state of the Dniester Estuary waters using TSI and TRIX trophic indices./ Materials of All-Ukrainian Scientific and Practical Conference "Estuaries of the North-Western Black Sea Area: Urgent Hydro-ecological problems and the ways to solve them". 12-14 Sept. 2012, Odesa: Odesa State Environmental University, 2012. – P. 94-97. (In Ukrainian).

Kovalova N.V., Medinets V.I. (2015) Integrated assessment of marine coastal waters quality at the Zmiinyi Island shoress / Proceedings of Ternopil State V. Gnatyuk Pedagogical University. Series Biology, Special Issue: Hydroecology. 2015. № 3-4 (64). P. 317-320. (In Ukrainian).

Kovalova N.V., Medinets V.I., Konareva O.P., Snigirov S.M., Medinets S.V., Soltys I.E. (2010) Hydroecologcal research monitoring of the Lower Dniester basin: Proceedings of Ternopil State V. Gnatyuk Pedagogical University. Series Biology, Special Issue: Hydroecology. – 2010. – № 3(44). – P. 113-116. ISSN 2078-2357. (In Ukrainian).

Kovalova N.V., Medinets V.I., Medinets S.V. (2018) Trophic status of the Dniester Estuary water in summer periods of 2012-2017.//XXI International Scientific and Practical Conference «Ecology, Environmental Protection and Balanced Nature Management: Education – Science – Production – 2018»: Theses of presentation, Kharkiv, 18-20 April 2018. P. 103-106. (In Ukrainian).

Kovalova, N., Medinets, V., Medinets, S., Konareva, O., Soltys, I., Gazyetov, E. (2018) Trophic status for deltaic lakes of Dniester in 2006–2017. *Kharkiv National University Herald. Series: Ecology,*18, 30–41. (in Ukrainian).

Kovalova, N., Medinets, V., Medinets, S. (2019). Results of bacterioplankton studies in the Dniestrovskiy estuary in 2003–2018. *Man and Environment. Issues of Neoecology ,*31, 57–66. (in Ukrainian).

Kovalova N.V., Medinets V.I., Medinets S.V. (2019) Quality and trophic status of the water bodies in the Dniester Delta in 2006-2018./ Materials of All-Ukrainian Scientific and Practical Conference «Rivers and Estuaries of the Black Sea Area at the Beginning of the 21 Century». Odesa State Environmental University. Odesa: TKS, 2019. P. 85-87. (In Ukrainian).

Kovalova N.V., Medinets V.I., Medinets S.V. (2020) Peculiarities of the long-term changes of bacteioplankton number if the Dniester Estuary in 2003-2018. Hydrobiological Journal, 2020. V. 56, №5, P. 42-51. http://www.hydrobiolog.com.ua (In Ukrainian).

Kovalova N., Medinets V., Medinets S. (2021) Peculiarities of Long-Term Changes in Bacterioplankton Numbers in the Dniester Liman/ Hydrobiological Journal, 2021, Vol 57, No 1. P. 27-36. ISSN 0018-8166.

Landsat 8. Internet resource: https://www.usgs.gov/landsat-missions/landsat-8

Materials (2012). Materials of All-Ukrainian Scientific and Practical Conference “Estuaries of the North-Western Black Sea Area: Urgent Hydro-ecological problems and the ways to solve them”. – Odesa: Odesa State Environmental University, 2012. 160 p. (In Ukrainian).

Methodology (1998). Methodology of surface waters environmental assessment according to respective categories. V.D. Romanenk, V.M. Zhukinskyi, O.P. Oksiyuk et al., K.: SIMVOL-T, 1998. 28 p. (In Ukrainian).

NOMAD (2008). NOMAD: NASA bio-Optical Marine Algorithm Dataset. Internet resource: https://seabass.gsfc.nasa.gov/wiki/NOMAD, 18 July, 2008.

O'Reilly J. E. et al. (1998) Ocean color chlorophyll algorithms for SeaWiFS. J Geophys Res Oceans 103(C11):24937-53.

O'Reilly, J.E., Carder, K., Kahru, M. (1998). Ocean color chlorophyll algorithms for SeaWiFS. *Journal of Geophysical Research: Oceans*, 103(C11) : 24937-53.

O'Reilly J. E., Werdell P. J. (2019) Chlorophyll algorithms for ocean color sensors - OC4, OC5 and OC6 // Remote Sensing of Environment. 2019. V. 229. P. 32-47.

OECD (1982). OECD (Organisation for Economic Cooperation and Development). Eutrophication of Waters, Monitoring, Assessment and Control. Paris, OECD, 1982. 145p.

Ogashawara, I., Mishra, D.R., Gitelson, A.A. (2017). Chapter 1 - Remote Sensing of Inland Waters: Background and Current State-of-the-Art // Bio-optical modeling and remote sensing of inland waters. Amsterdam: Elsevier, 1–24.

Pan, X. et al. (2010). Remote sensing of phytoplankton pigment distribution in the United States northeast coast. Remote Sensing of Environment, 114(11), 2403-2416.

Pan, X., et al. (2011) Remote sensing of phytoplankton community composition along the northeast coast of the United States. Remote Sensing of Environment, 115(12), 3731-3747.

PONTOS project (2021). Copernicus assisted environmental monitoring across the Black Sea Basin. Available at: https://pontos-eu.aua.am

Sentinel-2. Internet resource: https://sentinels.copernicus.eu/web/sentinel/missions/Sentinel-2

SENTINEL-3. Internet resource: https://sentinels.copernicus.eu/web/sentinel/missions/sentinel-3

SNAP. Internet resource: http://step.esa.int/main/toolboxes/snap/

Tikhomirov O.A., Bocharov A.V., Komissarov A.B., Khizhnyak S.D., Pakhomov P.M. (2016) Using Landsat 8 (OLI) sensor data to measure turbidity, color, and chlorophyll con tent in the water of the Ivankovo reservoir // Vestnik TvGU Seriya Khimiya. 2016. No. 2. P. 230–244 (in Russian)

Toner P., Bowman J., Clabby K., Lucey J., McGarrigle M., Concannon C., Clenaghan C., Cunningham P., Delaney J., O'Boyle S., MacCárthaigh M., Craig M. and Quinn R. (2005). Water Quality in Ireland 2001-2003. Ireland Environmental Protection Agency. 2005. - 233p.

Trifonova, I.S. (1990). Ekologiya i suktsessiya ozernogo fitoplanktona [Ecology and succession of lake phytoplankton]. Leningrad, 182 p. [in Russian]

Vollenweider R.A. (1998) Characterization of the trophic conditions of marine coastal waters with special reference to the NW Adriatic sea: proposal for a trophic scale, turbidity and generalized water quality index/ Vollenweider R.A., Giovanardi F., Montanari G., Rinaldi A// Environmetrics. 1998. № 9. P. 329-357.

Voronova A. E. (2020) Using satellite MSI data (Sentinel-2) to estimate the concentration of chlorophyll a in the Novosibirsk Reservoir, Siberian Center of State Research Center for Space Hydrometeorology “Planeta”. Current problems in remote sensing of the earth from space, 17(2), 2020 DOI: 10.21046/2070-7401-2020-17-2-199-205 (In Russian)

Wang G. & Moisan J. (2021) Remote Sensing of Phytoplankton Pigments. Chapter in Plankton Communities. DOI: http://dx.doi.org/10.5772/intechopen.95381

Watanabe, F., Alcântara, E., Imai, I., Rodrigues, T., Bernardo, N. (2018) Estimation of chlorophyll-a concentration from optimizing a semi-analytical algorithm in productive inland waters. *Remote Sensing*, 10, 227. doi: 10.3390/rs10020227

Witter DL. Ortiz JD. Palm S. Heath RT. Budd JW (2009) Assessing the application of SeaWiFS Ocean color algorithms to Lake Erie. J Great Lakes Res 35(3) : 361 - 370